STABILITY OF ANGLE-SECTION MEMBERS

by

R.T.G. Green, B.E. (Hons.)

submitted in partial fulfilment of the requirements

for the degree of

Master of Engineering Science,

UNIVERSITY OF TASMANIA

HOBART.

- AUGUST, 1967 -

SUMMARY

A simple treatment of the elastic stability of angle-section members, both columns and beams, has been developed, based on the measured deformations of typical members loaded in the laboratory. Detailed mathematical models describing the torsional or local buckling modes of the members are presented. Other buckling modes have been considered and the interaction of the various modes has been discussed. Angle-section columns, eccentrically loaded columns, cantilevers, centrally-loaded simply-supported beams, and laterally loaded columns, have been studied in particular.

I hereby declare that, except as stated herein, this thesis contains no material which has been accepted for the award of any other degree or diploma in any University, and that, to the best of my knowledge or belief the thesis contains no copy of paraphrase of material previously published or written by another person, except where due reference is made in the text of this thesis.

- I N D E X -

- I N D E X -

ACKNOWLEDGEMENTS

This work was carried out in the Civil Engineering Department of the University of Tasmania. The author wishes to thank the members of the staff of the University. In particular the author wishes to thank Professor A.R. Oliver, Professor of Civil Engineering, and Dr. M.S. Gregory, my supervisor of research, for their help and encouragement.

INTRODUCTION

Angle-section members, under various loading conditions, have been found to be unstable. In this thesis the conditions under which the instability occurs are presented and mathematical models are formulated to describe the geometry of the deformed member and to calculate the load capacity of the member. Equal-leg angle-section members were tested as columns, eccentrically loaded columns, cantilevers, centrally loaded beams, and laterally loaded columns. The mathematical models which are developed herein describe the torsional and local buckling of the members. However, where applicable, other types of instability have been investigated; also some types of interaction which can occur between the possible modes of buckling have been considered.

Only relatively recently, the torsional and local properties of structural members have become important. With the introduction of slender high-strength steel members, and materials such as aluminium and its alloys with low moduli of elasticity, the problem has been accentuated. Even today most design codes are based upon practices developed for mild steel members. In this century, considerable work has been carried out on the instability properties of columns. Two organisations which are particularly interested in the problem are the Column Research Council of America[1] and the Aluminium Research Development Association of Britain.[2] Both organisations have published results or codes which could be used by practising engineers. The German code is one of the most progressive codes.

In this thesis the problem of the buckling of angle-section members has been investigated using a new approach. Large field methods of measuring geometrical shapes have been used to obtain the deformed shape of the member. The basic geometry is then described analytically and the analytic function is used as a basis for the mathematical model. The forces required to sustain the measured deformation are calculated and a differential equation is obtained by considering the statical equilibrium of the whole member. The analytic function describing the geometry can be specified to any order of approximation and consequently

---

Ref. 1 Column Research Council Guide to Design Criteria for Metal Compression Members, John Wiley & Sons, Inc.

Ref. 2 Series of Aluminium Research Development Association Reports.

a number of successively more satisfactory mathematical models can be derived to describe the physical behaviour.

For most cross-sections the member can buckle either by the whole cross-section rotating, in an undeformed state, or by part of the cross-section deforming. The first type of instability is referred to as a torsional instability and the second as a local instability. For an equal-leg angle-section member, with both legs loaded identically, torsional buckling and local buckling are the same phenomena, and the two terms are interchanged freely in all the literature. Under this loading each leg acts as a simply supported plate, and there is no moment acting around the corner of the cross-section. The buckling of an angle member has been treated by these various methods, each of which will be considered.

The models tested were of such dimensions that the torsional mode was prominent. To emphasize torsional buckling behaviour the members tested had thinner walls, relative to width of leg, than are common in practice, but it has been indicated how the results obtained can be amended to give an understanding of the behaviour of more practical sections.

This thesis does not set out to present a large quantity of results and to derive empirical formulae or relationships. Rather, it relies on the similarity of the geometry of the deformation of members of different proportions and sizes. The mathematical models developed are based upon the deformed geometry of a number of members tested in the laboratory, and the results derived are compared with those obtained from a few physical models. In the future, large-scale testing programmes for more practical members might be contemplated; it is thought that the necessary basic ideas are established in this thesis.

* * * *

This thesis is divided into four parts. The first part is devoted to forming a foundation upon which the author's work is built. Although no new ideas are presented therein, the understanding of the ideas is basic to the remainder of the thesis.

The second section deals with the stability of a column which is axially loaded with a uniform stress distribution. Results presented

in this part have been derived in detail, because many of the ideas are used in the following sections. The work on a column under a pure axial load was presented by the author as a partial requirement for an honours bachelor's degree. In this thesis, the topic has been expanded by including the effect of non-uniform stress distribution produced by loading the member through a bolt. A detailed comparison with other mathematical models is also presented.

The third section deals with the instability of angle-section beams. This section leans heavily on the preceding section as it uses basically the same logic, although the mathematical models developed are more complicated. To the author's knowledge, there exist no other mathematical models which describe this problem, although beam-columns have been treated empirically.

The fourth section, a detailed comparison between the results obtained in this thesis and those obtained by other mathematical models is given. Present design codes are considered, and possible amendments are suggested in the light of the results of the work described in the thesis, and the fundamental understanding which it has encouraged or made possible.

This thesis establishes a new, simple mathematical model for the elastic behaviour of a column, and original mathematical models for the torsional buckling of a cantilever and a centrally loaded simply supported beam. Although the author has presented a mathematical model for a laterally loaded column, this topic needs further investigation. The thesis also considers the mathematical models describing the torsional-flexural buckling of a column developed by other workers, and the relevance of the lateral buckling model of beams developed by Tunoshenko.

GEOMETRY AS A WORKING TOOL

In the history of engineering structural science, the basic understanding of the geometry of the deformations of a loaded member has led to the necessary valuable simplifications on which all analysis is based, and has thus played an important part in the advancement of the science. Geometry has the advantage that it can be easily measured. From the earliest problem, that of a loaded cantilever, the geometry has been the basis for the mathematical description. The theory of bending is based upon the geometrical assumption that plane sections remain plane. However, the parameters of the geometry must be evaluated by considering the statical equilibrium of the member. The early development of the theory of bending was slow, as the experimenters failed to combine the geometry and the equations of equilibrium. In fact, this lack of completeness in the model led early engineers to assume that the neutral axis of a beam in bending was at the lower edge.

Later, prominent men, such as Timoshenko, have made advances because they have been able to base their mathematical descriptions upon geometry. One example, which was developed during this century, is the plastic analysis of members. Plastic analysis has become important because of the simplicity of its application, which in turn depends upon a simple deformation pattern. A framed structure in a fully plastic state is described by a rigid-plastic load-deformation relationship, in which all deformations occur within local regions known as plastic hinges. Lately, more sophisticated descriptions of elastic-plastic bending have been produced in which other deformations have been included.

The author will consider the torsional buckling of angle-section members by measuring the geometry of the member in its deformed or buckled state. The geometrical approach has been made possible by the development of optical methods of measuring geometry over large fields of view. Two such methods are the photo-elastic method, which measures stress in the plane of the model, and the moire fringe techniques, which measure deflections both in and normal to the plane of the model. For the work described here the moire fringe methods have been used, as they measure geometry directly.

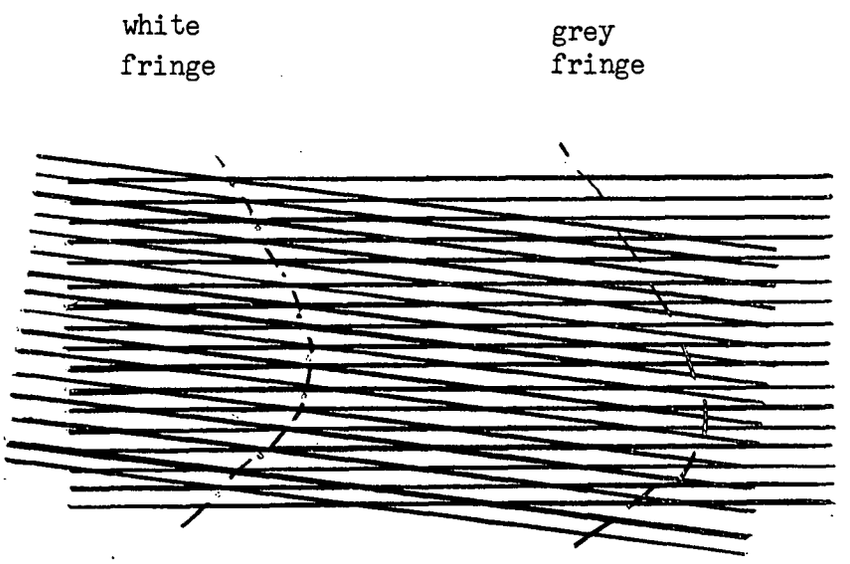

MOIRE FRINGES
FIGURE 1.

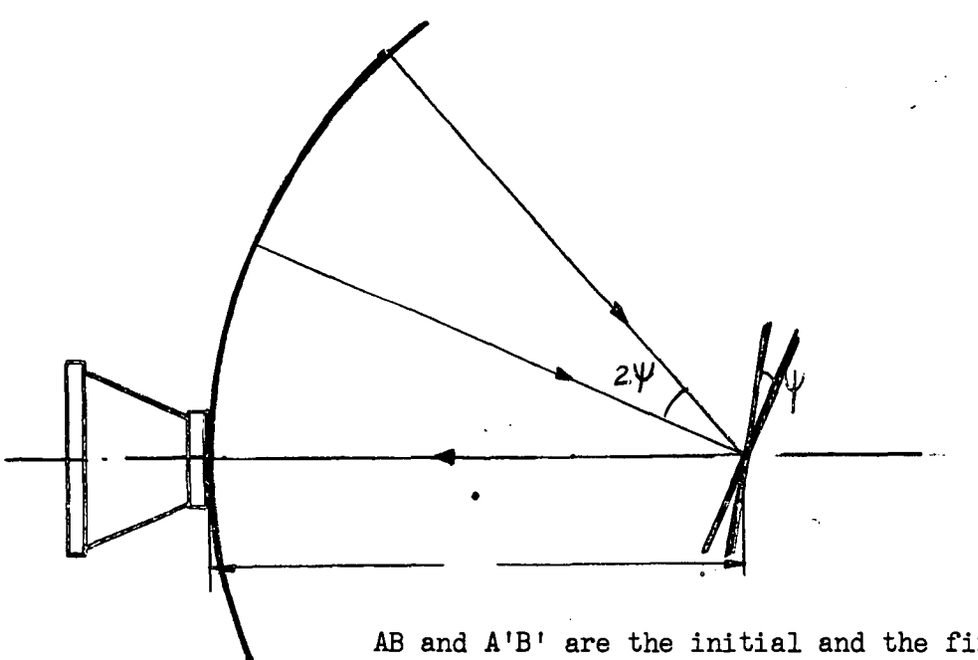

AB and A'B' are the initial and the final slopes of the plate at O.
ROI and QOI are two rays.
I is the image of both Q and R.

LIGTENBERG APPARATUS
FIGURE 2.

Moire Fringes

When two sets of parallel lines are interfered, a moire fringe pattern is formed as shown in fig. 1. Where two lines intersect, a "white" fringe is formed, while a grey fringe occurs when a white and a black line intersect. In interference terms, a "white" fringe occurs when the lines are in phase, that is displaced by an integral number of line spaces. The "grey" fringes are formed when the lines are out of phase.

Two of the available moire fringe methods have been used by the author in his experimental work. One method, the Ligtenberg method, measures changes in slope of a surface. The other method measures deflections in the plane of the surface. In this section of the thesis the author will only outline the experimental methods used. For complete details, such as the production of gratings, and the preparation of the models, reference may be made to Ligtenberg's[1] paper and two papers by Middleton, Jenkins and Stephenson;[2,3] the latter workers are engaged in the development of the techniques used at the University ofTasmania. The basic ideas involved in using the two methods are described in the following sections.

* * * *

The Ligtenberg Method[1]

The Ligtenberg method produces moire fringes which are contours of equal change in slope of a surface. The surface to be examined is made reflective by gluing a sheet of Melanex, a commercially available sheet of plastic coated with aluminium, to the surface. Kodaflat matte solution, a pressure-sensitive glue is used. A set of photographically reproduced lines is mounted on a part of a cylindrical surface and a camera is arranged so that the lens is at the centre of the screen. The lines are reflected from the model's surface and an image is produced on the camera film. The model is loaded and the second exposureis taken.

Ref. 1 Ligtenberg: "The Moire Method as a new experimental method for the determination of moments in small slab models". Vol. XII, No. 2, Proc. Soc. Experimental Stress Analysis.

Ref. 2 E. Middleton and C. Jenkins: "Moire methods for Strain Analysis for Student Use". Bulletin of Mech. Eng. Education, Issue 3, Vol. 5, 1966.

Ref. 3 E. Middleton and L.P. Stephenson: "A reflex Spectrographic Technique for in-plane Strain Analysis". In printers hands. SESA Paper No. 1250.

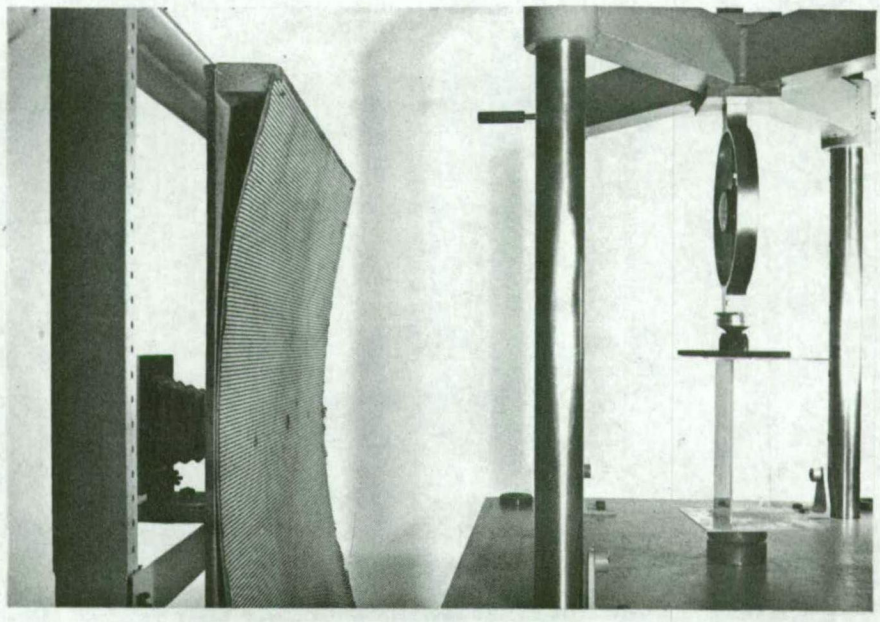

Ligtenberg moire apparatus for measuring slope.

FIG. 3

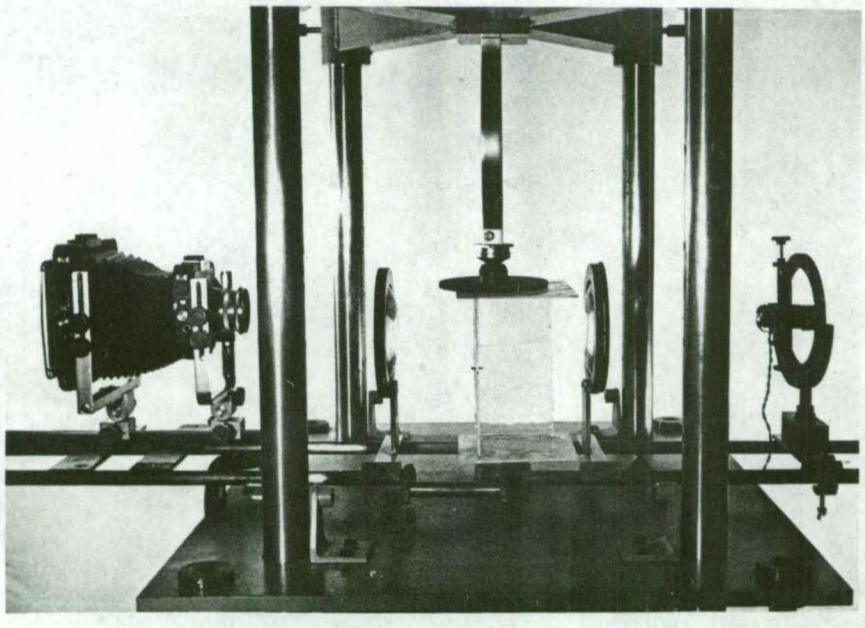

Crossed diffraction grating method of measuring displacements in the plane of the model.

FIG. 4

The double exposure produces moire fringes which are lines of constant slope. The general arrangement of the apparatus is as shown in figs. 2 and 3.

An approximate relationship between the change of slope at each fringe can be derived by considering the model point which lies on the screen. The following notation will be used; d is the line spacing of the grid, a is the radius of curvature of the screen, ψ is the change in slope of the model and n is an integer. In fig. 3, QOI and ROI are the ray traces for the unloaded and loaded cases respectively. The distance QR is given approximately by $2a\psi$. For a "grey" fringe to form at I, QR must be equal to $2(n + \frac{1}{2})d$. Thus the slope change is given by

$$\psi = (2n + \tfrac{1}{2})d/2a \qquad (1)$$

In the following experimental work this formula has been used for all points on the model surface. The errors involved in using this formula, when applied to off-centre points or when the model is not at the centre of curvature of the grid, have been indicated by Ligtenberg in his article. The slope measured is the slope in the direction normal to the grid lines. Two photographs, with the grid lines perpendicular must be taken to fully describe the geometry of the surface in terms of its slope in two directions at right angles to one another.

* * * *

Crossed Diffraction Grating Methods

A moire pattern is produced when two diffraction gratings are superimposed. Fringes are due to mis-matching of gratings or relative rotation of the two gratings. If one of the gratings is moved relative to the other, the pattern changes. A secondary moire fringe pattern can be obtained by superimposing the two primary patterns. The secondary fringes represent lines of constant displacement and are independent of the initial primary pattern.

A grating is glued to the surface of the model and a reference grating is fixed to the model, so that the relative movement between the two gratings is restrained kinematically[1]. Usually three connections are

---

Ref. 1 E. Middleton and L. P. Stephenson: "A reflex Spectrographic Technique for in-plane Strain Analysis". In printers hands. SESA Paper No. 1250.

used; a point at which there is no relative movement, a line where there is movement in one direction only and a plane which allows complete freedom of movement and is used to maintain a constant air gap. With the three point system the reference grating is mounted kinematically, and the loading of the model does not load the reference grating.

Two photographs are taken of the moire fringe pattern, one of the loaded model and another of the unloaded model. The secondary pattern obtained from the two primary patterns represents lines of constant displacement normal to the grating lines. The optical system required to take the photographs is shown in fig. 4. The system can be broken down into four sections, a collimator, the model, a condenser system, and a camera.

The models used for the transmission method are made of perspex. Gratings of one hundred, one thousand, and three thousand lines per inch are produced at the University of Tasmania.

* * * *

The moire fringes make it possible to measure the deformations of members under load, and hence to describe the deformations analytically. The analytic functions, in conjunction with stress-strain relationships, can be used to consider the statics of the problem, either to determine the loads applied or to enable a statical balance on any section or portion of a member to be carried out. It will be appreciated that the geometry is only approximated by the analytic functions and the degree of approximation is important. The complexity of the mathematics must be balanced by consideration of the accuracy with which the mathematical description is required to agree with the physical model.

* * * *

At this point it will be of benefit to introduce several terms to be used throughout this thesis. "Functional form" is a term used to indicate any one aspect of the geometry which is common to all problems of a certain type. For example, "plane sections remain plane" is the functional form for bending, and "radii remain straight" is the functional form for the torsion of a solid circular bar. The functional form does not necessarily describe the shape of the member fully. The "mode" of a buckled

member or structure is the critical or buckled shape (or "eigen" shape) of the perfect member or structure. For a given structure there is usually more than one mode.

A "mathematical model" refers to the mathematical description which can be built up once some basic assumptions have been made. It is important to realize there is more than one possible mathematical model suitable for describing a physical model. In the previous example of elastic bending, the basic assumptions are that plane sections remain plane and that the stress-strain relationship is linear. From these basic assumptions follow the relationships that the moment M is equal to EIK, and that the stress σ at a point equals My/EI, where E is Young's modulus, I is the moment of inertia about an axis through the centroid, K is the curvature of the line of centroids, and y is the distance from the centroidal axis. The next result, for example, is that the shear stresses and strains are parabolically distributed in a rectangular beam. The previous statements form one mathematical model of elastic bending. However, it should be noted that the model has a contradiction. It has been assumed that plane sections remain plane, but, as a result, the shear stresses and hence the shear strains are parabolically distributed. This result leads to another mathematical model in which plane sections do not remain plane. For most engineering purposes the first mathematical model describes the physical model sufficiently well.

In some cases more than one mathematical model arises due to a mathematical approximation. Consider the beam again. If one derives the curvature distribution along the beam and uses the differential expression for curvature,

$$K = \partial^2 w/\partial x^2/(1 + \partial w/\partial x)^{3/2}$$

the shape of the beam can be calculated. In most cases the approximate expression for the curvature $K = \partial^2 w/\partial x^2$ is sufficiently accurate. Any mathematical approximation should be included in the basic assumptions and also the limits of its application, because if the model is extended to apply for large deflections the approximations may not apply.

In a mathematical model one tries to satisfy three conditions; compatible geometry, the equations of statical equilibrium and the boundary

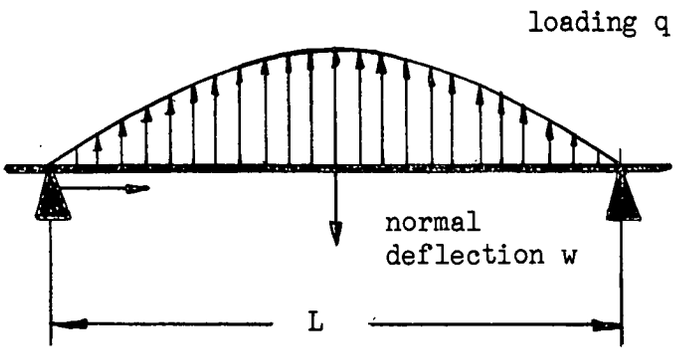

FIGURE 5

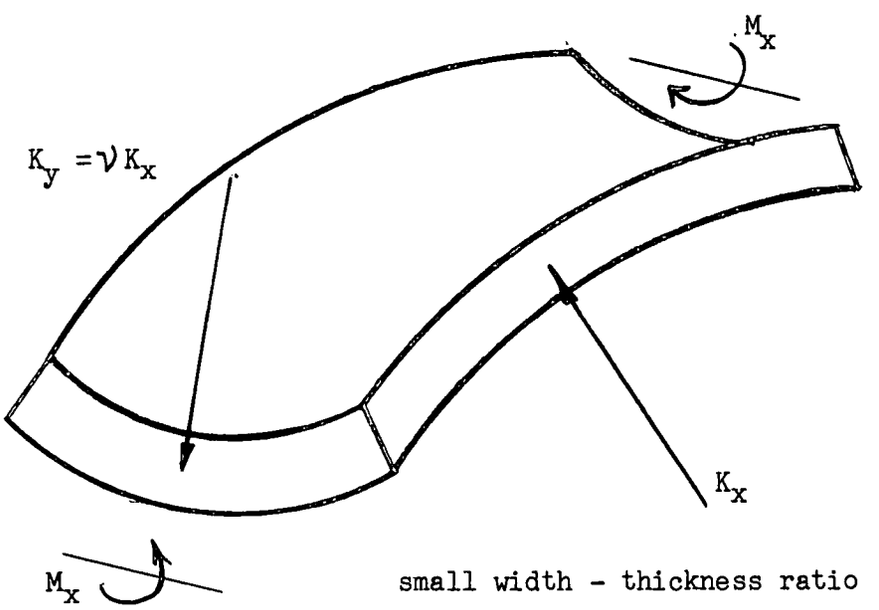

small width - thickness ratio

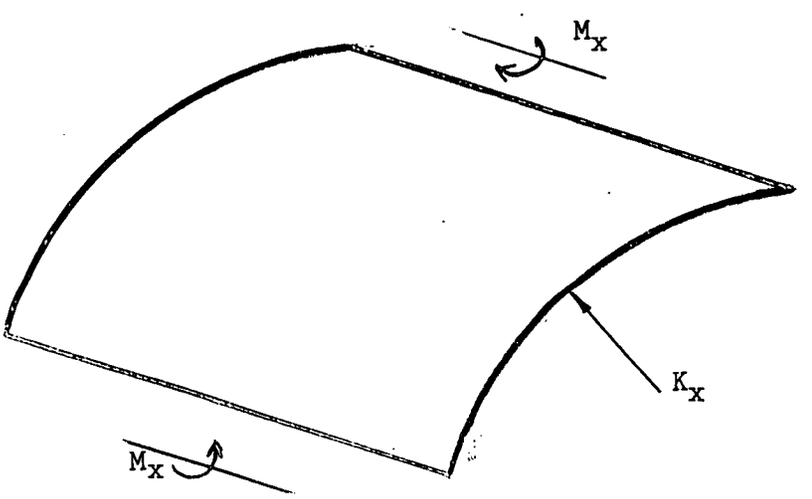

large width - thickness ratio

THE SHAPE OF A SLAB BENT BY A UNIFORM MOMENT

FIGURE 6

conditions, all to a certain level of approximation. As no mathematical model fully describes the physical model, a compromise must be reached. in the approach taken it is relatively simple to describe a system of compatible geometrical deformations which satisfy the boundary conditions. However, usually only some of equations of statics are satisfied. The potential energy method is a means of obtaining an approximate solution in which all the equations of statics are satisfied on an average. In fact, if the correct geometry is fed into the energy equation it reduces to the equations of statics.

In establishing a mathematical model it is advisable to start with the simplest functional form possible. Using large field measurements the salient functional form is usually obtained easily, and the order of magnitude of any secondary component can be determined. In the previous paragraph, it has been stated that the functional form must satisfy the boundary conditions. For certain problems some of the boundary conditions have little effect on the strength of the member. The contours of measured deformations, obtained by the moire methods, aid the investigator in appreciating the important boundary conditions. Consider two beams one with a width-thickness ratio of approximately two and another with a large width-thickness ratio. Both beams have a curvature K_x in the direction of the applied moment. But the orthogonal curvature is equal to $-\nu K_x$ for the first beam and zero for the second, where ν is Poisson's ratio (see Fig. 5). Obviously the second beam does not satisfy the boundary conditions of zero moment and shear stress along the edge of the beam. In fact, it does, because the curvature changes from zero to $-\nu K_x$ in a local region near the edge. If the curvature is assumed to change in a certain manner the consequences of neglecting the local edge effect can be calculated. The assumption of zero curvature across a long flat strip leads to a simpler mathematical model. As an example, consider a strip as a long beam, length L, simply supported at each end and carrying a load

$$q = q_0 \sin \frac{\pi x}{L}$$

see fig. 6, the differential equation for the normal deflection w of a plate carrying a lateral load q is

$$\partial^4 w/\partial x^4 + 2\ \partial^4 w/\partial^2 x\ \partial^2 y + \partial^4 w/\partial y^4 = q/D \qquad (2)$$

If we take $w = aW(x)$, where $W(x)$ is a function at x only, the differential equation simplifies to

$$\partial^4 W/\partial x^4 = q_0/D \sin \frac{\pi x}{L}$$

and the shape is

$$w = q_0(L/\pi)^4 y \sin \frac{\pi x}{L},$$

when the boundary conditions are satisfied. Alternatively, if we use

$$w = W(y) \sin \frac{\pi x}{L}$$

then the differential equation becomes

$$W(\pi/L)^4 \sin \pi x/L - (\pi/L)^2 \sin \pi x/L \; \partial^2 W/\partial y^2 + \sin \pi x/L \; \partial W/\partial y$$

$$= q_0/D \sin \pi x/L .$$

This equation could be solved and the boundary conditions, zero moment and shear stress applied. However, the mathematics are much more complicated.

In buckling problems the end conditions have an important effect on the load capacity of the model. In developing a mathematical model for the buckling of a column, most experimenters aim either for fully built in end conditions or for a simply supported condition. In the experimental work associated with this thesis, no particular effort was made to obtain a certain type of end condition. The Ligtenberg apparatus was used to determine the end conditions. However, the mathematical models established have been adopted to apply to members with simply supported ends, and have been presented for this case.

In this section it is hoped that the benefits of measuring the geometry of deformations of a loaded member have been indicated: Firstly in establishing the problem, that is in determining the boundary conditions and indirectly the loads applied; secondly in appreciating the salient features of the functional form. Geometry is a readily measurable property which forms a foundation stone from which can be built, in a logical manner, a mathematical model.

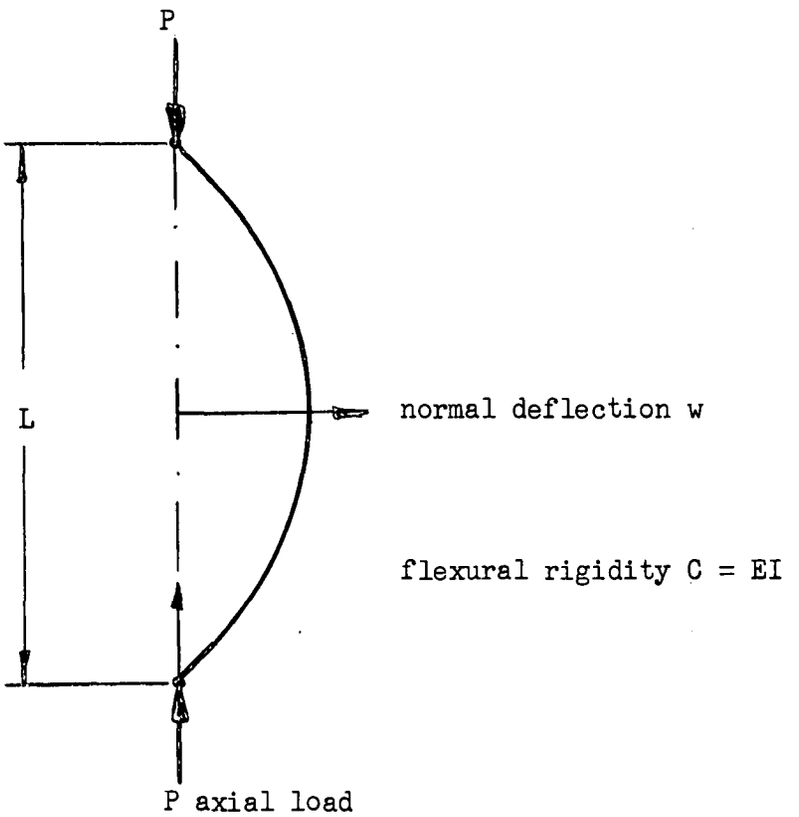

SIMPLY SUPPORTED, AXIALLY LOADED COLUMN

FIGURE 7

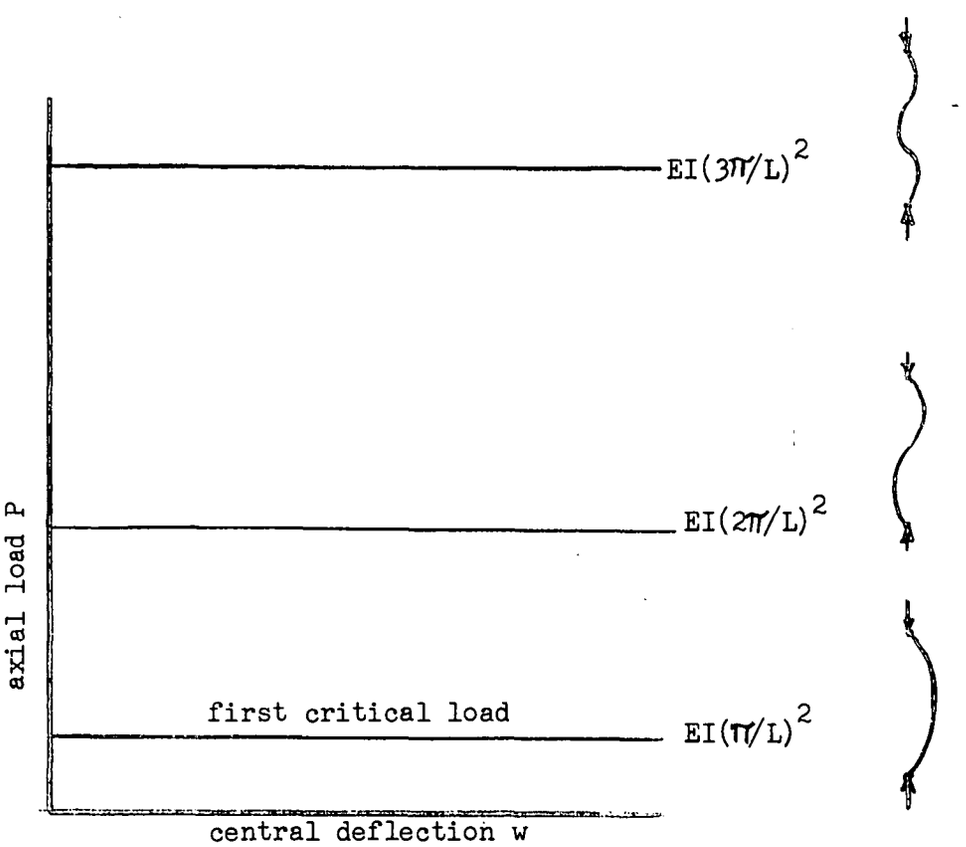

LOAD-DEFORMATION RELATIONSHIP FOR AN INITIALLY STRAIGHT, SIMPLY SUPPORTED COLUMN.

FIGURE 8

BUCKLING

A practical structure can be said to be unstable if it experiences large deformations in the neighbourhood of a given load. The given load is called the critical load. One type of instability is plastic collapse due to the non-linearity of the load-deformation relationship of the material. Other structures are unstable in the elastic range. Generally the term "instability" applies only to elastic structures. It is important to realize that the stability of the structure depends not only on the structure but also on the loading method.

This chapter is presented as a historical review of the of instability. However, the progress in understanding the behaviour of a single column is considered first, as most of the ideas associated with the general topic of buckling were established by considering a simply supported column. Next, the buckling of plates will be considered. Chronologically the development of the theory of the buckling of plates lagged slightly behind that of a column. The final part of this chapter will be devoted to ideas which apply generally to all structural and dynamic instability problems. Both types of problems have similar differential equations.

Columns

The mathematician, Euler, first introduced a mathematical model for the instability of an axially loaded, simply supported column in the year 1744, see Fig. 7. Basing his model on a linear moment-curvature relationship and the approximate curvature expression

$$K = \partial^2 w / \partial x^2 , \tag{3}$$

he obtained the equation of equilibrium for the column in terms of the normal deflection w,

$$\text{Moment} = Pw - C\, \partial^2 w / \partial x^2 . \tag{4}$$

The solution of the differential equation is trivial unless the load has the value

$$P_{crit} = C(\pi/L)^2$$

in which case the deflection is indeterminate. The constant C is the flexural rigidity EI, where E is Youngs Modulus and I is the smallest moment of inertia. Lagrange (1770) enlarged upon Euler's work

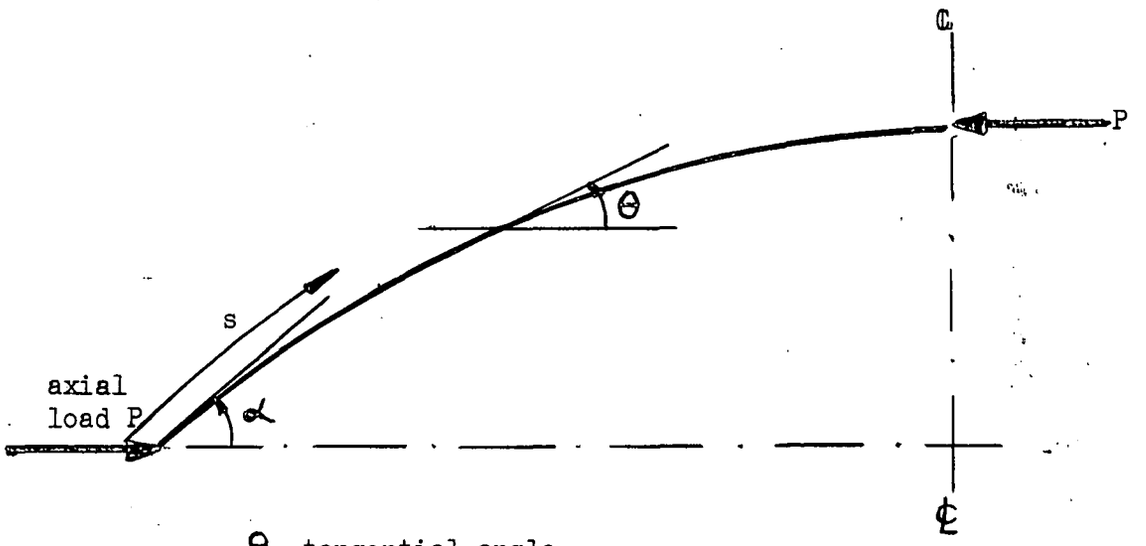

θ tangential angle
α end angle
s ordinate measured along the member

FIGURE 9

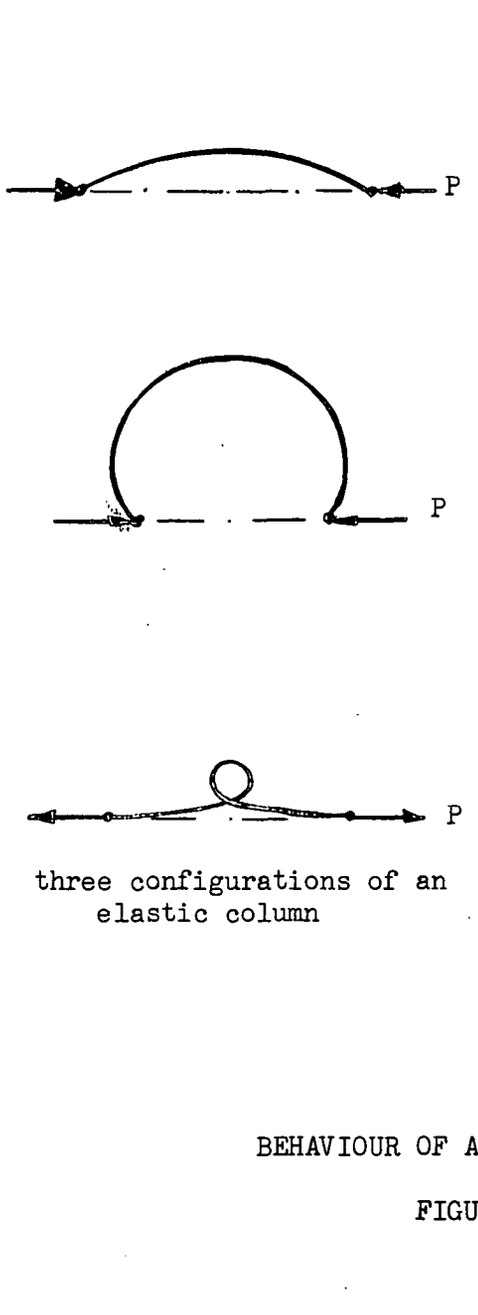

three configurations of an elastic column

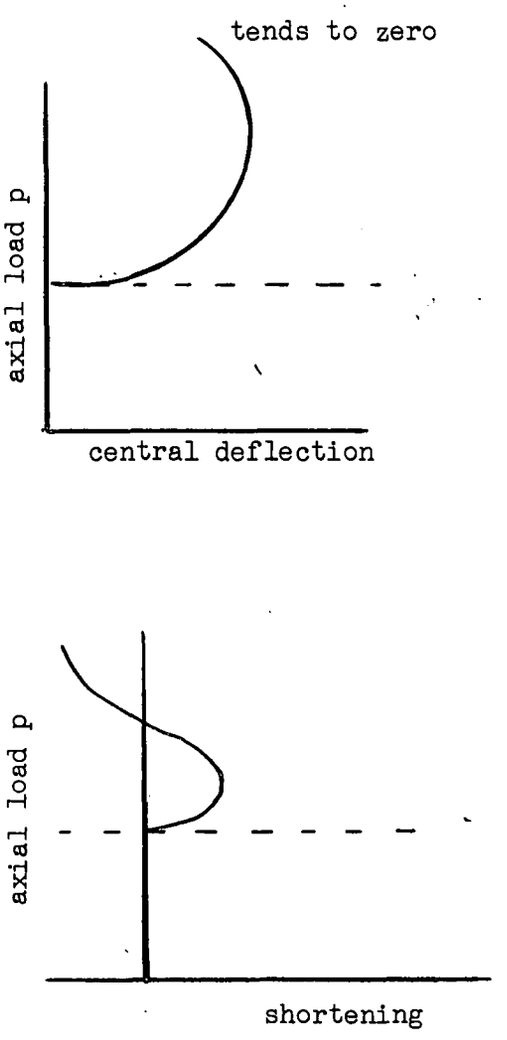

BEHAVIOUR OF AN ELASTIC COLUMN (ELASTICA)

FIGURE 10

by indicating that there is an infinite number of solutions which satisfy the boundary conditions and a corresponding load for each:

$$y = A \sin \frac{n\pi x}{l} \quad \text{and} \quad P_n = \left(\frac{n\pi}{l}\right)^2 C \tag{5}$$

The shapes $y = A \sin \frac{n\pi x}{l}$ are called the modes, or in mathematical terms eigen functions or characteristic functions. The loads are the critical loads or the eigen-values or the characteristic values. A model will be said to be mathematically unstable if the load-deformation relation bifurcates at a number of buckling loads and at each load the deflection is indeterminate. (see fig. 8)

When the more accurate expression for curvature is used, it is well known that there is a one-to-one correspondence between the load and the deformation as shown in fig. 10. In terms of the symbols defined in fig. 9 the differential equation becomes

$$EI\, \partial\theta/\partial s + Py = 0 \quad \text{or} \quad E\, \partial^2\theta/\partial s^2 + P\partial y/\partial s = 0 ,$$

which is equivalent to

$$EI\, \partial^2\theta/\partial s^2 + P \sin\theta = 0 . \tag{6}$$

If the equation is multiplied by $2\partial\theta/\partial s$ and integrated, in conjunction with the boundary conditions, the equation becomes

$$EI(\partial\theta/\partial s)^2 - 2P\cos\theta = \text{constant} = -2P\cos\alpha .$$

Using the following coordinate changes

$$s = u\sqrt{EI/P} , \quad k = \sin\alpha/2 \quad \text{and} \quad k \sin\phi = \sin\theta/2 ,$$

that is $k\cos\phi = \frac{1}{2}\cos\theta/2\,(d\theta/d\phi)$, the solution is the first elliptic integral

$$u = \int_{\frac{\pi}{2}}^{\phi} d\phi/\sqrt{1 - k^2\sin^2\phi} \tag{7}$$

The relationship between the load and the end slope follows from this expression,

$$\frac{L}{2}\frac{P}{\sqrt{EI}} = (\text{complete elliptic function}) \int_{\frac{\pi}{2}}^{0} d\phi/\sqrt{1 - k^2\sin^2\phi} .$$

In the mathematical sense the second, more complicated, model is stable. Consequently the mathematical stability (or Eulerian stability) is a property of the mathematical model and not of the physical model.

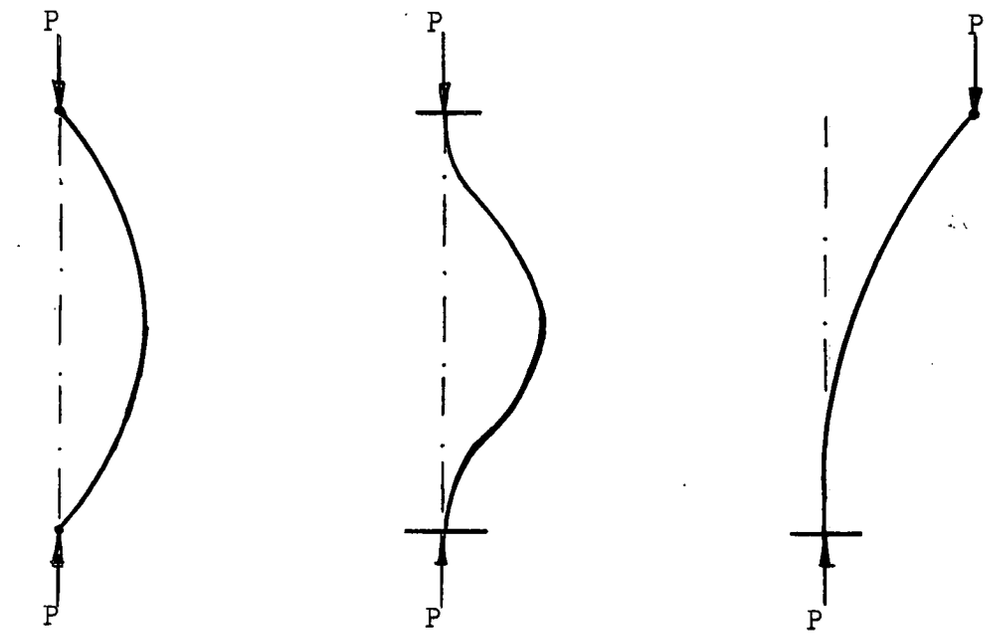

EFFECTIVE LENGTH OF COLUMN

FIGURE 11

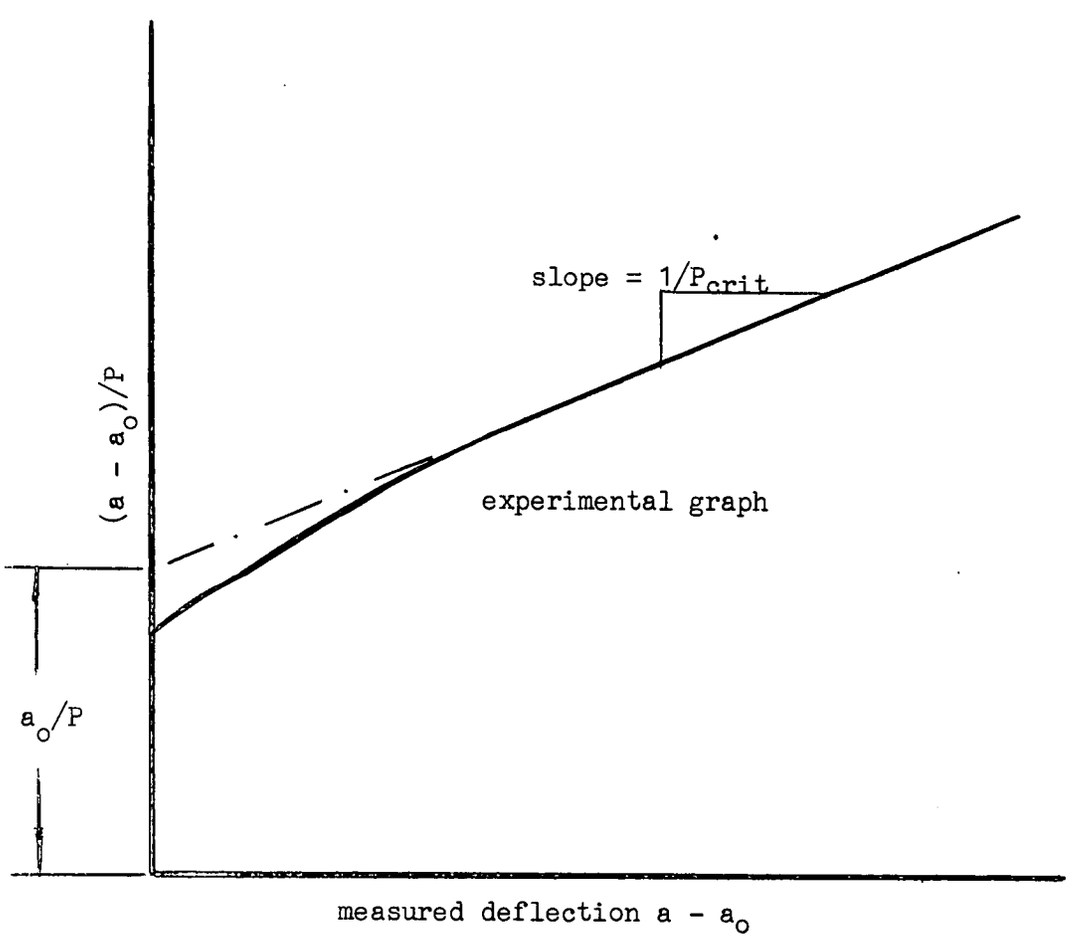

TYPICAL SOUTHWELL PLOT

FIGURE 12

The Eulerian critical load is a useful number since, in a large number of applications the member can be said to be physically unstable at this load. Often the instability is emphasized by the yielding of the material near the critical load. In the plate and shell analysis it is not so useful since strains in the central planes of the shell or plate vary with deformations and the critical load has little relevance to the failure load. This applies for some of the members considered in this thesis.

The analysis of Euler holds for simply supported boundary conditions; that is the end moment and deflection is zero. It is possible to describe the shape for other boundary conditions by

$$w = a \sin \frac{\pi x}{l} ,$$

where l is equal to kL and is known as the effective length, k is a constant. Then the Euler load becomes

$$P = \left(\frac{\pi}{kL}\right)^2 EI . \qquad (8)$$

For an axially loaded column the effective length has the physical meaning that it is the length of the column which acts as a simply supported column. However when a lateral load is applied the effective length derived from the shape can not be used in Euler's load formula. (see fig. 11)

Euler also derived the differential equation for a member with an initial curvature,

$$\text{Moment} = Pw = -\left(\partial^2 w/\partial x^2 - \partial^2 w_0/\partial x^2 \right) , \qquad (9)$$

where w_0 is initial deflection. But it was Young who, early in the nineteenth century, derived the first expression for deflection of an initially crokked member. He assumed that the initial shape was the same form as the lowest buckling mode,

$$w_0 = a_0 \sin \pi x/L .$$

From this assumption it follows that

$$a = \frac{a_0}{1 - P/P_{crit}} .$$

Young also gave the solution to a column built in at one end and loaded eccentrically.

In the early twentieth century, Southwell showed that by a simple transformation of co-ordinates Young's result could be linearized. He then suggested that the relationship, now known as a Southwell Plot, was a good means of determining the critical load of a physical model. Southwell[1] developed the theory to show the validity of this expression for a simply supported column. He also suggested that it could be applied generally, except for the buckling of some shell structures. Southwell expressed the initial shape as an infinite Fourier series of the buckling modes

$$w_0 = \sum_{n=0}^{\infty} a_{0n} \sin (n\pi x/L) .$$

Then from the differential equation he obtained

$$w = \sum_{n=0}^{\infty} a_n \sin (n\pi x/L) ,$$

where

$$a_n = a_{0n} (1/(1 - P/P_n)) \qquad (10)$$

and P_n are the eigen values. For loads near the critical load, the first term in the series dominates and the deflection is given approximately by

$$a = \frac{a_{01}}{1 - P/P_1} ,$$

which can be rearranged to give

$$(a - a_0)/P = (a - a_0)/P_1 + a_0/P_1 \qquad (11)$$

If $(a - a_0)/P$ is plotted against the measured deflection $a - a_0$ as in fig. 11, then the inverse of the slope is the critical load and the intercept is a measure of the initial crookedness. The initial crookedness is a useful quantity in estimating the load capacity of a member which yields before the critical load is reached. Southwell indicated, that for the method to give a reasonable result the member must deform elastically, the first mode must predominate, and the deflections must be small.

Following Southwell's suggestion, the Southwell plot has been

---

Ref. 1 R. V. Southwell "On the Analysis of Experimental Observations in Problems of Elastic Instability", Proc. Roy. Soc. Series A, p.135, 1932.

used for various buckling problems. However, its validity has only been indicated for some structures, such as frames. In general it has been used blindly. Gregory[1] has shown that it is often more convenient to use a Southwell plot on strains, but the strain typical of the buckling mode must be separated from the total strain. In the case of a column, only the bending strains must be considered, not the axial strains. To use any Southwell plot the investigator must have some idea of the buckling mode, so that he measures a geometric quantity which is indicative of the buckling mode. Gregory also showed, for a column loaded eccentrically, that the Southwell plot can be used for measuring the critical load, but in this case the intercept is a function of the eccentricity and the initial crookedness. For an eccentrically loaded column the Southwell plot cannot be shown to be linear, but for most purposes it is approximately linear.

Euler's formula for the ultimate load of a column was not generally accepted, as many members tested failed at loads less than those predicted by Euler. Larmarle realized that for stocky members the material yields before Euler's load is reached. He suggested that the failure stress should be given by

$$P_{crit} = EI \left(\frac{\pi}{L}\right)^2$$

if this value is less than yield stress and the yield stress if it is greater.

Simultaneously, Considere and Engesser extended Euler's mathematical model to allow for the non-linearity of the material's stress-strain curve. Both gave the buckling load as

$$P_{crit} = \bar{E}I \left(\frac{n\pi}{L}\right)^2 .$$

Engesser gave $\bar{E}$ as the tangent modulus, and defined it as

$$\bar{E} = \partial s / \partial t ,$$

where s is stress and t strain. Considere said $\bar{E}$ is the reduced

---

Ref. 1 M. S. Gregory "The Buckling of Structures" Ph.D. thesis, University of Tasmania.

Ref. 2 M. S. Gregory "The Use of Measured Strains to obtain Critical Loads", Civ. Engineering. London, Vol. 55, No. 642, p.80-82.

modulus, the value of which lies between the elastic modulus and the tangent modulus. He did not evaluate the reduced modulus, but stated that it was less than the tangent modulus, as only a portion of the cross-section experienced a non-linear stress-strain relationship. Lately, the tangent modulus has been re-introduced as most columns tested fail near the tangent modulus critical load. This is thought to be due to the initial crookedness, which causes deformations for loads less than the critical load, and consequently at the critical load most of the cross-section is plastic.

With the use in practice of slender iron struts, empirical column formula were developed. The earlier formulae were based upon the test results obtained by Hodgkinson. The first English engineers used Tredgold's formula for rectangular columns and hinged ends

$$\sigma_{max} = P/bh\,(1 + a\,L^2/h^2)\,, \qquad (12)$$

where a is a constant, L the length, b the width and h the depth. Gordon evaluated the constant for wrought iron using Hodgkinson's results. For a simply supported column

$$\sigma_{max} = 36{,}000/(1 + L^2/12{,}000\,h^2)$$

and for a built in column

$$\sigma_{max} = 36{,}000/(1 + L^2/3{,}000\,h^2)\,.$$

Today, Perry-Robertson's formula is the most commonly used, this states

$$\sigma_a = (\sigma_y + \sigma_e\,(1 + \delta_0 c/\rho^2)) - \sqrt{(\sigma_y + \sigma_e\,(1 + \delta_0 c/\rho^2))^2 - 4\sigma_y\sigma_e}\,,$$

where $\sigma_e = \frac{EI}{A}\left(\frac{\pi}{L}\right)^2$ and σ_y is the yield stress, δ_0 is a measure of the crookedness and eccentricity. Lately with the introductions of high strength steels the effect of residual stresses has become important and the Column Research Council[1] has indicated ways of including the effects of residual stresses.

Plate Structures

The study of the buckling of plate structures has developed along

---

Ref. 1 Column Research Council Guide to Design Criteria of Metal Compression Members.

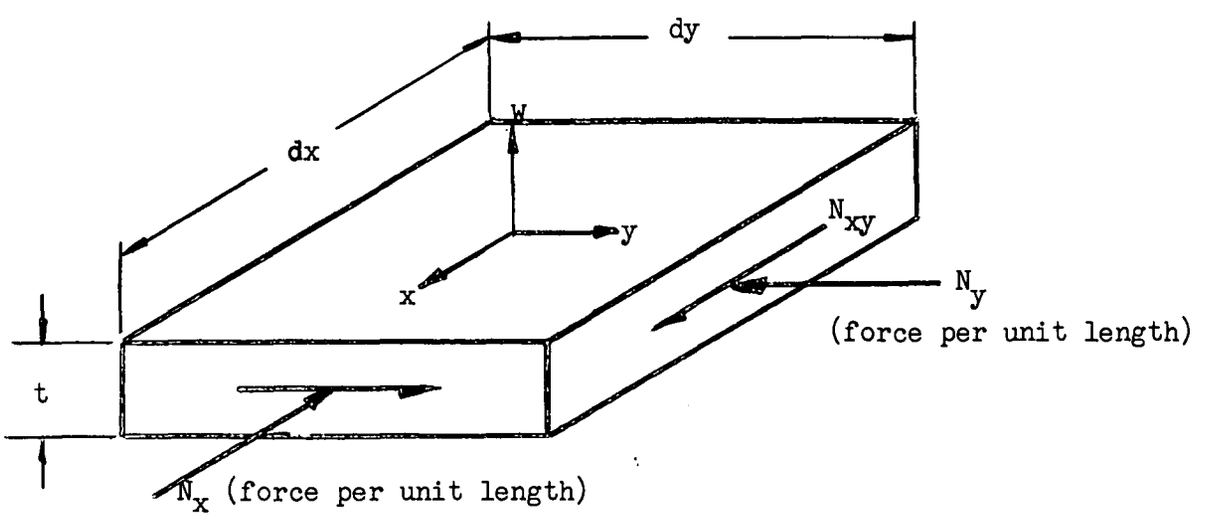

FORCES ON THE CENTRAL PLANE OF A PLATE ELEMENT.

FIGURE 13

similar lines to that of columns. However, the bulk of the mathematical work has been carried out in this century. The importance of these problems has been emphasized by the introductions of, first, steel ships, then aeroplanes and submarines. Also the uses of lightweight, low modulus of elasticity materials in aeroplanes has played an important part in the development of the understanding of plate buckling.

In the early analysis of plates, the plate was simulated by two sets of orthogonal elastic beams. The differential equation for the normal deflections w of the plate,

$$+ D\,(\partial^4 w/\partial x^4 + \partial^4 w/\partial y^4) = N_x\,\partial^2 w/\partial x^2 ,$$

derived by this means, neglected the effect of the twisting moments in the plates. It was Navier who in 1820 developed the correct differential equation for a plate under an axial load N_x ,

$$+ D\,(\partial^4 w/\partial x^4 + 2\,\partial^4 w/\partial^2 x\,\partial^2 y + \partial^4 w/\partial y^4) = N_x\,\partial^2 w/\partial x^2 , \qquad (13)$$

but he was unable to provide a solution. (see fig. 13)

The first occasion when plate buckling was met in practice was in 1845 when Robert Stephenson was commissioned to build railway bridges in England. Stephenson decided upon a tube design, through which the trains would pass. Fairbairn, an experimenter, was called in. He tested various models and came to the conclusion:

"Some curious and interesting phenomena presented themselves in the experiments - many of them are contrary to our preconceived notions of the strength of materials, and totally different to anything yet exhibited in any previous research. It has invariably been observed, that in almost every experiment the tubes gave evidence of weakness in their powers of resistance on the top side, to the forces tending to crush them".

Simply, the top flange of the tube was failing by local instability due to the compressive bending stresses before the lower flange failed by yielding. Fairbairn called in his theoretical colleague, Hodgkinson, to examine the results. However, as time was short, Fairbairn was forced to test a large model with a span of seventy five feet. As a result of the test the cross-section of the tube remained rectangular but the top and bottom flanges were reinforced using a cellular structure. The tests

also indicated that the sides were unstable, and the instability could be improved by the use of vertical stiffeners.

Jourawski in an extensive criticism of the tube bridges observed that the buckling of the sides of the tubes was due to compressive stresses at forty five degrees to the axis of the bridge. He demonstrated with models that it was more efficient to have stiffeners at forty five degrees. Hodgkinson's examination of the failures produced the conclusion that the buckling load varied with the ratio of the thickness of the plate to the width of the plate. He also suggested that circular tubes are far more stable than rectangular tubes.

Early in the investigation of plates, engineers, one of whom was Rankine, developed formulae for buckling loads of plates and I-beams, which were of the same form as those used for columns (equation 12). The appropriate constants were evaluated using the experimental results of the time.

In the late nineteenth century, Bryan (1891) investigated mathematically the stability of thin rectangular plates with simply supported edge conditions, and produced the first acceptable result. Bryan used his theory to aid him in the proper selection of plates for ships' hulls. In the 20th century, the buckling of plates became of paramount importance and Bryan's work formed a foundation for much of the mathematics which followed.

In the twentieth century men such as Prandtl, Wagner, Goodier, Kappus, Vlasov, Bleich, and Timoshenko, have developed the theory of plate, torsional and lateral buckling. Their work will not be discussed in detail here as it will be referred to where applicable in the following chapters.

Energy

The general differential equation for the normal deflection w of a plate is

$$D\left(\frac{\partial^4 w}{\partial x^4} + 2(1-\nu)\,\partial^4 w/\partial^2 x\,\partial y^2 + \partial^4 w/\partial y^4\right) = N_x\,\partial^2 w/\partial x^2 + 2N_{xy}\,\partial^2 w/\partial x\,\partial y + N_y\,\partial^2 w/\partial^2 y$$

where N_x, N_y are the normal and N_{xy} the shear forces per unit length

on the central plane of the plate. The differential equation must be solved in conjunction with the boundary conditions of the plate. For most problems the solution of the differential equation is too difficult. Timoshenko popularised the energy method of obtaining approximate solutions of structural problems. Energy had been used previously by Rayleigh in dynamic eigen value problems, such as solving for the frequencies of the linear vibrations of a system.

The potential energy for a plate with no lateral loads is

$$u = \iint \tfrac{1}{2}D\left(\left(\partial^2 w/\partial x^2 + \partial^2 w/\partial y^2\right)^2 - 2(1-\nu)\left(\partial^2 w/\partial x^2\right)\left(\partial w^2/\partial y^2\right) - \left(\partial^2 w/\partial x \partial y\right)^2\right) + \tfrac{1}{2}\left(N_x(\partial w/\partial x)^2 + N_y(\partial w/\partial y)^2 + N_{xy}(\partial w/\partial x) \times (\partial w/\partial y)\right)dxdy \qquad (15)$$

The energy can be considered in two parts. The first bracket is the internal strain energy of the deformed plate, and the second is the external energy of the applied loads.

The energy expression can be treated in two ways. Timoshenko states that if N_x, N_y and N_{xy} can be expressed as $N_x = \lambda C_x$, $N_y = \lambda C_y$ and $N_{xy} = \lambda C_{xy}$ then conservation of energy gives

$$\lambda = \frac{\iint D\left(\left(\partial^2 w/\partial x^2 + \partial^2 w/\partial y^2\right)^2 - 2(1-\nu)\left(\partial^2 w/\partial x^2\, \partial^2 w/\partial y^2 - \left(\partial^2 w/\partial x \partial y\right)^2\right)\right)dxdy}{\iint C_x(\partial w/\partial x)^2 + C_y(\partial w/\partial y)^2 + 2C_{xy}(\partial w/\partial x)(\partial w/\partial y)dxdy} = F_1/F_2 \qquad (16)$$

and that the load parameter λ must have a minimum value with respect to all geometric parameters. Ritz on the other hand states that the potential energy u must be a minimum, that is

$$\partial u/\partial a_i = 0 \qquad \text{for any parameter } a_i .$$

Both approaches arrive at similar results. Timoshenko gives

$$\partial\lambda/\partial a_i = \partial(F_1/F_2)/\partial a_i = (F_2\, \partial F_1/\partial a_i - F_1\, \partial F_2/\partial a_i)/F_2^2$$

which simplifies to

$$\partial\lambda/\partial a_i = (\partial F_2/\partial a_i + \partial F_2/\partial a_i)/F_2 ,$$

when the expression for the load parameter is substituted into the expression. The term in the brackets is a statement that the potential energy must be a minimum, or the Ritz criterion.

Usually the shape is expressed as a finite sum of orthogonal functions, each of which satisfies the boundary conditions,

$$w = \sum_{i=1}^{n} a_i \phi_i \, . \tag{17}$$

The functions need not be orthogonal. The expression for the deflection w is substituted into either expression (15) or (16), which is then minimized with respect to all the n parameters. The result is a system of n linear equations,

$$[A - \lambda B][a_i] = [0]. \tag{18}$$

For the solution to be non-trivial the determinant of $[A - \lambda B]$ must be zero, which leads to a characteristic equation of n^{th} order which has n eigenvalues, λ_n . In the case where only a single term of the series is used, the espression for the conservation of energy (16) is sufficient to obtain a result.

The energy expression can be obtained from the differential equation by a series of mathematical manipulations. Thus potential energy can be thought of as a process by which all the equations of statics of the member are satisfied on a weighted average. Later, only part of the energy expression will be used, and it will be shown that this is equivalent to obtaining a weighted solution of certain of the equations of statics. If the true solution of the mathematical model is substituted into the energy expression, the results obtained are the same as those obtained from the differential equation.

For the series describing the approximate shape to converge rapidly the functions should be orthogonal, and a reasonable approximation to the true eigen functions. In general the value of the load parameter obtained is an upper bound on the exact solution of the mathematical model. As the differential equation is self adjoint, the series can be expressed as a series of the eigenfunction ϕ_i then the load parameter

$$\lambda = \frac{F_1(\phi_1) + F_1(\phi_2) + F_1(\phi_3) + \ldots}{F_2(\phi_1) + F_2(\phi_2) + F_2(\phi_3) + \ldots}$$

which is greater than $F_1(\phi_1)/F_2(\phi_2)$ since

$$\int \phi_i^2 dx > 0 \, ,$$

which is the definition for positive definite. The ratio of $F_1(\phi)$ to $F_2(\phi_1)$ is the lowest critical load.

* * * *

Stability of Systems governed by Differential Equations

Ariaratnam[1] showed, using an energy analysis, that for the buckling of a column, certain types of trusses, and torsional-flexural buckling an infinite number of modes were obtained and these were all mutually orthogonal. Hence any shape could be expressed as a unique, infinite sum of the buckling modes. He also showed the validity of the Southwell plot for each of the cases considered.

Kjar[2] has generalized these concepts. He states that if a differential equation

$$L(x) - \lambda N(x) = 0$$

is self adjoint and positive definite with respect to the given boundary conditions then this is a sufficiency condition for the equation to have an infinite number of eigen functions ϕ_n which are mutually orthogonal, and a corresponding number of eigen values $_n$. Positive definite is defined to be

$$\int_a^b \phi_r \, N(\phi_r) > 0 \quad \text{and} \quad \int_a^b \phi_r \, L(\phi_r) > 0 \tag{18}$$

and self adjoint as

$$\int_a^b \phi_r \, N(\phi_s) - \phi_s \, N(\phi_r) = 0$$

and (19)

$$\int_a^b \phi_r \, L(\phi_s) - \phi_s \, L(\phi_r) = 0 \,,$$

where ϕ_r and ϕ_s are any two solutions to the differential equation, which satisfy the boundary conditions, and a and b are the two limits within which the differential equation applies. The condition has been extended to apply when the equation is self adjoint and positive definite with respect to a certain weighting function.

* * * *

Ref. 1 S. T. Arairatnam "The Southwell Method of Predicting Critical Loads of Elastic Structures". Quart. J. Mechs and Appl. Maths, 14, 1961.

Ref. 2 A. R. Kjar, Doctor of Philosophy Thesis, University of Tasmania.

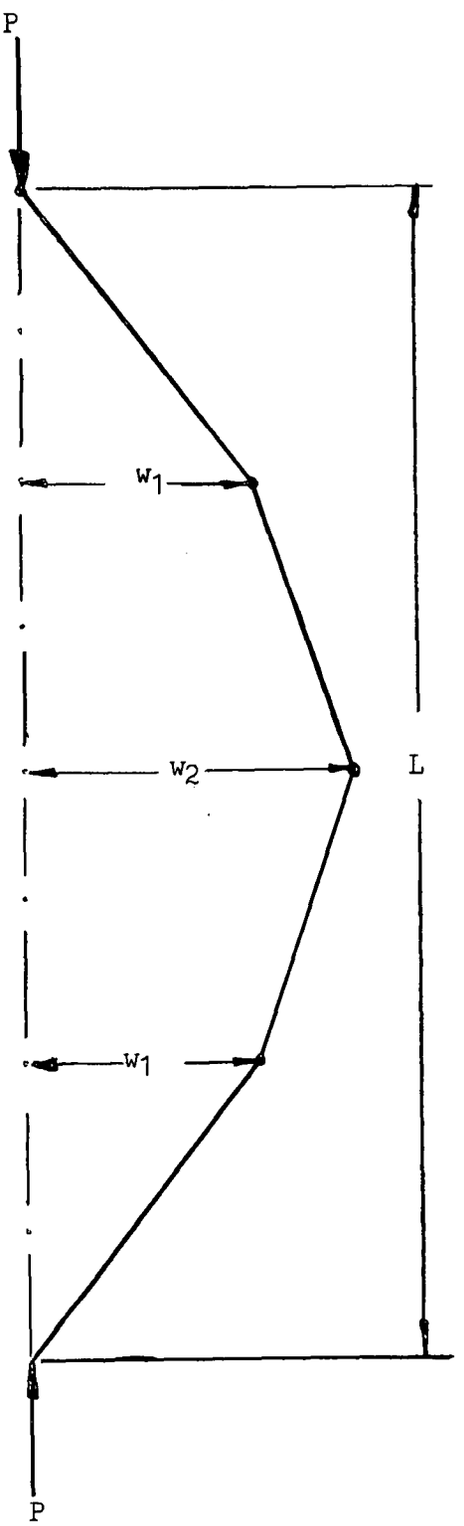

Moment at hinge
$M = EI(w_{i+1} - 2w_i + w_{i-1})/L$

Length of link $L/4$

FOUR LINK COLUMN USED FOR A FINITE DIFFERENCE ANALYSIS

FIGURE 14

Stability of System governed by Simultaneous Linear Equations

The last section described some conditions for the stability of a differential equation. In the following section the stability of a set of homogeneous linear equations is considered. Most of the ideas involved have been introduced in the section on energy. Other ideas will be established by means of the following two examples.

Finite Difference Methods

The problem of a column can be solved by a finite difference method. One finite difference method treats the column as a series of rigid rods hinged so that the moment applied at the hinges is related to the deformations. The relationship can be a straight finite difference moment-curvature relationship,

$$M = EIK = EI\,(w_{i+1} - 2w_i + w_{i-1})/dx^2 , \qquad (20)$$

or it can be weighted to take into account that the rods in a column are not rigid. Using the moment-deformation relationship (20) the equations of statics for a four bar chain, in terms of symbols defined in fig. 14, become

$$16EI\,(w_2 - 2w_1)/L^2 = -Pw_1$$

and (21)

$$16EI\,(2w_1 - 2w_2)/L^2 = -Pw_2 .$$

The eigen values of the system can be obtained from the characteristic equation, which is the condition that the determinant is zero. The eigen values are

$$P_1 = \frac{16EI}{L^2}\,(2 - \sqrt{2}) \quad \text{and} \quad P_2 = \frac{16EI}{L^2}\,(2 + \sqrt{2})/L^2 \qquad (22)$$

and the eigen functions are

$$\frac{w_{11}}{w_{12}} = \frac{1}{\sqrt{2}} \quad \text{and} \quad \frac{w_{21}}{w_{22}} = -\frac{1}{\sqrt{2}} , \qquad (23)$$

which are linearly independent since

$$w_{11}/w_{21} \neq w_{12}/w_{22} .$$

Hence any shape can be expressed as a sum of the two ratios

$$w_1 = Aw_{11} + Bw_{21} \quad \text{and} \quad w_2 = Aw_{12} + Bw_{22} .$$

A sufficiency condition for the matrix to have real, positive eigen values

is that the matrix be positive definite and symmetric. The load-deflection graph is the same as for a column, except, now, there are only two bifurcations. It should be noted that if the column is split into an infinite number of links there are an infinite number of modes and loads, and the system of equations is equivalent to the differential equation.

A System of n Degrees of Freedom

A structure or member, with n degrees of freedom can be described by n differential equations. When a set of solutions is substituted into the differential equations, n simultaneous homogeneous linear equations are obtained. The condition for the solution to be non-trivial,(that the determinant is zero) leads to n relationships, or ratios, between the n degrees of freedom, which are linearly independent of each other. However, there is an infinite number of modes, as for each ratio there exists an infinite number of modes.

* * * *

This chapter has presented a review of the buckling phenomena as it is applicable to the author's work. Mainly it emphasizes the basic points which have been employed, both as mathematical and experimental techniques. The following references have been used in the compiling of this chapter and they give a more detailed discussion on the various topics.

References

S. P. Timoshenko: History of Strength of Materials, McGraw-Hill Book Co. Inc.

H. Straub: A History of Civil Engineering, The M.I.T. Press.

S. P. Timoshenko & J. M. Gere: Theory of Elastic Stability, McGraw-Hill Book Co. Inc.

M. S. Gregory: Elastic Instability - Analysis of Buckling Modes and Load of Framed Structure, Spon Ltd. London.

W. G. Godden: Numerical Analysis of Beam and Column Structures, Prentice-Hall Inc., Englewood Cliffs, N.J.

D. N. de G. Allen: Relaxation Methods," McGraw-Hill.

S. P. Timoshenko & S. Woinowsky-Krieger: Theory of Plates and Shells, McGraw-Hill Book Co. Inc.

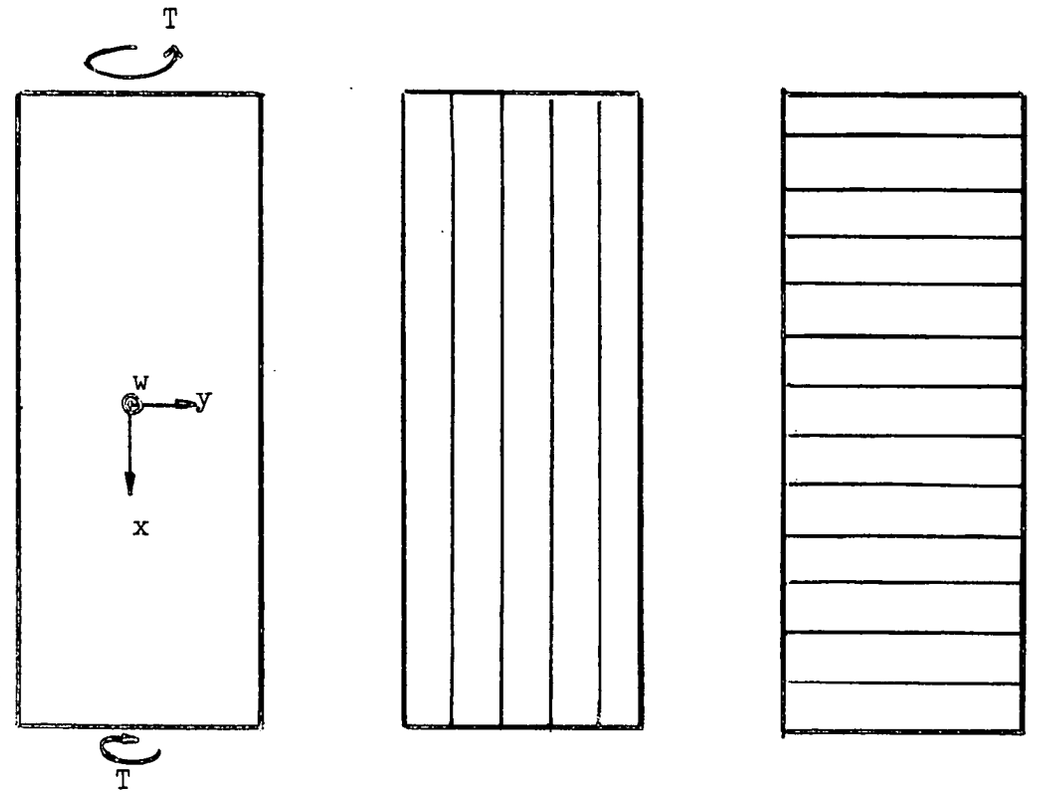

LIGTENBERG FRINGES OF A TWISTED PLATE,
AN ANTICLASTIC SURFACE

FIGURE 15

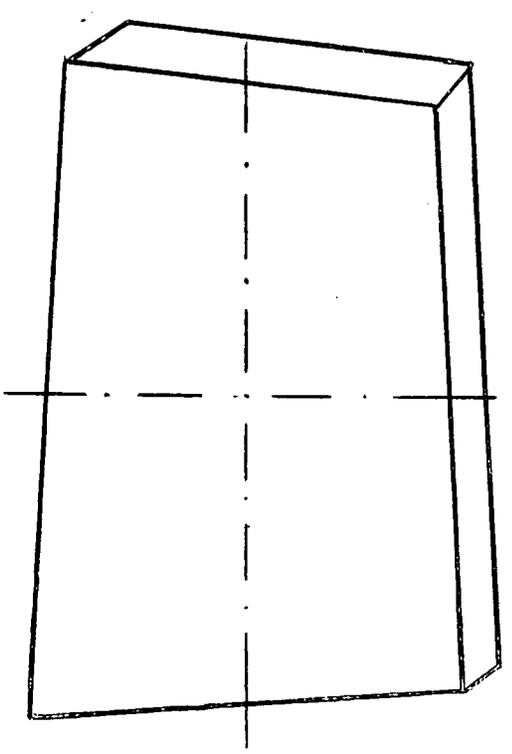

TWISTED SURFACE

FIGURE 16

TORSION

The torsional properties of thin open-section members, with a special emphasis on a flat strip and angle section members, will be investigated in this section. The aspects which are relevant for angle section members have been examined experimentally. The results are applicable for elastic materials only, although both large and small deflections have been considered.

* * * *

If a flat, rectangular plate is twisted, then the surface is defined by the Ligtenberg, moire fringe patterns in fig. 15. The surface, known as an anticlastic surface, has the property that in two perpendicular directions the curvature is zero. If a co-ordinate system is set up such that the x-y axes lie in these directions, then the deflections w normal to the plane of the undeflected surface may be described analytically by the function

$$w = Cxy$$

where C is a constant.

From this geometrical model, the relationship,

$$\text{Torque } T = Gbt^3 \left(\partial^2 w / \partial x \partial y \right)/3 , \qquad (23)$$

may be derived, where G is the shear modulus, b the width of plate, t the thickness and $\partial^2 w / \partial x \partial y$ is the twist. The torque-twist relationship was first obtained by St. Vennant. The model applies for small twists only, for large twists the surface becomes a helix. All the surfaces of the strip, including the edges, deform into anticlastic surfaces, thus the opposite ends of the plate are no longer parallel but slope towards each other as in fig. 16.

When an open-section member made of flat plates is twisted, each plate element deforms to an anticlastic surface. Hence St. Vennant's formula may be extended to apply to these sections, by replacing the width b by the perimeter m , that is the sum of the widths of the constituent plates. However, the relationship only applies when the ends of the members are free to warp. The product $mt^3/3$, or the torsional stiffness, is denoted by J , and GJ is known as the torsional rigidity.

The twist of a plate has been defined as $\partial^2 w / \partial y \partial x$. In the

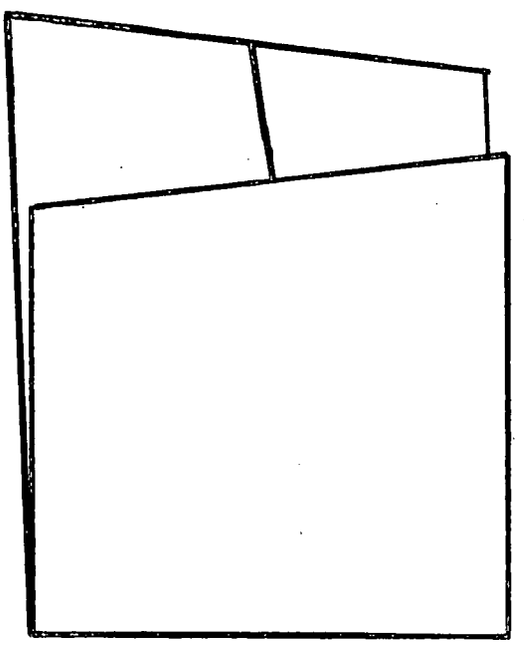

WARPING OF A TWISTED I-MEMBER

FIGURE 17

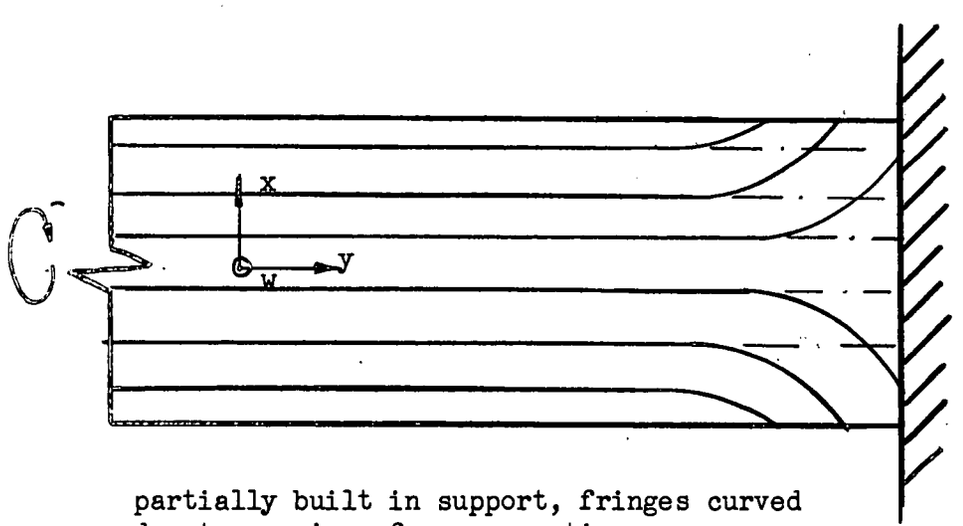

partially built in support, fringes curved due to warping of cross section.

LIGTENBERG FRINGES OF A TWISTED CANTILEVER STRIP

FIGURE 18

case of a member where the cross-section rotates, in an undeformed state, then the twist is independent of the y ordinate. If ϕ is the rotation of the cross-section relative to some point, usually the shear centre, then the twist is $\partial\phi/\partial x$, where x is the abscissa measured along the member. It is important to realize that both the torque and the rotation must be considered relative to the same point.

For some composite sections the cross-section does not remain plane, because the ends of each plate are no longer parallel. As an example consider the cross-section of an I-beam which is shown in fig. 17. The cross-section is said to have warped. When the member is restrained in some way to force plane sections to remain plane, or is twisted with varying twist, then longitudinal stresses and shear stresses are developed in the member. These stresses modify the torque-twist relationship to

$$T = GJ\,\partial\phi/\partial x + C_w\,\partial^3\phi/\partial x^3, \qquad (24)$$

where C_w is a warping constant. Reference may be made to one of the references at the conclusion of this section for the derivation of the relationship.

The following work is concerned with equal leg, angle-section members; for these members the shear stresses do not effect the torque, hence the parameter C_w is zero. However, it should be pointed out that secondary warping does occur, as the cross-section of each leg of the angle warps and deforms into an anticlastic surface. The effect of the secondary warping can be noticed when a flat strip, which is built in at one end, is twisted. Near the built-in end, the cross-section is partially restrained against warping and the twist decreases. One could consider a fully built-in cantilever as one in which the end did not warp, and hence the twist is zero. From the Ligtenberg fringes in fig. 18 it can be seen that this is a very local effect.

Bleich derived an expression for the torque of an equal leg, angle-section member involving the secondary warping of each leg using an energy approach. He gives

$$T = GJ\,\partial\phi/\partial x + (2bt)^3\,\partial^3\phi/\partial x^3/144 .$$

In this thesis, the author derives the same expression by considering

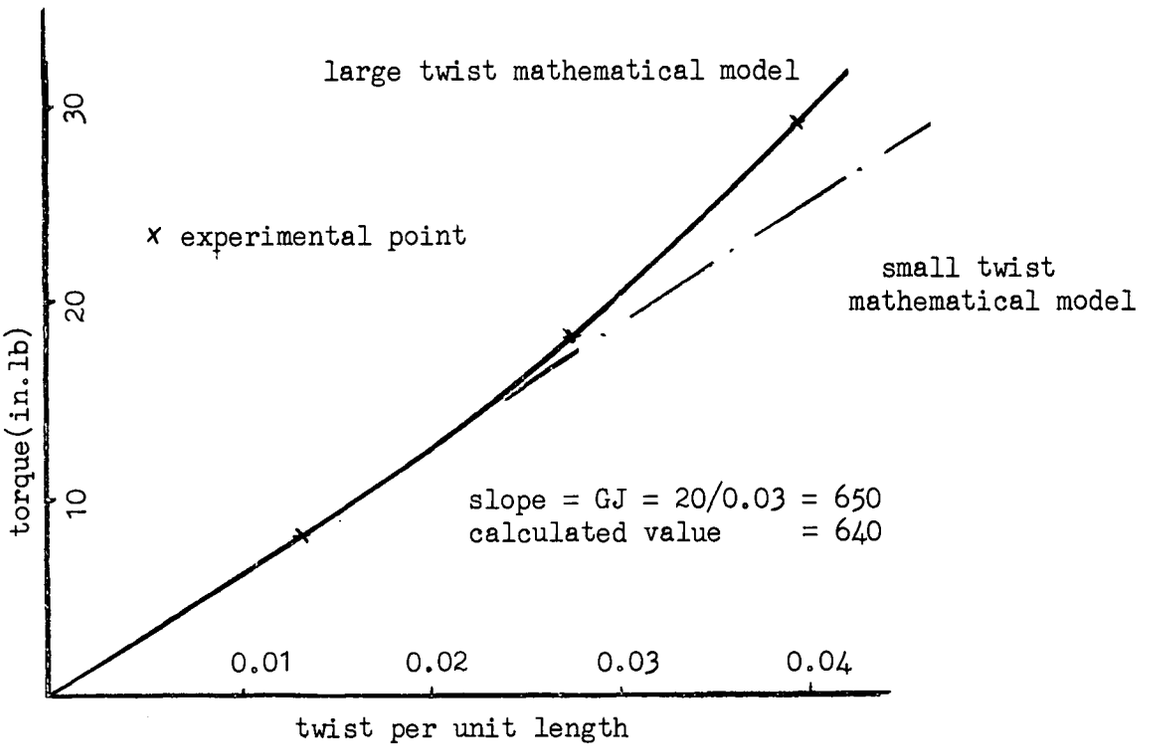

TORQUE TWIST CURVE OF A 2" x 2" x 0.05"
ANGLE-SECTION MEMBER

FIGURE 19

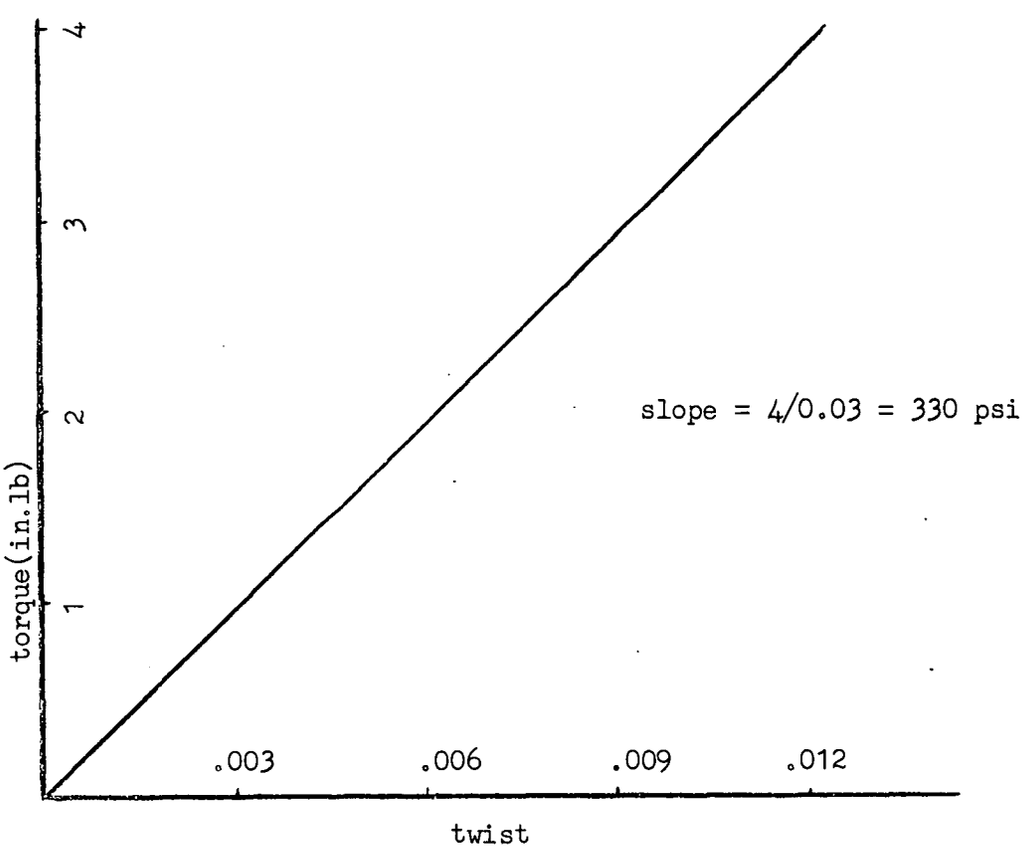

TORQUE TWIST CURVE OF A 2" x 0.05"
RECTANGULAR SECTION

FIGURE 20

the bending stiffness of the legs of the angle. For any section with primary warping the secondary warping may be neglected.

The torque twist relationships both for a flat plate and for an angle member are shown in figs 19,20 and the elastic constants of proportionality are evaluated.

For large twists, the torque-twist relationship of an angle-section member deviates from a straight line, although the material is still elastic. This phenomena has been investigated by Cullimore[1] and Gregory[2] and it was found to be due to the development of longitudinal strains arising from the deformations out of the plane of the model. During twist, straight lines across the leg of the angle remain straight. Therefore the first component of the strain, the derivative of the displacement in the direction of the axis of the member with respect to the ordinate in this direction, is linear across the leg.

Consider an angle section member which is deforming such that ϕ is the rotation of the cross-section about the shear centre. Let r be a radial ordinate measured from the shear centre. Then the strain ϵ due to twisting is

$$\epsilon = r^2(\partial\phi/\partial x)^2/2 ,$$

and, as straight lines remain straight, the total strain is

$$\epsilon = A + Br + r^2(\partial\phi/\partial x)^2/2 .$$

By considering the equilibrium of axial forces and moments, the values of A and B can be determined. The expression for the strain is

$$\epsilon = (\partial\phi/\partial x)^2(r^2/2 + b^2/12 - br/2) , \qquad (25)$$

where b is the leg width of the angle. Geometrically, the strains mean that the member not only twists, but also bends. Notice that there is a line which remains straight; it is not the line of shear centres. Gregory[3] has shown that the derived results are independent of the point chosen as the origin of the coordinate system.

The longitudinal strain of an angle-section cantilever

Ref. 1 M. S. G. Cullimore & A. G. Pugsley "Torsion of A1 Alloy Structural Members", Aluminium Research Development Association Report No. 9.

Ref. 2 3 M. S. Gregory, Australian Journal of Applied Science, Vol 11, Nos. 1 & 2, 1960, Vol. 12, No. 2, 1961.

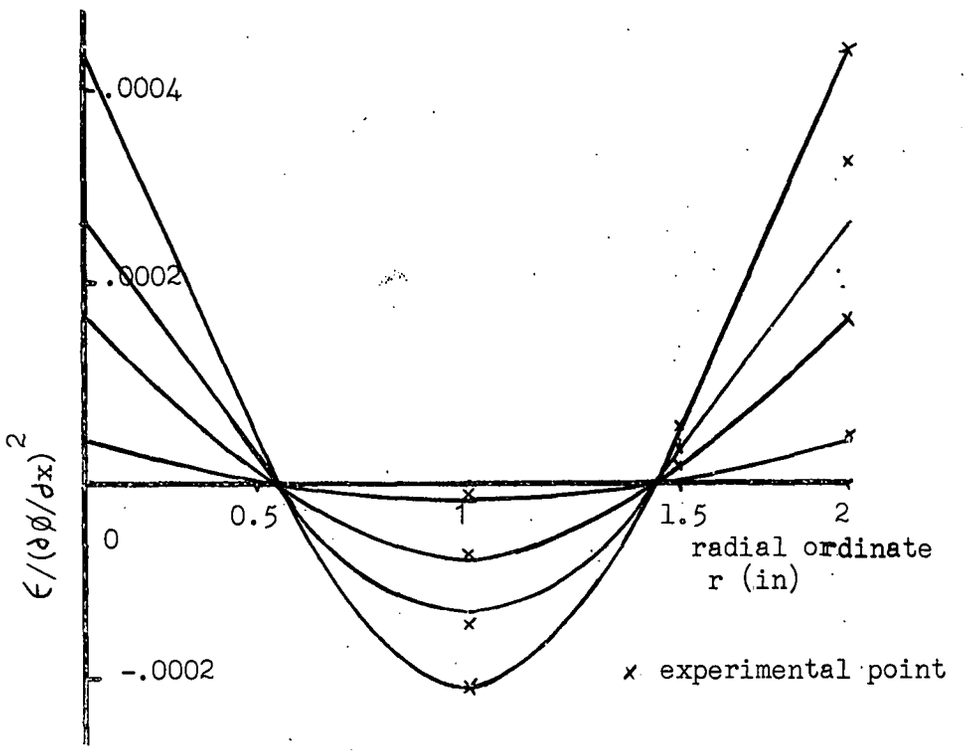

STRAINS IN A TWISTED ANGLE SECTION MEMBER
b = 2", t = 0.05", L = 11.5"

FIGURE 21

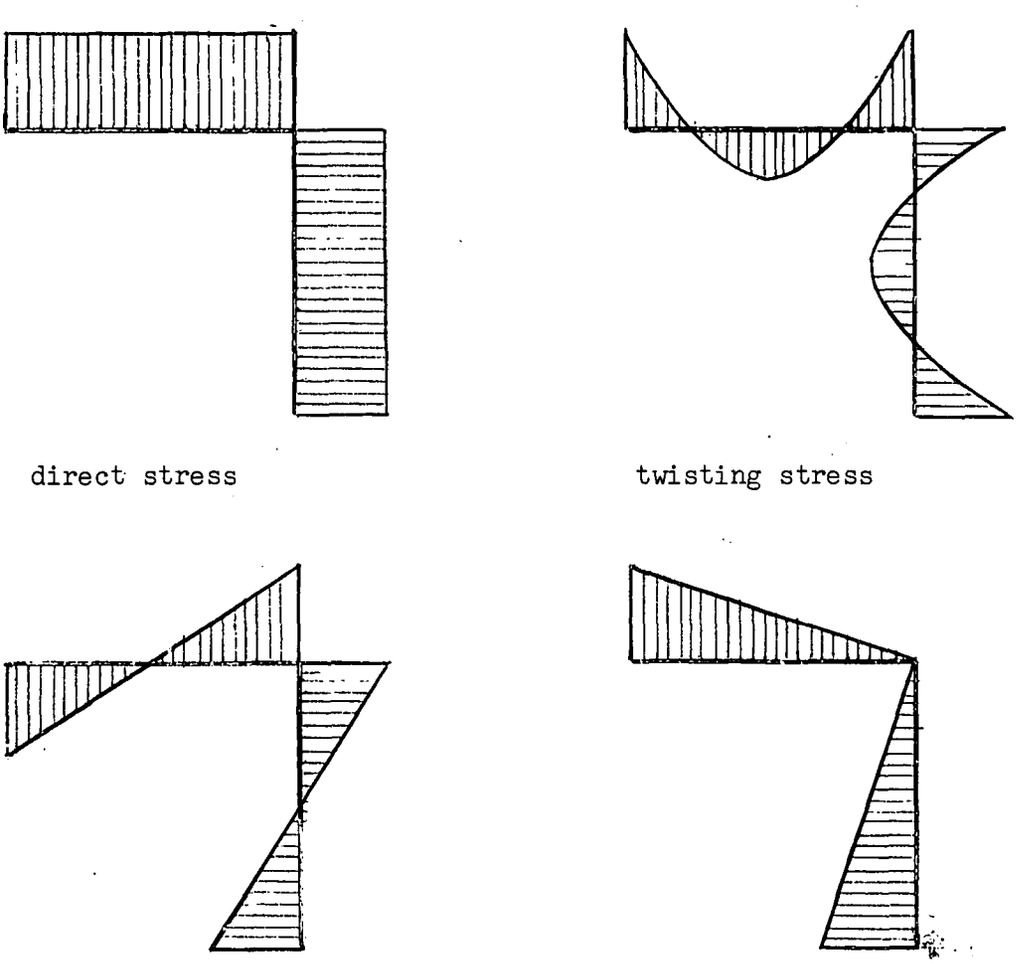

FIGURE 22

experiencing a twist were measured with Huggenberger strain gauges. The results obtained are given in fig. 21, where they are compared with the results estimated by the previous mathematics. In this experiment a "built-in" cantilever was used, but the strains were measured where the twist was constant. The region was found using the Ligtenberg apparatus.

For a section in which warping is important the torque twist relationship for a small twist is

$$T = GJ\partial\phi/\partial x + C_1 \partial^3\phi\partial x^3 .$$

When large deflections are considered, two more terms must be considered. The first is derived in the same manner as for an angle, $C_2(\partial\phi/\partial x)^2$. The second term is due to the shear forces which act along the section N_{xy}, and is related to the derivative of the longitudinal forces $\partial N_x/\partial x$. The form of this term is $C_3\partial\phi/\partial x\,(\partial^2\phi/\partial x^2)$. The total torque becomes

$$T = GJ\partial\phi/\partial x + C_1\,\partial^3\phi/\partial x^3 + C_2(\partial\phi/\partial x)^3 + C_3\partial\phi/\partial x\,(\partial^2\phi/\partial x^2) . \quad (26)$$

For an elastic material, four local strain readings were used to determine the loads applied to a member under test experiencing an axial load, a torque and two bending moments. The twist and bending deflections were checked using Ligtenberg's apparatus. The four strain distributions are shown in fig. 22.

This section has aimed at being a concise review of elastic torsion. It has introduced the terminology and derived the relationships used by the author. The effect of warping has been included, because, in the conclusions of the thesis, the methods available for generalizing the approach developed in this thesis, will be suggested. The section has also indicated, by means of geometry, the important features, which the author has included in the following sections on torsional buckling.

References

S. P. Timoshenko: "Theory of Elastic Stability" McGraw-Hill Book Co., Inc., New York.

H. Wagner: "Torsional Buckling of Open Sections" Technical Memorandum No. 807, U.S. National Advisory Committee of Aeronautics 1936.

H. Wagner and W. Pretscher: "Torsion and Buckling of Open Sections" Technical Memorandum No. 784, U.S. National Advisory Committee of Aeronautics 1936.

Weber: "Die Lehre der Drehungsfestigkeit" Forschungs beiten auf dem Geibiete des Ingenieurswesens, Heft 249.

V. Z. Vlasov: "Thin Walled Elastic Beams".

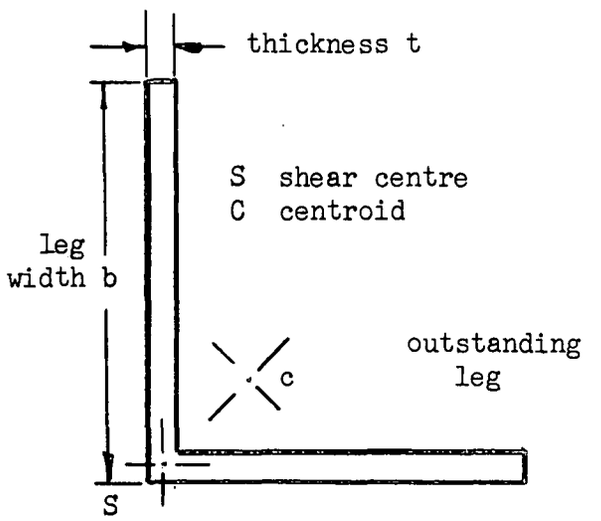

dimensions

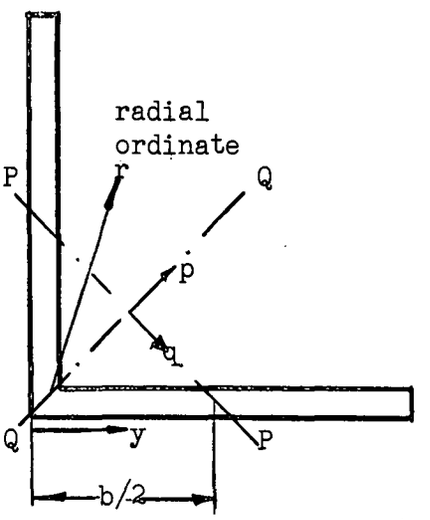

co-ordinates

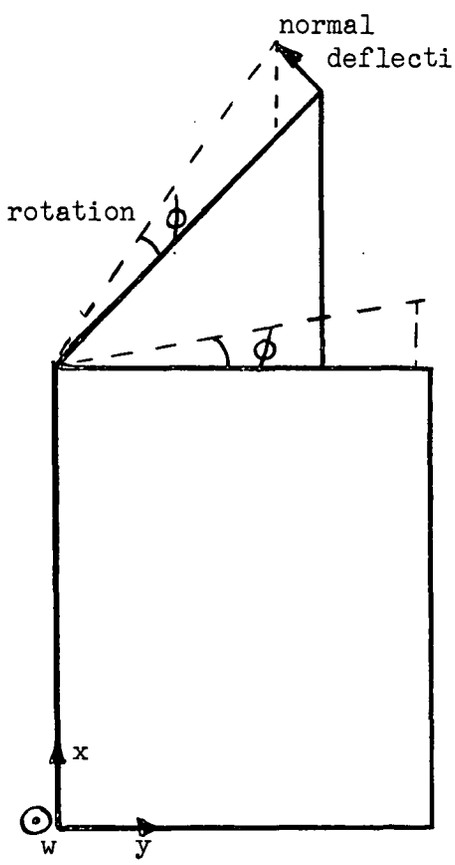

deformations

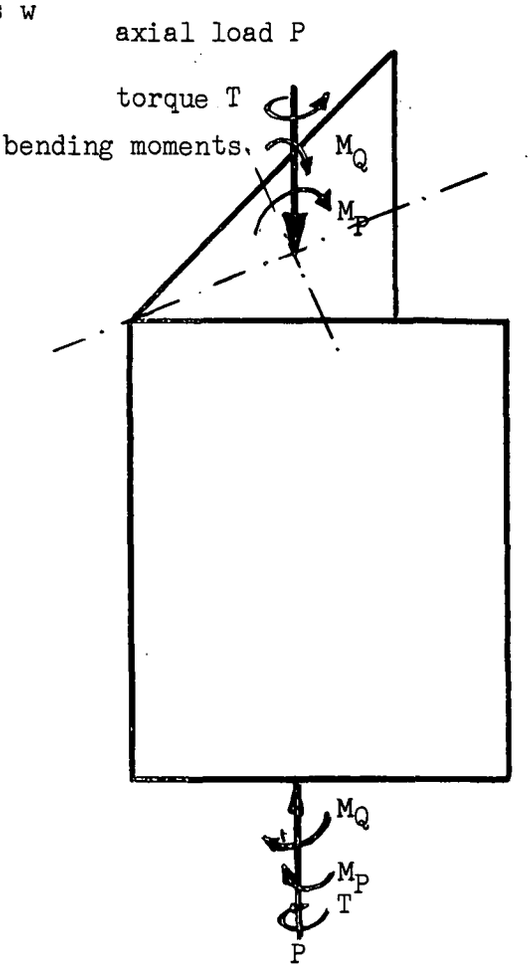

applied forces

NOTATION ASSOCIATED WITH AN ANGLE- SECTION COLUMN.

FIGURE 23.

COLUMNS

Three mathematical models will be developed in this chapter to describe the behaviour of columns. These models will describe the local buckling of the column under a uniform axial load and a linearly distributed end moment, provided the cross-section does not distort. The second part of the chapter deals with eccentric loads which cause the cross-section to distort. The treatment given results from work on angle-section columns, loaded through one leg by a single bolt connection. The effect of the longitudinal stress distribution, produced by loading the column through a bolt, has also been estimated using a "partial energy" approach.

LOAD APPLIED THROUGH A BASE PLATE

The first loading to be considered is an axial load, uniformly distributed across the cross-section. Simply supported end conditions are assumed, that is the rotation, the torque, and the moment, are zero at each end of the member.

The notation associated with the problem is p, q are the co-ordinates about principal axes of the cross-section. The x, y and r coordinates are associated with one leg of the angle. The ordinate y is measured across the leg from the root of the angle, the abscissa x is measured along the line of shear centres of the member from one end of the member, and the r ordinate is a radial ordinate measured from the shear centre. The displacements in the x and y directions are u and v respectively, and the displacements normal to the x-y plane are w. The properties of the angle are leg width b thickness t, and length L. The notation is defined also in figure 23.

Experimental Work

The experimental models used to measure the deformations were made of perspex; the dimensions were: leg width 4", length 8" and thickness 1/8". These members were loaded through their centroids using a system of ball bearing supports as shown in fig. 24. The deflections w normal to the leg were measured using the Ligtenberg Moire method. The fringes obtained are shown in fig. 25.

In the experimental work, the ideal pin-ended conditions were

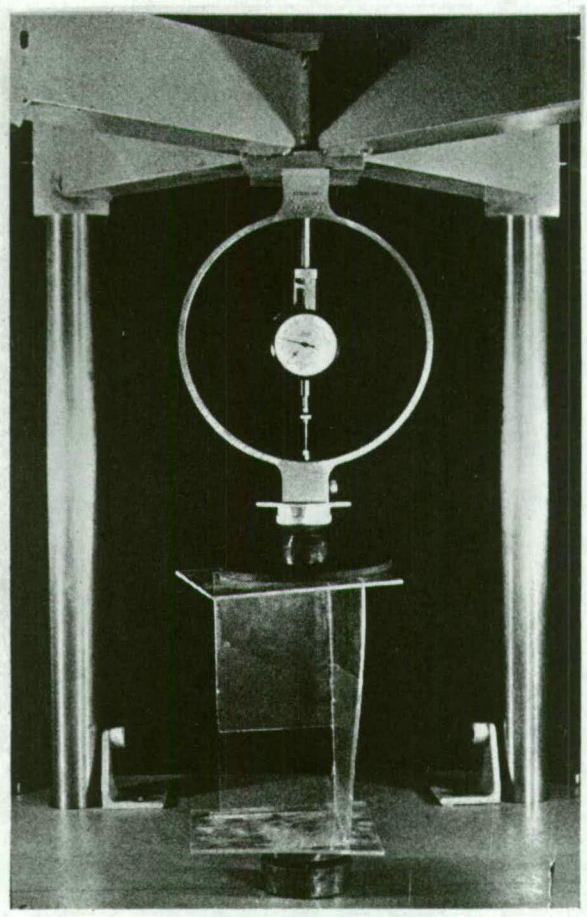

An angle-section column deforming under a uniformly distributed axial load. Note an approximate analytic function describing the shape is

$$w = at \cos \pi x/L \ .$$

FIG. 24

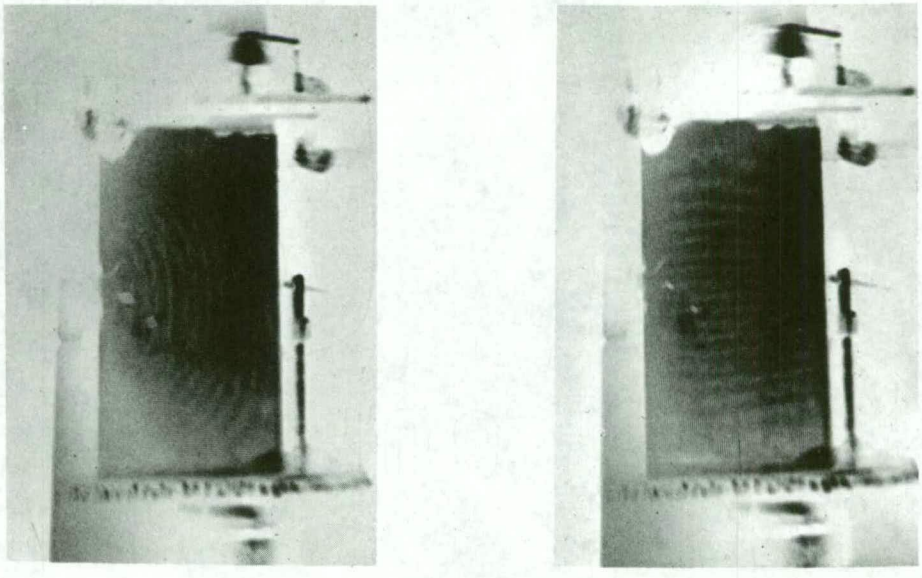

(a) (b)

Ligtenberg fringes for one leg of an angle-section column deforming into the shape shown in Fig. 24. The root of tha angle is on the right (a) dw/dx (b) dw/dy. The quality of the fringes is the same as obtained forall experimental work.

FIG. 25

not attained at the end of the column. Consequently only the section of the member with pin-ended boundary conditions was considered. The length of this section was measured directly from the $\partial w/\partial x$ fringes, see fig. 26. But the "effective length" l can be measured in this manner only if the shape of the member is symmetrical about the centre line. If this is not so then the end condition that the deflection at each end is zero is not satisfied. Another approach would be to calculate the geometrical boundary conditions from the measured deformations and to use the load-deformation relationships to derive the forces applied to the member. The calculated geometrical and statical boundary conditions are then fed into the mathematical model. The second approach will not be used in this chapter.

For the short members tested, the approximate shape the member deformed into was

$$w = ay \cos \pi x/L ,$$

which has the boundary conditions of zero twist at each end, and not zero moment and zero rotation as for a simply supported column. However, by similar calculations to those that follow, it can be readily shown that a column with these boundary conditions has the same load capacity as a simply supported column. Thus the experimental results will be compared with the mathematical model which is to be developed.

The crossed-diffraction grating method was used to measure the displacements u and v in the x and y directions in the plane of the leg of the angle. The moire fringes represent lines of constant displacement u or v.

Basic Form of the Deformation

From the $\partial w/\partial x$ fringes (fig. 25) it is seen that the line of shear centres remained straight, that is, for a short member, the deflections produced by the bending of the member were small compared with those produced by the twisting. The $\partial w/\partial y$ fringes (fig. 25) indicate that the section rotated as a whole and without distortion, and hence w can be expressed as

$$w = y\phi(x) , \qquad (27)$$

where $\phi(x)$ is a function of x only, and is the angle through which

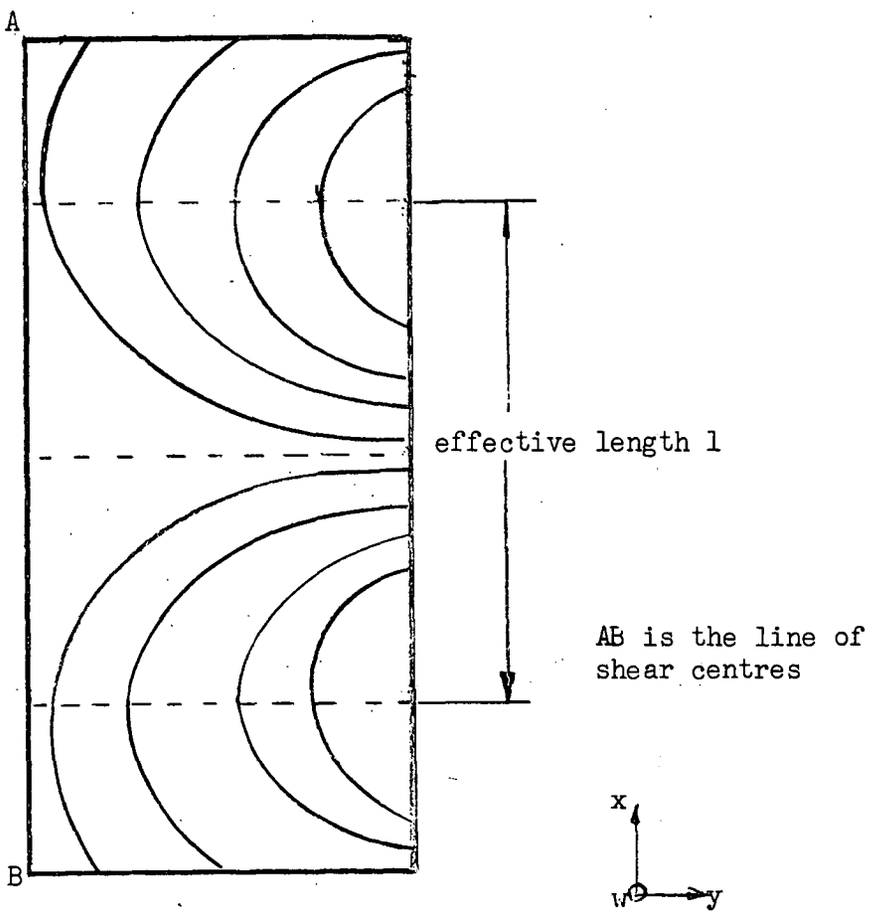

LIGTENBERG $\partial w/\partial y$ FRINGES FOR ONE LEG OF AN ANGLE -SECTION COLUMN

FIGURE 26

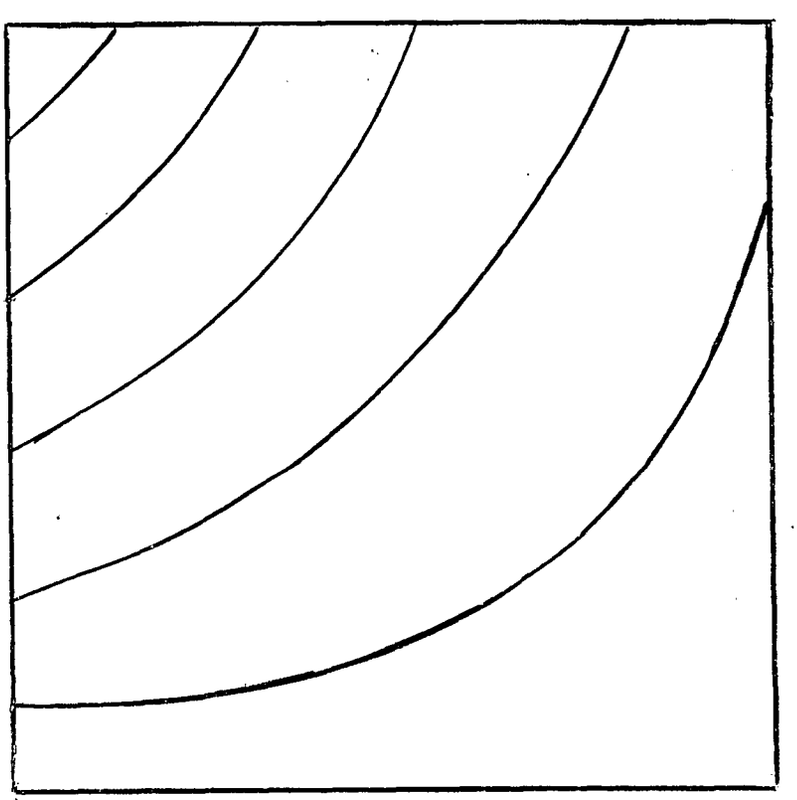

CROSS DIFFRACTION GRATING FRINGES, LINES OF CONSTANT DISPLACEMENT (u, v)

FIGURE 27.

the section has rotated. The movement of the centroid of any section with x constant, under these conditions was $b/(2\sqrt{2})\phi(x)$. From the fringes for u and v it was found that horizontal lines, that is lines with x a constant, remained straight during deformation and $\partial u/\partial x$ was much greater than $\partial v/\partial y$. In algebraic terms u and v were linear in y and x respectively.

First Mathematical Model

In the first mathematical model, all the internal stresses will be assumed to be small compared with the twisting moment per unit length, which is given by the expression

$$m_{xy} = D(1 - \nu)\ \partial^2 w/\partial x \partial y ,$$

where D is the flexural rigidity and ν is Poisson's ratio. The applied longitudinal forces per unit length N_x are assumed to be constant and invariant with the deformations,

$$N_x = P/A ,$$

where P is the total axial load and A is the cross-sectional area. The longitudinal forces have a component in the direction of the w deflections, which is equivalent to a shear force per unit length Q_x acting across the leg of the angle

$$Q_x = N_x \partial w/\partial x = P/A\ \partial w/\partial x .$$

The equation of torque equilibrium on a plane with x constant is

$$\int_A Q_x r\, dA + \int_A M_{xy} dA = 0,$$

or in terms of the deflection w

$$\int (P/A) \partial w/\partial x\ r\ dA + \int D(1 - \nu)\ \partial^2 w/\partial x \partial y\ dA , \qquad (28)$$

which simplifies to the differential equation

$$GJ\ \partial\phi/\partial x - (PI_p/A)\ \partial\phi/\partial x = 0 \qquad (29)$$

when the functional form of equation 27 is used. The torsional stiffness J equals $2bt^3/3$, the polar moment of inertia about the shear centre I_p equals $2b^3t/3$ and G is the elastic shear modulus. The strut remains in the undeformed state for all loads except the load

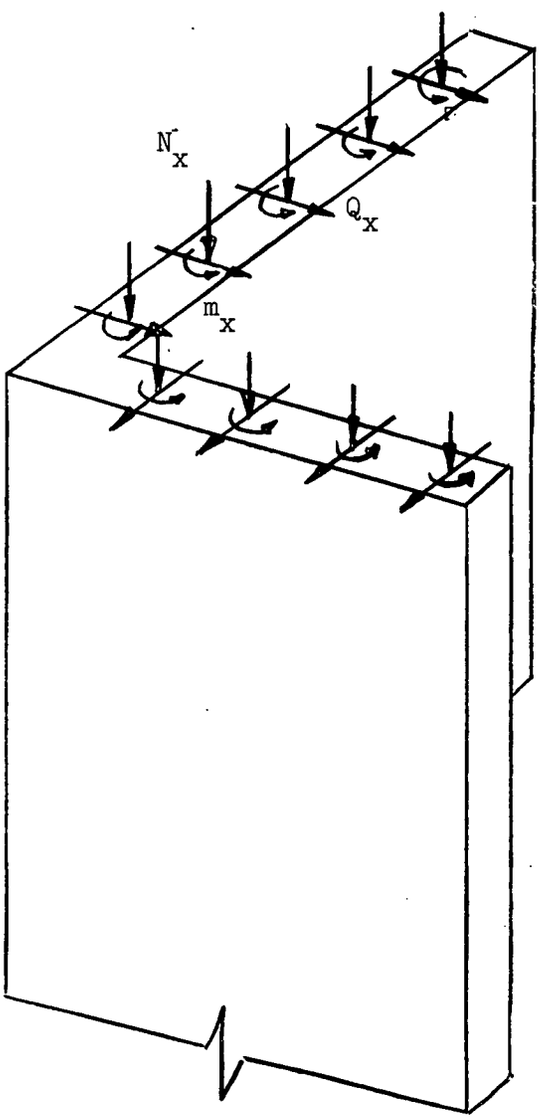

FORCES ON AN ANGLE CROSS -SECTION

FIGURE 28

$$p_{crit} = GJA/I_p \,, \tag{30}$$

at which load the deformations are indeterminate.

Second Mathematical Model

The experimental work has determined the deformations and not the shape of the member. In setting up the equations of statical equilibrium the shape is important. The initial shape is taken to be $u = w = v = 0$. The mathematical model has as its basis the displacements or deformations u, v and w; where u is linear in y, v is linear in x and $w = y\phi(x)$. If the problem is limited to one of small deflections the change in curvatures K_x and K_y of the leg, consistent with the specified deflections are

$$K_x = \partial^2 w/\partial x^2 \,,$$

$$K_y = \partial^2 w/\partial y^2$$

and the change in twist, or torsion, is

$$K_{xy} = \partial^2 w/\partial x \partial y = \partial \phi/\partial x \,. \tag{31}$$

From the expressions for u and v, the first approximations of the longitudinal strains are

$$\epsilon_x = \partial u/\partial x = (py + r)h(x)$$

and (32)

$$\epsilon_y = \partial v/\partial y = (Sx + t)j(y) \,,$$

where p, r, s, t are parameters and h and j are functions.

Internal Stresses

The problem is further restricted in that the load-deformation relationship is taken to be linear, that is the material is elastic. When this is so the moments per unit length m_x, m_y and m_{xy} required to maintain the deformations expressed in equation (31) are:

$$m_x = -Dy\,\partial^2\phi/\partial x^2$$

and $$m_y = -D\,y\,\partial^2\phi/\partial x^2 \tag{33}$$

$$m_{xy} = (1 - \nu)D\,\partial\phi/\partial x \,,$$

where the flexural rigidity D denotes $Et^3/12(1 - \nu)^2$. Using the expressions (32) for the longitudinal strains the longitudinal forces per unit length acting on the central plane of the leg becomes

$$N_x = Et(cy + d)q(x) \text{ .} \qquad (34)$$

In order to determine the other internal stresses the statical equilibrium of an element of the leg must be studied. When an element of the leg, thickness t, and defined by the planes x, $x + dx$, y, $y + dy$ is considered, the following equations are obtained (see fig. 29).

Force equilibrium in w-direction:

$$\partial Q_x/\partial y + \partial Q_y/\partial x = 0 ,$$

moment equilibrium in w-x plane:

$$Q_x = \partial m_x/\partial x - \partial m_{xy}/\partial y - N_x \partial w/\partial x - N_{xy} \partial w/\partial y \qquad (35)$$

and moment equilibrium in w-y plane:

$$Q_y = \partial m_y/\partial y - \partial m_{xy}/\partial x - N_y \partial w/\partial y + N_{xy} \partial w/\partial x \text{ .}$$

The equilibrium equations (35) in conjunction with the load deformation relationships (33) give an expression for the shearing force per unit length,

$$Q_x = - Dy \partial^3\phi/\partial x^3 - N_xy \partial\phi/\partial x - N_{xy}\phi \text{ .} \qquad (36)$$

Applied Forces

As the axial force is applied through the centroid of the section of the member, the only applied end force is an axial force P and hence the resultant forces on a section D-D (see fig. 23) with x constant are:

Axial force	P ,	
moment about minor axis	$M_P = \phi Pb/2\sqrt{2}$,	(37)
moment about major axis	$M_Q = 0$,	
and torque about x-axis	$T = 0$.	

The forces on any section must be balanced by the stress resultants on that section. These are obtained by integrating the internal stresses. When three of these forces, the axial thrust and two moments, are considered the following three equations are obtained

$$M_P = \oint_A N_x \, q dA = \phi \, Pb/2\sqrt{2}$$

$$M_Q = \oint_A N_x \, p dA = 0 \qquad (38)$$

and $$P = \oint_A N_x \, dA \, ,$$

where $\oint_A dA$ denotes the integral over the whole section. From equations (38) the values of the parameters, c and d in the functions describing the longitudinal forces per unit length in both legs are determined.

$$N_{x1} = tP/A + 3P\phi y/4b^2$$

and $$N_{x2} = tP/A - 3P\phi y/4b^2 \qquad (39)$$

The fourth force, the torque, is balanced by the moment of the internal stresses about the shear centre. The moment of the internal stresses is independent of the point about which it is taken. The shear centre was chosen so that the shear forces N_{xy} need not be evaluated. The torque balance gives

$$\oint_A M_{xy} \, dA - \oint_A Q_x \, y dA - \oint_A N_{xy} \, y \partial w/\partial y \, dA = 0 \qquad (40)$$

When the expressions for m_{xy}, Q_x, and N_x obtained in equations (33), (36), (39) are substituted into the equation (40) the differential equation is obtained as

$$GJ \partial\phi/\partial x - D \partial^3\phi/\partial x \, I_p/t - P \partial\phi/\partial x \, I_p/A = 0 \, ,$$

in which G is the shear modulus, J the torsional rigidity $= 2bt^3/3$ and I_p is the polar moment of inertia $= 2b^3t/3$. After rearrangement the equation becomes

$$\partial^3\phi/\partial x^3 + (P/2Db - GJt/DI_p) \partial\phi/\partial x = 0 \, . \qquad (41)$$

A solution of the mathematical model is

$$w = a_n \sin n\pi x/L \, ,$$

where n is an integer, as it satisfies both the differential equation (41) and the boundary conditions: $M_P = M_Q = T = 0$ and $w = 0$ at $x = 0$ and $x = L$. But there are two conditions on the solution: either $a_n = 0$ or

$$-(n\pi/L)^3 + (P_n t/AD - tGJ/DI_p)\pi/L = 0 \qquad (42)$$

Hence equation (41) has an infinite number of eigenvalues of P, given by (42), corresponding to an infinite number of eigen functions

$$w_n = a_n y \sin n\pi x/L , \quad n = 1(1)\infty .$$

Energy

When a differential cannot be solved explicitly an approximate solution can often be found using a weighted integral of the differential equation. The expression for the weighted integral can be obtained from the differential equation. In this case the differential equation is multiplied by $\partial^2\phi/\partial x^2$ and integrated twice with respect to the x variable to give

$$\int_0^L DI_p/2t\,(\partial^2\phi/\partial x^2)^2 + \int_0^L GJ/2\,(\partial\phi/\partial x)^2 + \int_0^L N_x\,(\partial\phi/\partial x)^2 = 0 \qquad (43)$$

which is identical to the energy expression

$$u = \int_0^L\int_0^b \tfrac{1}{2}D\,(\partial^2 w/\partial x^2 + \partial^2 w/\partial y^2)^2 - 2(1-\nu)(\partial^2 w/\partial x^2\,\partial^2 w/\partial y^2 - (\partial^2 w/\partial x\partial y)^2)\,dy\,dx + \tfrac{1}{2}\int_0^L\int_0^b N_x\,(\partial w/\partial x)^2\,dy\,dx , \qquad (44)$$

when the functional form and the loading conditions are applied and the expression is integrated with respect to y. Thus the minimization of the energy expression is equivalent to the least squares method of averaging the differential equation.

Initial Shape

No physical member is initially straight, and as the mathematical model is non-linear, it is expected that the behaviour of the member depends upon the initial shape. When the initial shape is $w = w_0$ the differential equation must be modified as the moments per unit length depend upon the change in curvatures and the change in twist:

$$\partial^2(w - w_0)/\partial y^2 , \quad \partial^2(w - w_0)/\partial x^2 \quad \text{and} \quad \partial^2(w - w_0)/\partial x\partial y$$

respectively. When these corrections are included, equation (41) becomes

$$\partial^3(\phi - \phi_0)/\partial x^3 + Pt/DA\,\partial\phi/\partial x - GJt/I_p\,(\partial\phi/\partial x - \partial\phi_0/\partial x) = 0 . \qquad (45)$$

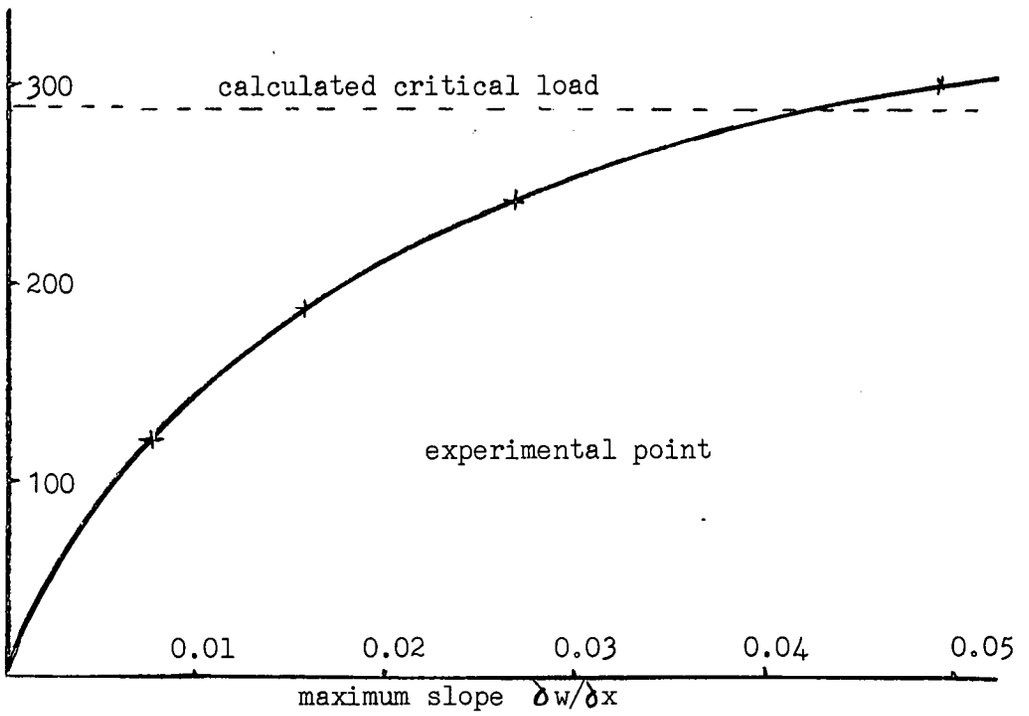

LOAD-DEFORMATION FOR AN 8" x 4" x 4" x 1/8" ANGLE-SECTION MEMBER

FIGURE 30

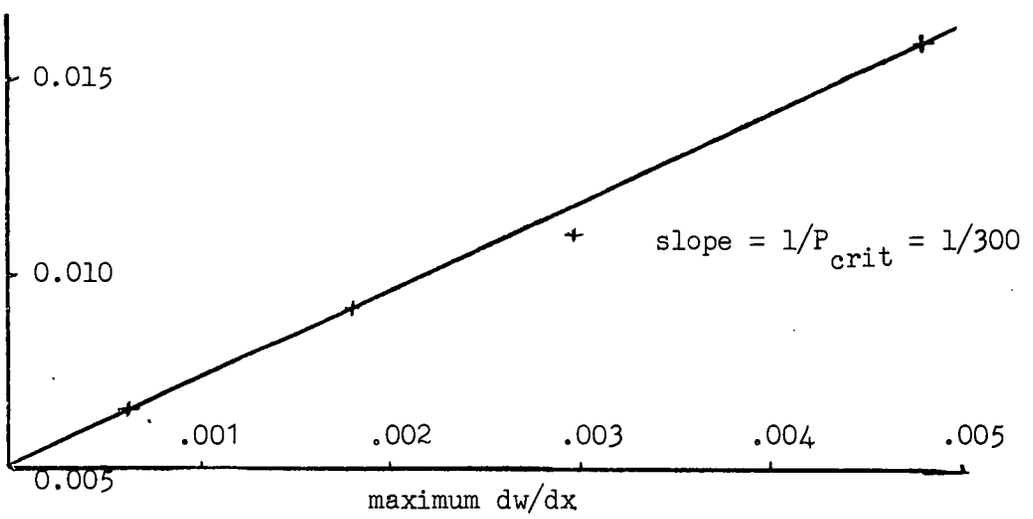

SOUTHWELL PLOT FOR THE ABOVE MEMBER

FIGURE 31

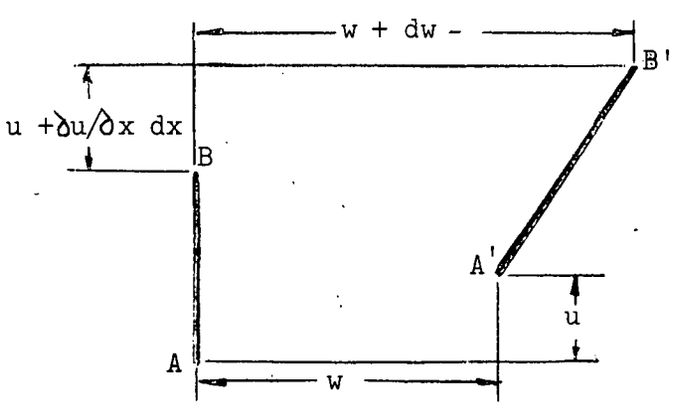

AB original state
A'B' deform state

Strain = $\partial u/\partial x + \frac{1}{2}(\partial w/\partial x)^2$

FIGURE 32

The initial shape can be expressed as an infinite series of the eigen function of the differential equation (41),

$$\phi_0 = \sum_{n=1}^{\infty} a_{0n} \sin n\pi x/L \ .$$

This is possible as the eigen functions are orthogonal. The solution of the differential equation is then

$$\phi = \sum_{n=1}^{\infty} a_n \sin n\pi x/L$$

with the coefficients a_n given by

$$a_n = a_{0n} (1 - P/P_n) \ , \quad n = 0(1) \ \infty \ . \tag{46}$$

In the neighbourhood of P_1 , the first term of the series predominates and the shape is approximately $\phi = a_1 (1 - P/P_1) \sin \pi x/L$. P_1 is the lowest eigen value, which is called the critical load and is calculated using

$$P_1 = 2(Db\pi^2/L^2 + GJbt/I_p)$$

This mathematical model buckles in the Eulerian manner like a simple column. If the member is initially straight it can be in either one of two states, zero deflection or indeterminate deflection. The second state occurs only for well defined loads P_n . When initial shape is included, the load deflection relationship of the mathematical model approaches the lowest critical load asymptotically (fig. 30). Equation (46) justifies the use of the Southwell plot, that is plotting $(w - w_0)/P$ against $w - w_0$. The slope of the graph is the inverse of the first eigen value or critical load. The Southwell plot was used to evaluate the critical loads of the experimental members (see fig. 31).

Third Mathematical Model

In the first model the longitudinal strains on the centre plane of the leg were taken as $\epsilon_x = \partial u/\partial x$. In the model to be studied next, the shortening due to bending is also to be considered. The approximate expression for curvature is still to be employed as the twists measured experimentally are not large enough to justify the use of more complex expression. From fig. 32 it can be seen that the bending deflections w modify the longitudinal strain to give

$$\epsilon_x = \partial u/\partial x + \tfrac{1}{2}(\partial w/\partial x)^2 . \qquad (47)$$

Following the steps of the previous section, using the load-deformation relationship and the equations of statical equilibrium on the section with x a constant, gives the longitudinal stresses as

$$N_{x1} = Pt/A - (Pb\phi/2\sqrt{2} - (b^2P/\sqrt{2}\,\partial\phi/\partial x)y - (\partial\phi/\partial x)^2(y^2/2 + b^2/12 - by/2)) \qquad (48)$$

and

$$N_{x2} = P/A + b^3t/2(Pb\phi/2\sqrt{2} - (b^2P/\sqrt{2}\,\partial\phi/\partial x)y - (\partial\phi/\partial x)^2 x \times (y^2/2 + b^2/12 - by/2)) .$$

When these values of the stresses are substituted into the torque equilibrium equation the differential equation is

$$GJ\,\partial\phi/\partial x - D\,\partial^3\phi/\partial x^3 I_p/t + 2\int_0^b (\partial\phi/\partial x)^3(y^2/2 + b^2/12 - by/2)^2\, y\, dy - PI_p/A\,\partial\phi/\partial x = 0 ,$$

which on rearrangement gives

$$\partial^3\phi/\partial x^3 + (P/2Db - GJt/DI_p)\,\partial\phi/\partial x - Eb^5t^2(\partial\phi/\partial x)^3/180DI_p = 0 . \qquad (49)$$

When $\partial\phi/\partial x$ is replaced by ϕ', $P/2Db - GJt/DI_p$ by Ω^2 and $b^5t/180DI_p$ by β equation (49) simplifies to

$$\partial^2\phi'/\partial x^2 + \Omega^2\phi' - \beta\phi'^3 = 0 , \qquad (50)$$

or after integrating once

$$dx = d\phi'/(c - \phi'^2(\Omega^2 - 2\beta\phi'^3/3)^{\frac{1}{2}} ,$$

where c is a constant of integration (see Appendix B). This can be expressed in the form of an elliptic integral

$$dx = B'd\theta/(1 - k^2\sin^2\theta)^{\frac{1}{2}} ,$$

where B', θ and k are defined appropriately.

As discussed previously the approximate shape of the physical members was not

$$w = ay \sin \pi x/L \quad \text{but} \quad w = ay \cos \pi x/L .$$

For this section of the work, the members are considered to have the same end conditions as the physical members. This is thought advisable as geometrical results of the third mathematical model are compared with

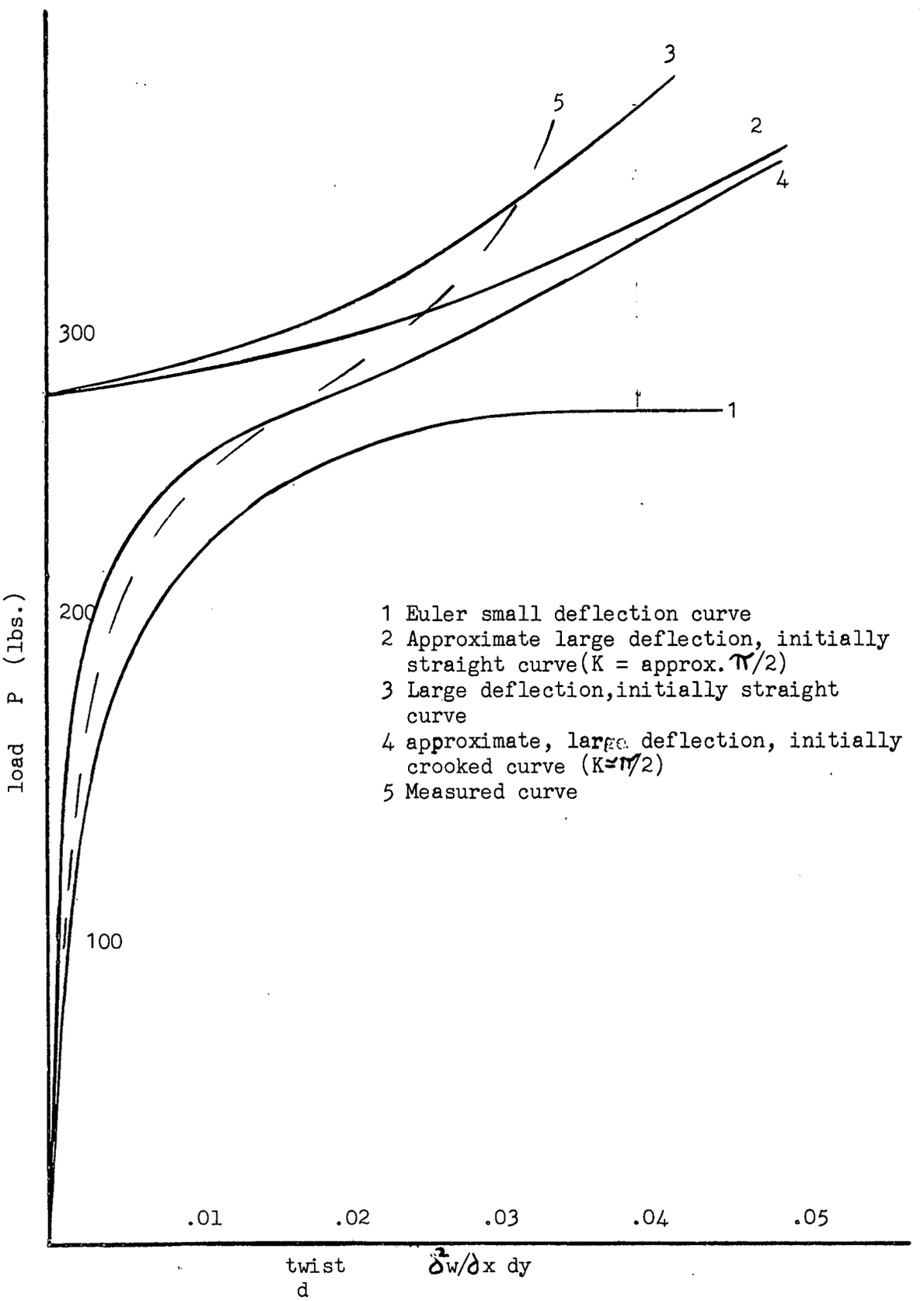

LOAD - DEFORMATION CURVE FOR A COLUMN

FIGURE 33

the geometrical results of the physical model.

The functions $\phi' = B \sin 2Kx/L$ satisfies the boundary conditions and when substituted into the differential equation (50) gives

$$B(2K/L)^2(2k^2 sn^3 2Kx/L - (1 + k^2) sn\ 2Kx/L) + \Omega^2 B sn\ 2Kx/L - \beta B^2 sn^3 2Kx/L = 0 ,$$

$4K$ is the period of the sn function and K is equal to the complete elliptic function,

$$K = \int_0^{\pi/2} (1 - k^2 \sin^2\varphi)^{-\frac{1}{2}} d\varphi$$

(see Appendix B for properties of sn z). By equating the coefficients of $sn(2Kx/L)$ and $sn^3(2Kx/L)$ two conditions are obtained:

$$2(2KkL)^2 - \beta B^2 = 0$$
$$\text{and} \qquad (1 + k^2)(2K/L)^2 = \Omega^2 . \qquad (51)$$

These two equations in conjunction with the k-K relationship is solved for a load-deformation relationship (P, B) ; the form of which is shown in fig. 33. For small deflections an approximate load-deformation relationship is obtained by combining equations (51) and using the fact that $K = \pi/2$ for small k. Hence

$$P/Db2 - GJt/I_pD - b^5tB^2/3b0DI_p - (\pi/L)^2 = 0 . \qquad (52)$$

For $P < 2(Db(\pi/L)^2 + GJtb/I_p)$ the deflection is zero, which is identical with the simpler model. However, the third model predicts a unique deflection for each load, which is in contrast to the second mathematical model which buckles in the sense that the deflections are indeterminate at the critical load. Thus it appears that Eulerian buckling is a property of the mathematical model and not the physical member. In this respect the second model bears the same relationship to the first model as the "elastica" does to Euler's column. The mathematical model of the elastica includes a more exact expression for the curvature of the column.

In order to calculate the magnitude of this effect we shall calculate deflection for a $4" \times 4" \times \frac{1"}{8}$ perspex angle member, 8" long, with $E = 480{,}000$ p.s.i. and $\nu = 0.3$. For $P = P_{crit} + 100$

$$B^2 = 120 \times 8 \times 100/(480{,}000 \times 64) = .00313$$

and hence

$$B = 0.56 \text{ rads/in.}$$

The maximum deflection can be estimated when it is assumed that the shape is

$$w = By\,(\sin \pi x/L + 1) \quad \text{and} \quad \partial\phi/\partial x = B\pi/L \cos \pi x/L \,.$$

The assumption is of the same order as that made in obtaining the approximate equation.

Then

$$w = 2 * 4 * 0.56 * 8/\pi$$

$$= 1.14 \text{ in.}$$

When $P - P_{crit} = 50$ the deflection w is 0.808 inches.

The two simultaneous equations (51) can be solved by trial and error to give the true load deflection relationship. For the same member

$$\beta = Eb^5t^2/180DI_p = 92.2$$

and

$$\Omega^2 = P/(2Db) - GJt(6(1 - \nu))/b^2I_pD$$

$$= 0.00144P - 0.262 \,.$$

Using the same deflection as above, $B^2 = 0.00316$, equation (51), $8(Kk/L)^2 = B^2/2$, gives

$$k^2 = 0.59 \quad \text{and} \quad K^2 = 3.74 \,.$$

With these values the second equation, $(1 + k^2)4K^2/L^2 = \Omega^2$, becomes

$$\Omega^2 = 0.372$$

or

$$0.00144P = 0.372 + 0.262 \,,$$

which reduces to

$$P = 440 \text{ lbs} \quad \text{or} \quad P - P_{crit} = 158 \text{ lbs.}$$

Other points on the true load deflection curve have been calculated by the same method. The true curve is plotted with the approximate curve on graph 33. As can be expected the two curves agree in the region of small deflections, the region in which the assumption holds.

The third mathematical model does not include the initial shape of the member. The importance of initial shape can be appreciated from the load deflection curve based upon the small deflection model. This curve is plotted on graph 33 for a $4'' \times 4'' \times 8'' \times \frac{1''}{8}$ perspex

model with an initial twist of 0.001 in. The differential equation (49) can be modified to allow for any initial shape. The shear strains, the plate bending strains, and the longitudinal strains due to twisting depend upon the change in shape. When the initial shape is

$$w_0 = B_0 y \phi_0$$

the modifications give

$$\partial^3(\phi - \phi_0)/\partial x^3 + P\partial\phi/\partial x/2Db - GJt/DI_p \partial(\phi - \phi_0)/\partial x -$$
$$- b^5 t\, \partial(\phi - \phi_0)/\partial x\, ^2 \partial\phi/\partial x/180DI_p = 0$$

or
$$\partial^2(\phi' - \phi'_0)/\partial x + \Omega'\phi' - \Omega''\phi' - \beta(\phi' - \phi'_0)^2\phi = 0 . \qquad (53)$$

The differential equation cannot be solved easily, if at all, and consequently an approximate solution is obtained. It can be expected that the shape of the member changes with the load, as it did for the initially straight member. To obtain an approximate solution it is assumed that the change in shape is not appreciable, and that the initial shape is of the same form as the deformations. Take

$$\partial w_0/\partial x = B_0 y \text{ sn } 2Kx/L \quad \text{and} \quad \partial w/\partial x = By \text{ sn } 2Kx/L .$$

As for the initially straight member, two equations are obtained when the values of $\partial\phi/\partial x$ and $\partial\phi_0/\partial x$ are substituted into the differential equation (53). These are

$$2k^2 (B - B_0)(2K/L)^2 - \beta(B - B_0)B = 0 \qquad (54)$$

and
$$-(B - B_0)(2K/L)^2(1 + k^2) + \Omega'B - \Omega''(B - B_0) = 0 .$$

The value of K is assumed to be $\pi/2$, which is in keeping with the earlier assumption that the shape does not change to any extent. Physically, these assumptions mean that the shape is approximately described by

$$\partial w/\partial x = By \sin \pi x/L .$$

Under these conditions, the above two equations (54) combine to give

$$\Omega'B/(B - B_0) = \Omega'' + (\pi/L)^2 + \beta B(B - B_0)/2 \qquad (55)$$

For a $4" \times 4" \times \frac{1"}{8} \times 8"$ perspex model with an initial deflection of $B_0 = 0.001$ rads./in. this becomes

$$0.00144B/(B - B_0) = 0.416 + 46.1B(B - B_0) .$$

The load deformation curve corresponding to the above equation is also plotted on graph 33. It can be seen that for small deflections the curve is asymptotic to the initial deflection curve for the Euler type model, and for large deflection it approaches the approximate large deflection curve. It appears reasonable to assume that the true curve will be asymptotic both to the curve for the Euler type model and to the true large deflection curve. The load-deflection curve, obtained experimentally, for a member with an initial maximum twist of 0.001 rads./in. is given on graph 33. The curve lies within the region expected, except for very large twists. Under these conditions the loading conditions have probably changed from those used in the mathematical model.

Eccentric Loading

In this section of the thesis the second mathematical model is expanded to cover the behaviour of an angle-section member under an eccentric load. It was shown previously that while the deflections due to bending of the line of shear centres are neglected, bending about the major principal axis has no effect on the differential equation, provided the section does not distort, a property of a symmetrical section. However, when the load is applied off the minor principal axis the differential equation is altered.

When the eccentricity e is sufficiently large, then the moment $P(w_s - P_e)$ about the minor axis can be approximated by $-Pe\phi$, where w_s is the deflection of the centroid of the section (see fig. 34). By considering the equilibrium of the elements on a section with x equals a constant the longitudinal stresses are found to be

$$N_{x1} = N_{x2} = P/2tb + b\sqrt{2}\,Pe(y - b/2)/b^3t ,$$

therefore

$$\oint N_x y \, \phi'/\partial x = \left[2\int_0^b y(P/2b + b\ 2\,Pe(y - b/2)/b^3t)\ \phi'/\partial x\, dy\right] - (Pb^2/3 - Peb/\ 2)\ \phi'/\partial x .$$

The equation for torque equilibrium on this section then becomes

$$I_p D/t\partial^3\phi/\partial x^3 + GJ\,\partial\phi/\partial x + (Pb^2/3 + Peb\sqrt{2})\,\partial\phi'/\partial x = 0 \qquad (56)$$

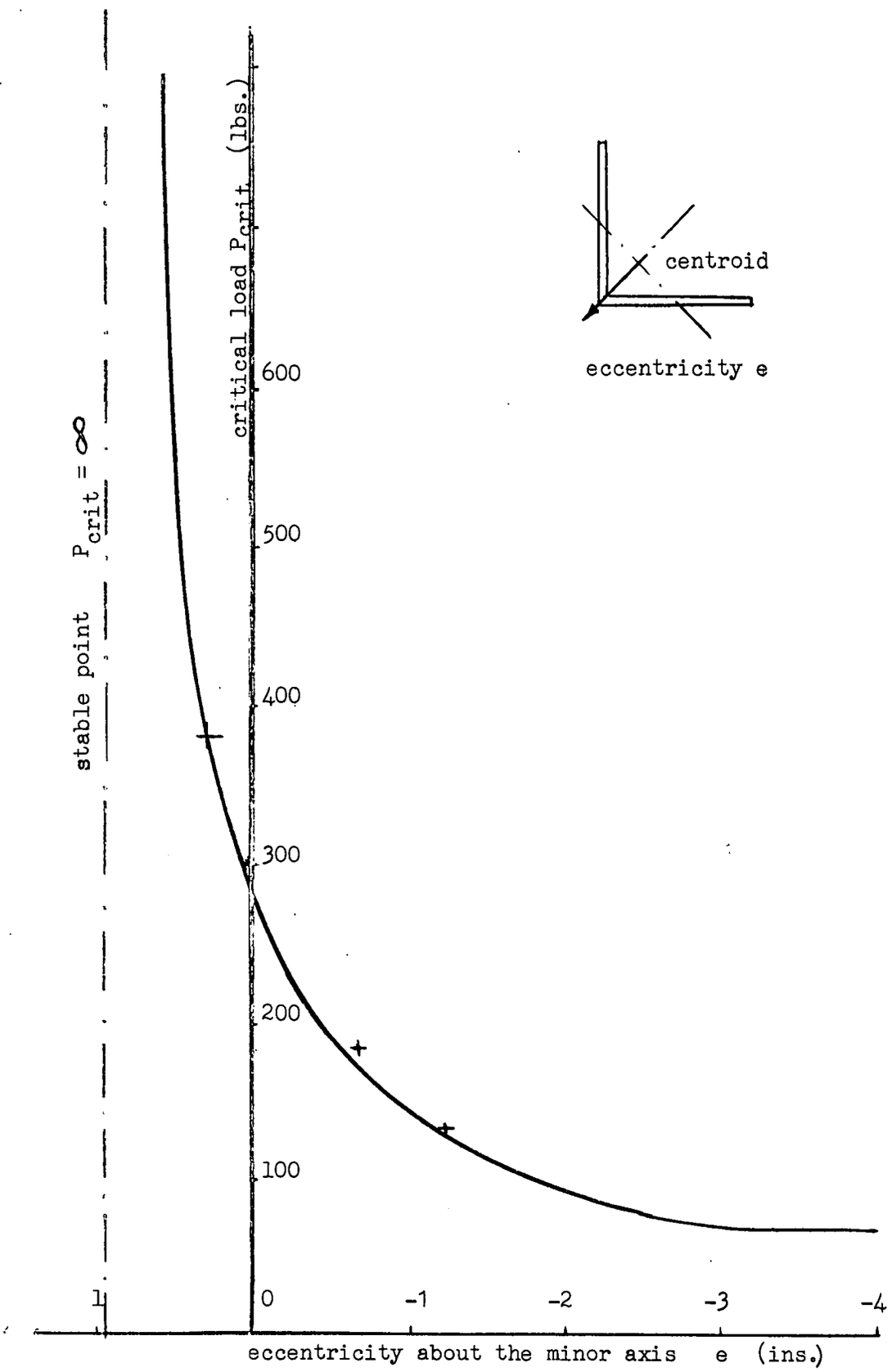

CRITICAL LOADS FOR AN ECCENTRICALLY LOADED 8" x 4" x 4" x 1/8" PERSPEX MODEL BASED ON THE THIRD MATHEMATICAL MODEL

FIGURE 34

and from this

$$w = ay \sin n\pi x/L$$

and

$$P_{crit} = P_1 = 2(Db(\pi/L)^2 + GJbt/I_p)b/(b + 3\sqrt{2}b) . \qquad (57)$$

See graph on fig. 34.

From fig. 34 it can be seen that there is a good agreement between the load capacity of the physical member and the mathematical model. When the eccentricity is $- b/3\sqrt{2}$ the critical load is infinite and the member is stable. If the eccentricity is less than $- b/3\sqrt{2}$ the mathematical model predicts that the member will buckle in tension but not in compression. At this stage a member has not buckled in tension as the member has failed by another mechanism. This thesis has only presented the torsional buckling of the whole member. For some of the models tested with large eccentricities local compressional buckling occurred under the loading position.

Applied Torque

When a torque T is applied at the end of the column the differential equation is modified to give

$$DI_p/t\, \partial^3\phi/\partial x^3 + (PI_p/A - GJ)\partial\phi/\partial x = T,$$

the solution of which is

$$\phi = a \sin(kx/L) + Tx/(DI_p/A - GJ) + C ,$$

where C is a constant. The boundary conditions are $\phi = 0$ at $x = 0$ and $x = L$. Thus

$$C = 0$$

and $$a = - TL \operatorname{cosec}(k)/(PI_p/A - GJ) .$$

The expression for the rotation is

$$\phi = T(x - L(\operatorname{cosec} k)(\sin kx/L))/(PI_p/A - GJ)$$

and the central rotation is

$$\phi_C = TL(1 - \sec k/2)/2k(PI_p/A - GJ) . \qquad (58)$$

As the load tends to the critical load the parameter k tends to one, as shown by equation (58); the central rotation approaches infinity.

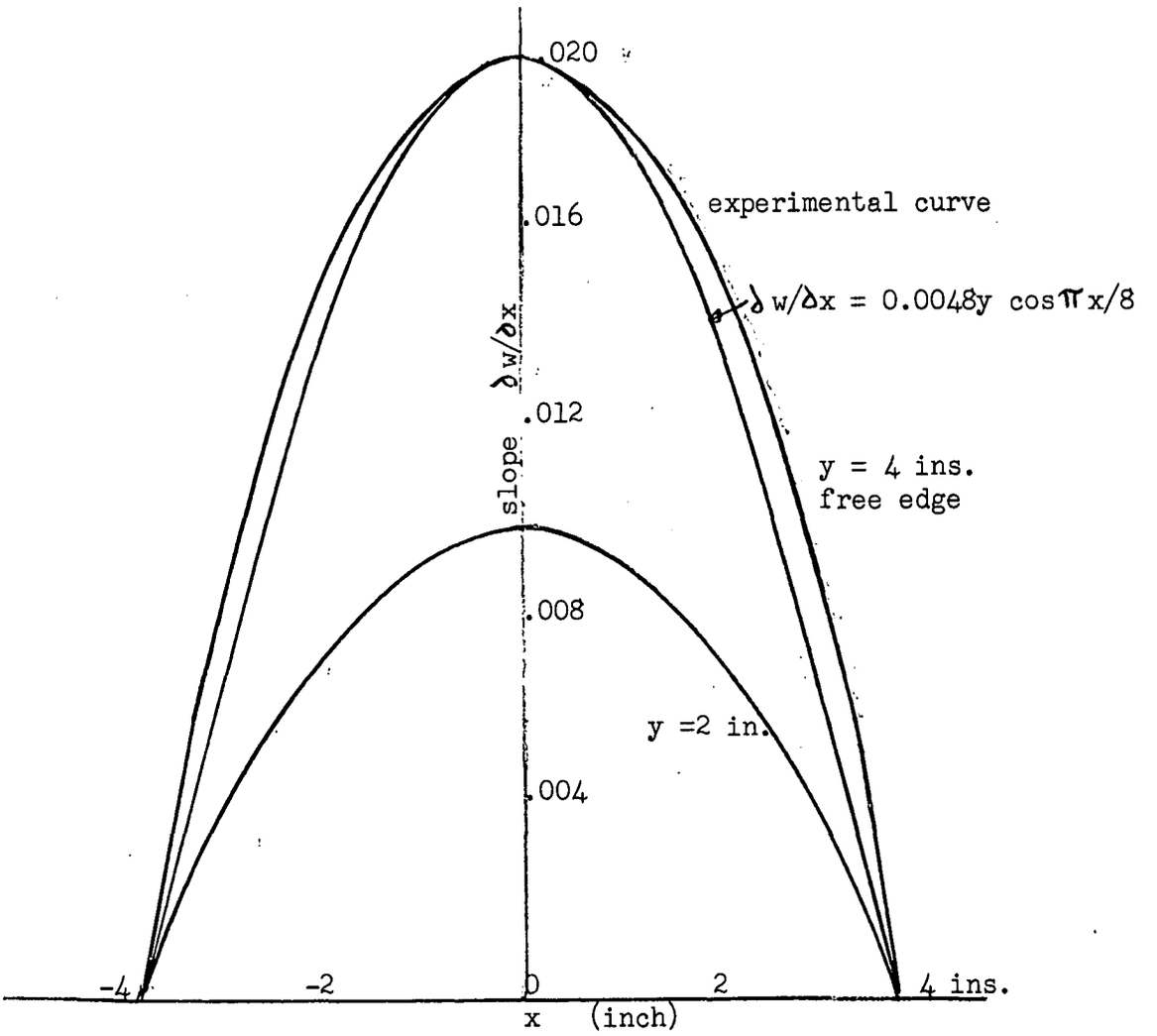

COMPARISON OF THE EXPERIMENTAL AND THE CALCULATED SHAPE OF A COLUMN WITH A UNIFORMLY DISTRIBUTED AXIAL LOAD

FIGURE 35

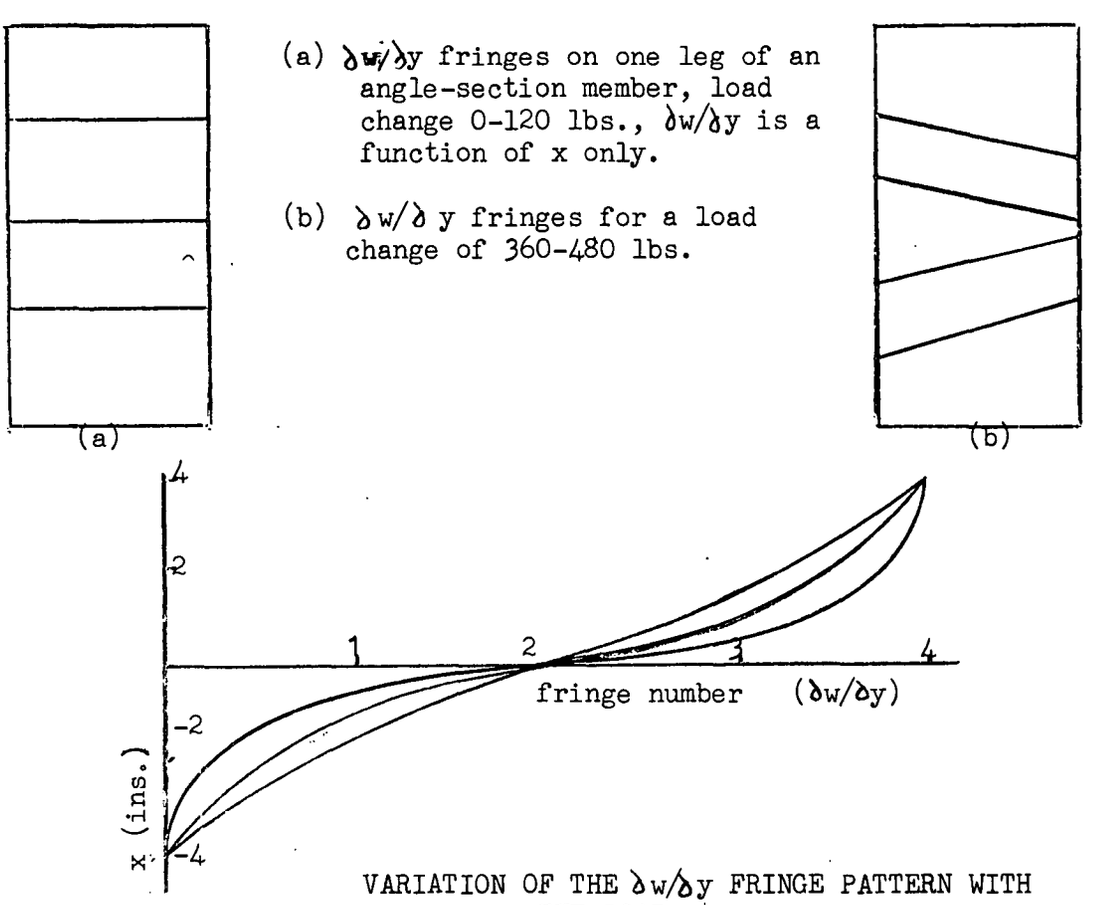

(a) ∂w/∂y fringes on one leg of an angle-section member, load change 0-120 lbs., ∂w/∂y is a function of x only.

(b) ∂w/∂y fringes for a load change of 360-480 lbs.

VARIATION OF THE ∂w/∂y FRINGE PATTERN WITH THE LOAD

FIGURE 36.

In the same manner that the relationship between the end slope of a column and the applied axial load and end moment is used in the analysis of buckling of frames, the relationship above could be used to modify the analysis of the buckling of frames out of their plane. The state of knowledge of the analysis of the instability of frames is given in Gregory's "Elastic instability - Analysis of Buckling Modes and Loads of Framed Structures" and his Doctor of Philosophy Thesis submitted at the University of Tasmania.

* * * *

It is suitable at this point to discuss the value of the mathematical models developed so far. First the shape of the deformed members is considered. In fig. 35 the measured values of the slope $\partial w/\partial x$ are compared with the analytic expression

$$w = ay \cos \pi x/L$$

Theconstant a has been chosen so that the maximum slope values agree. There is a slight difference in the shape and this can be accounted for if the analytic expression

$$\partial w/\partial x = ay \, sn \, 2Kx/L$$

is used.

For large deformations the functional form, used as a basis for all the mathematical models, was no longer valid, as the legs of the angle member began to bow. For large deflections the physical model deflected into the shape

$$w = a_1 y \cos \pi x/L + a_2 y^2 \cos 2\pi x/L$$

instead of

$$w = ay \cos \pi x/L \, .$$

Note that the physical models do not have simply supported boundary conditions. For the Ligtenberg fringes and a graph of the twist, see fig. 36. If a mathematical model were developed, based upon the new shape, the lowest critical buckling load would be the same, but some more, higher valued, buckling loads and modes would be introduced.

If there is a component of the shape of the form

$$w = a_1 y \cos \pi x/L + a_2 y^2 \cos \pi x/L$$

then the lowest or critical load would change and it would depend upon the ratio of a_1 to a_2. From the Ligtenberg fringe photographs this ratio is large and consequently the critical load derived from this shape is approximately equal to the critical load obtained from the second mathematical model.

Another approach to the problem is to consider each leg of the angle-section member as a plate, as Timoshenko did. Then the leg of the angle members bows. In fact, the shape of the member depends upon the size of the member. The critical load obtained by considering the leg as a buckled plate is very close to the value from the second mathematical model. The mathematical model developed by Timoshenko is discussed in fuller detail in the conclusions.

The calculated and measured values of the lowest critical load are quoted in the table below. All the members tested were made of perspex. The calculated values are obtained from the second mathematical model. For the members tested the first mathematical model predicts a lower critical load. From the form of the expression for the critical load, derived in the second mathematical model, it is sufficiently accurate to use the first mathematical model only for long members.

Member	Calculated Critical Load (lbs)	Measured (lbs.)
8" 4" 4" $\frac{1}{8}$"	280	300
4" 4" 4" $\frac{1}{16}$"	73	83
8" 3" 3" $\frac{1}{8}$"	435	440
30" 4" 4" $\frac{1}{8}$"	185	178

The maximum error is seventeen percent for the very short member. The errors for the remaining members are of the order of five percent. The critical loads for 8" x 4" x 4" x $\frac{1}{8}$" perspex angle-section member loaded eccentrically about the minor axis are shown in fig. 34. The differences between the calculated and measured values are of the order of five percent. This difference is considered satisfactory, when it is realized that in a practical application the "effective length" of the member must be guessed, thus introducing an error of a larger magnitude.

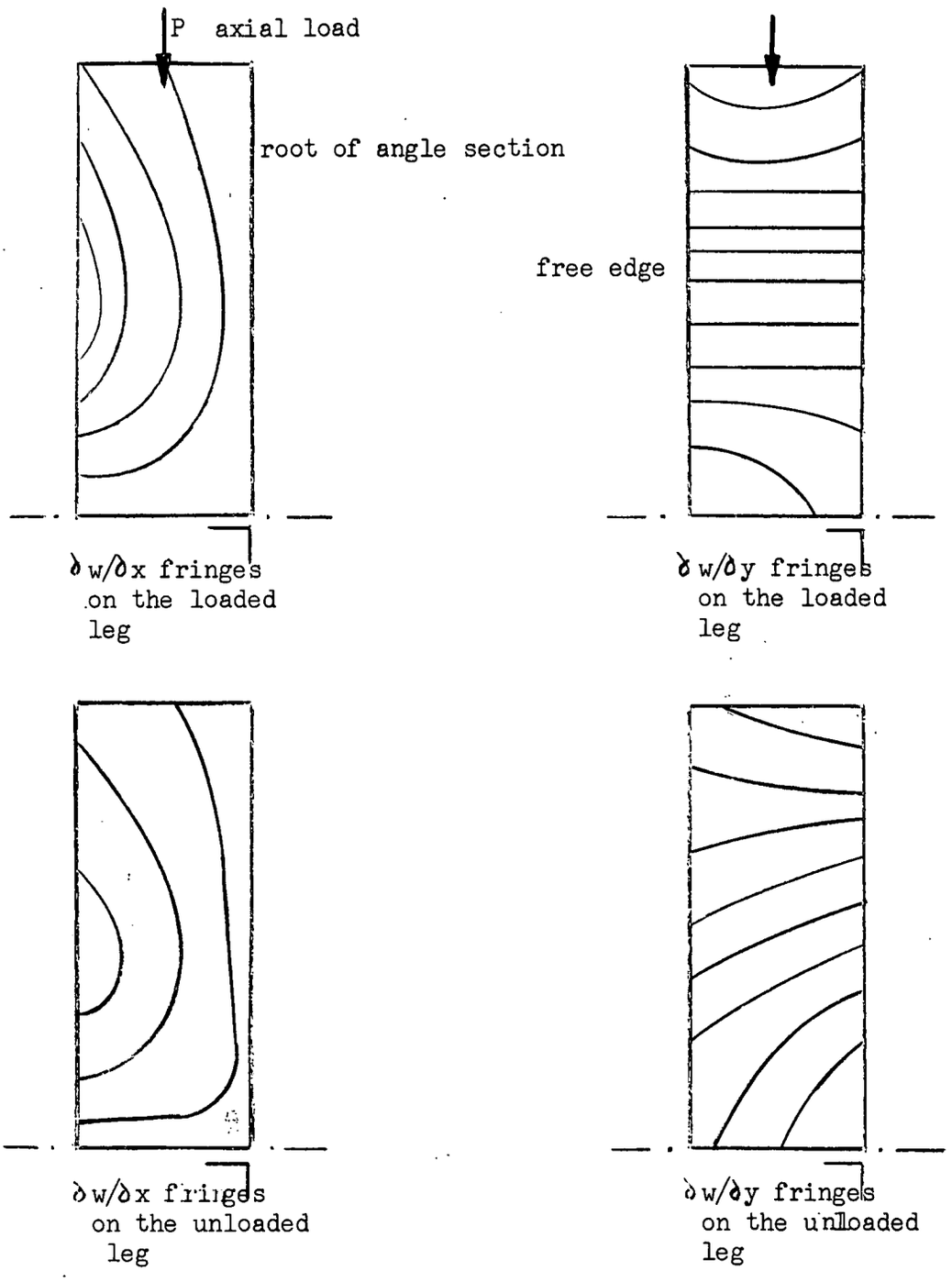

LIGTENBERG FRINGES OF SLOPE ON HALF OF EACH LEG OF AN ANGLE-SECTION COLUMN LOADED THROUGH ONE LEG

FIGURE 39

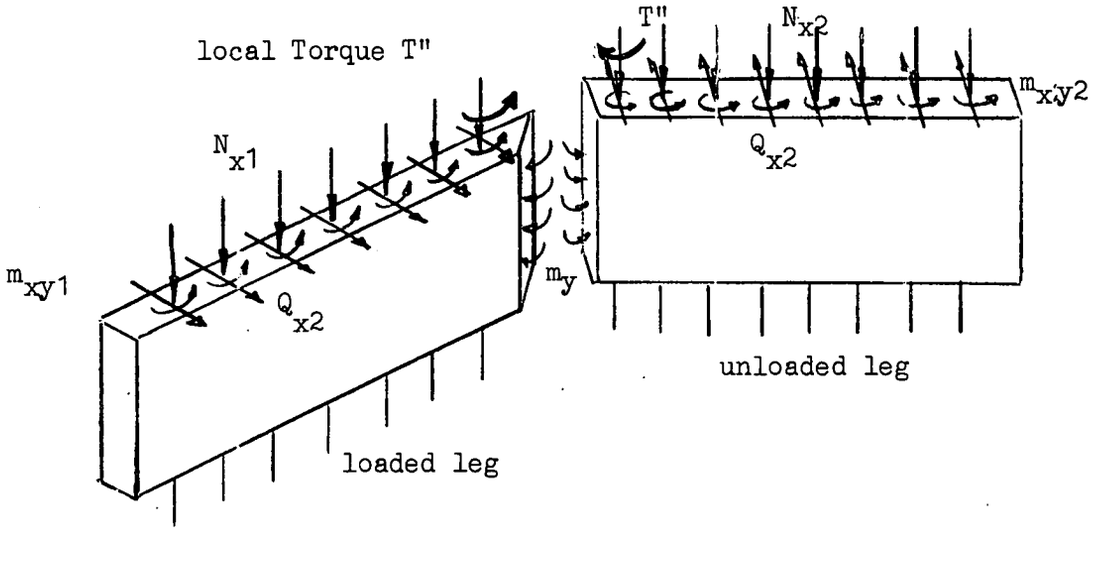

THE INTERNAL ACTIONS ON ELEMENTS FROM EACH LEG OF THE ANGLE SECTION COLUMN

FIGURE 40

Although some of the physical members failed above the critical load when the material yielded, the author does not suggest that a large deflection analysis is of value in general practice. This opinion is based upon two points. Firstly, the displacement is too large to be tolerated in practice, and secondly, any small lateral load will produce a large change, both in shape and maximum deflection. In other words, the members must be considered as physically unstable.

COLUMNS WITH BOLTED END-CONNECTIONS

Earlier work has shown that if an angle-section member is loaded eccentrically about the minor axis, then the critical load increases as the load moves towards the shear centre, and if the column is loaded eccentrically about the major axis there is no change in the critical load. These results are true only if the cross-section does not distort.

Several aluminium angle cross-section members, bent from aluminium sheet, were loaded through bolts placed at the centre of one leg as shown in fig. 38, that is, with an eccentricity of $b/2\sqrt{2}$ about the major axis. The most noticeable fact about the geometry of the loaded structure is that both legs no longerundergo the same deflection. The loaded leg experiences a much larger deflection than the unloaded, or outstanding leg. The ratio of the deflection near the critical load appears to depend primarily upon the type of root of the angle. Several perspex models were made with different amounts of glue at the root. Each had a different deflection ratio. Also the critical load for this member was much lower than the load given by the mathematical model based upon an undistorted cross-section. For the overall, or torsional mode of buckling to occur, the bolt must be tightened sufficiently to prevent any local buckling directly under the bolt. The local buckle was observed in all of the early columns tested.

Ligtenberg moire fringes were obtained for both legs. These fringes are shown in fig. 39. A straightline across the legs no longer remained straight. The bowing is most noticeable in the region of the bolt. Although in the central portion of the structure the legs are not straight, the bow is not appreciable. Hence it appears that the

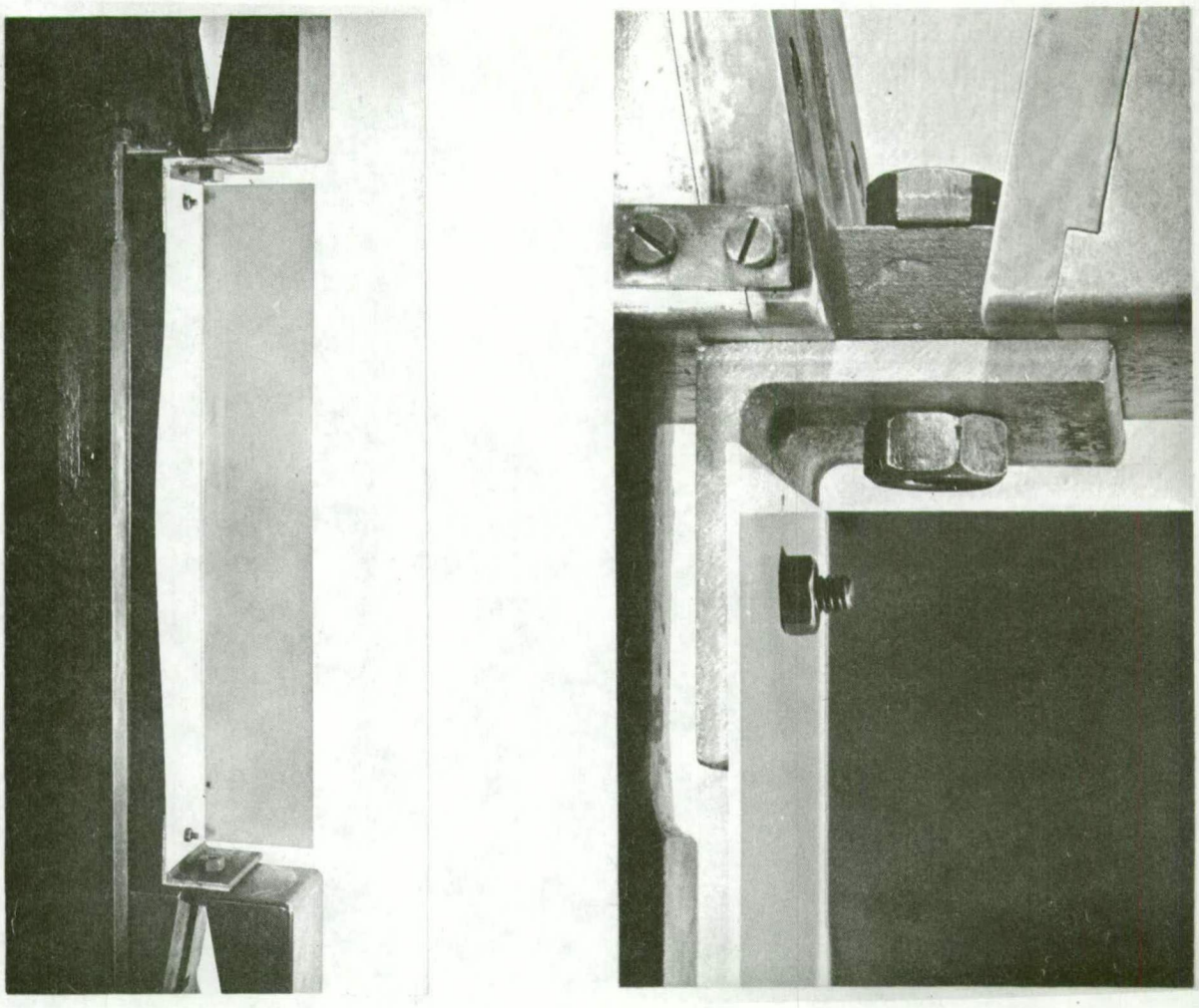

The mechanism for loading an angle column through one leg. The member is deformed into the elastic buckling mode.

FIG. 37

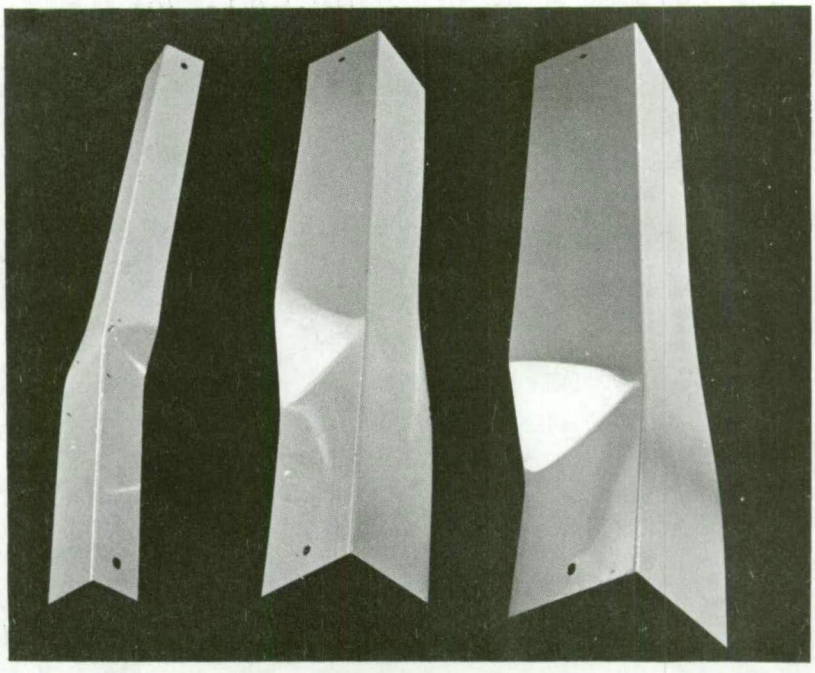

The shape of a column which has been loaded past the elastic buckling load until plastic deformations have occurred. Note that the triangular mode only forms in one leg.

FIG. 38

difference in the deflection of the two legs is taken up by the opening of the angle at the root. From the fringes in the other direction, the x direction, the shape of the central portion is roughly sinusoidal, which suggests that the longitudinal stress in the central region of the member is constant, as is to be expected for members with large length-leg width ratios. The effective length of the member is roughly half the total length, as the bolted connections produced built-in end conditions.

First Mathematical Model

The first mathematical model has the longitudinal stress on the central plane of the legs constant in the central half of the column,

$$L/4 \leq x \leq 3L/4 ,$$

the leg remaining straight and the included angle at the root changing. The shape of the deformations of both legs will be assumed to be of the same form within the central half of the member, and given by

$$w_1 = a_1 y\phi \quad \text{for the loaded leg}$$

and

$$w_2 = a_2 y\phi \quad \text{for the unloaded leg} \tag{59}$$

This model induces a finite moment at the root and zero moment in the legs. Naturally the moment is not discontinuous, but as a first approximation the discontinuous model will be used. It has further been assumed that the moment at the root of the angle is linearly related to change in the angle contained between the legs

$$m_y = C(a_1 - a_2)\phi .$$

Actually the root of the angle is at a high stress as it will have high residual stresses from the formative process, and also high shear stresses due to stress concentration at the corner. These facts could produce the weakness at the root. The constant of portionality has been evaluated experimentally, and it would appear that the constant must be so evaluated for each different type of angle section member.

As before, only certain equations of equilibrium are satisfied. Two elements are considered; a strip width b , thickness t and length dx from each leg, see fig.40. When the linear bending theory

is applied to the bending moment about the major axis the longitudinal stresses are

$$N_{x1} = P/A + My/I_{pp}2\sqrt{2}$$

and $$N_{x2} = P/A - My/I_{pp}2\sqrt{2} .$$

The shear stress across the thickness Q_x are obtained by considering the internal statical balance. The expression for the shear stress,

$$Q_x = - Dy\, \partial^3\phi/\partial x^3 - N_xy\, \partial\phi/\partial x - N_{xy}\phi , \qquad (60)$$

is derived in appendix A.

The above formula (60) for the shear stresses does not take into account the rapid change of moment m_y around the root of the angle-section member, which produces shear stresses and twisting moments on the planes, with x constant, in the vicinity of the root of the member (see fig. 40). In the following analysis, the torque of these two quantities about the shear centre is combined, and considered as the one torque, called the local torque. The total local torque is assumed to vary linearly with the x-ordinate. The torque equilibrium of one leg of the member gives the value of the local torque at the end of the member as

$$T'' = - \int_0^{L/2} C(a_1 - a_2)\phi\, dx = + (a_1 - a_2)T' ,$$

and thus the distribution of local torque is

$$+ (a_1 - a_2)T'(L/2 - x)2/L .$$

The torque equilibrium for an element from the loaded leg gives

$$\partial \left(\int_0^b m_x y\, dy\right)/\partial x\, dx + \partial\left(\int_0^b Q_x y\, dy\right)/\partial x\, dx = m_y\, dx + (a_1 - a_2)2T'/L\, dx .$$

When the appropriate expressions for m_y, m_{xy}, Q_x and N_x are substituted into the equilibrium equation the following differential equation in ϕ is obtained.

$$a_1 DI_p/2t\, \partial^4\phi/\partial x^4 + a_1(PI_p/2A + Peb^4/4\sqrt{2}I_{pp} - GJ/2)\, \partial^2\phi/\partial x^2 =$$

$$= C(a_1 - a_2)\phi + 2T'(a_1 - a_2)/L \qquad (61)$$

In the same manner the equation for the torque equilibrium of the element from the unloaded leg gives the differential equation

$$a_2 DI_p/2t\, \partial^2\phi/\partial x^4 + a_2(PI_p/2A - Peb^4/4\sqrt{2}I_{pp} - GJ/2)\, \partial^2\phi/\partial x^2 =$$

$$= C(a_1 - a_2)\phi - 2T'(a_1 - a_2)/L \qquad (62)$$

We shall assume that the boundary conditions are that the rotation is zero at $x = 0$, the twist iszero at $x = L/2$, and the moment is zero at $x = L/4$ and $3L/4$. The solution is then

$$w_1 = a_1 y(\cos(2n\pi x/L) - 1)$$

and

$$w_2 = a_2 y(\cos(2n\pi x/L) - 1).$$

If l is the effective length, then two linear equations in the unknowns a_1 and a_2 are obtained,

$$\begin{bmatrix} (DI_p/2t)(\pi/l)^4 - (PI_p/2A + Peb^4/4\sqrt{2}\,I_{pp} - GJ/2)(\pi/l)^2 - C, & +C \\ +C, & (+DI_p/2t)(\pi/L)^4 - (PI_p/2A + Peb^4/4\sqrt{2}\,I_{pp} - GJ/2)(\pi/l - C \end{bmatrix} \begin{bmatrix} a_1 \\ a_2 \end{bmatrix}$$

$$= [0] \qquad (63)$$

For the solution to be non-trivial the determinant of theleft-hand side must be zero, which gives a quadratic characteristic equation in P. For each value of n there are two solutions for P, and, although at these loads both displacements are indeterminate, the ratio of the two displacements can be determined. The ratio has two values, one corresponding to each load. Nevertheless there are an infinite number of modes and critical loads, as n can vary from zero to infinity.

The two ratios obtained for the one value of n are linearly independent, or orthogonal, and, as the functions $\cos n\pi x/L + 1$ and $\cos m\pi x/L$ are orthogonal, all the modes are orthogonal and any shape can be expressed as a unique sum of the modes, such as

$$w_1 = y \sum_{n=1}^{\infty} a_{1n}(\cos n\pi x/L + 1) + a_{2n}(\cos n\pi x/L + 1)$$

and

$$w_2 = y \sum_{n=1}^{\infty} R_{1n}a_{1n}(\cos n\pi x/L + 1) + R_{2n}a_{2n}(\cos n\pi x/L + 1),$$

where a_{1n} and a_{2n} are constant and R_{1n} and R_{2n} are the critical ratios for the shape $\cos(n\pi x/l) - 1$.

One of the members which was tested was made of aluminium sheet, having Young's modulus $E = 10$ psi, and thickness $t = 0.65"$, and length $L = 24"$ and leg width $4"$. For this member the two simultaneous linear equations are

$$(260.6 - 0.394P)a_1 - 143a_2 = 0$$

and

$$-143a_1 + (260.6 - 0.022P)a_2 = 0,$$

which combine to give the characteristic equation

$$(261 - 0.394P)(261 - 0.022P) = 143^2$$

or

$$0.00993P^2 + 97.4P - 47,800 = 0 .$$

The lowest critical load is 485 lbs and the ratio is 0.49. The results of the other tests will be discussed at the end of the second, more complicated, mathematical model, at which stage the two mathematical models will be compared.

When the initial shapes $w_{01} = a_{01}y\phi_0$ and $w_{02} = a_{02}y\phi_0$ are included, the torque equilibrium equations become

$$(DI_p/2t)\,\partial^4(a_1\phi - a_{01}\phi_0)/\partial x^4 + a_1(PI_p/2A + Peb^4/4\sqrt{2}\,I_{pp})\,\partial^2\phi/\partial x^2 -$$

$$- GJ/2\,\partial^2(a_1\phi - a_{01}\phi_0)/\partial x^2 = (C + 2T'/L)(a_1 - a_{01} - a_2 + a_{02})$$

and

$$DI_p/2t\,\partial^4(a_2\phi - a_{02}\phi_0)/\partial x^4 + a_2(PI_p/2A - Peb^4/4\sqrt{2}\,I_{pp})\,\partial^2\phi/\partial x^2 -$$

$$- GJ/2\,\partial^2(a_2\phi - a_{02}\phi_0)/\partial x^2 = -(C + 2T'/L)(a_1 - a_{01} - a_2 + a_{02}) .$$

If the initial shape is

$$\phi_0 = \cos(n\pi x/L) + 1$$

then the solutions to the equations are

$$\phi_1 = a_1(\cos(n\pi x/L) + 1) \quad \text{and} \quad \phi_2 = a_2(\cos(n\pi x/L) + 1)$$

provided the following two linear equations are satisfied

$$\begin{aligned}(a_1 - a_{01})(\pi/L)^4 DI_p/2t - a_1(\pi/L)^2(PI_p/2A + Peb^4/4\sqrt{2}\,I_{pp}) + \\ + (a_1 - a_{01})GJ(\pi/L)^2/2 = C(a_1 - a_{01} - a_2 + a_{02})\end{aligned}$$

and

$$\begin{aligned}(a_2 - a_{02})(\pi/L)^4 DI_p/2t - a_2(\pi/L)^2(PI_p/2A - Peb^4/4\sqrt{2}\,I_{pp}) + \\ + (a_2 - a_{02})GJ(\pi/L)^2/2 = -C(a_1 - a_{01} - a_2 - a_{02}) .\end{aligned} \tag{64}$$

In order to simplify the mathematical manipulations, a simpler notation will be used;

$$E = DI_p(\pi/l)^4/2 + GJ(\pi/l)^2/2$$

$$F = (\pi/L)^2 PI_p/2A$$

$$G = (\pi/L)^2 Pb^5/16I_{pp} = (\pi/L)^2 Peb^4/4\sqrt{2}\,I_{pp}$$

and

$$\gamma = (E - (C - (F + G)P)(E - C - (F - G)P) - C^2 .$$

Under these conditions the equations (64) become

$$(a_1 - a_{01})E - a_1(F + G) = C(a_1 - a_{01} - a_2 + a_{02})$$
$$(a_2 - a_{02})E - a_2(F - G) = -C(a_1 - a_{01} - a_2 + a_{02}) . \tag{65}$$

If P' is a critical load and we assume that the ratio of a_{01} and a_{02} is the corresponding critical ratio, then

$$\frac{a_{02}}{a_{01}} = \frac{C}{(EC) - P'(F - G)} = \frac{(E - C) - (F + G)P'}{C} \tag{66}$$

and $$((E - C) - (F - G)P')((E - C) - (F + G)P') = C^2 .$$

Solving the equations for the deflection a_1 gives

$$\gamma a_1 = ((E - C)((E - C) - (F - G)P) - C^2)a_{01} - (F - G)Pa_{02}$$

or $$\gamma a_1/a_{01} = (E - C)^2 - C^2 - PP'(F^2 - G^2) \tag{67}$$

when the ratio of the initial shapes is critical. On applying equation (65), equation (66) becomes

$$\gamma\, a_1/a_{01} = 2FP'(E - C) - (F^2 - G^2)(P' + P)P' ,$$

which on multiplying by $(P - P')$ gives

$$(P - P')\gamma a_1/a_{01} = -P'((F^2 - G^2)(P^2 - P'^2) - 2F(P - P')(E - C))$$

or

$$(P - P')\gamma\, a_1/a_{01} = -P'((F^2 - G^2)P^2 - 2F(E - C)P - (F^2 - G^2)P'^2 - 2F(E - C)P') .$$

When the characteristic equation,

$$(E - C)^2 + (F^2 - G^2)P' - (E - C)2FP' - C^2 = 0 ,$$

and the expression for γ are substituted into the equation for $(P - P')\gamma a_1/a_{01}$, then

$$(P - P')\ a_1/a_{01} = -P'(\gamma - (E - C)^2 - 0 + (E - C)^2 - C^2)$$

therefore

$$a_1 = -P'a_{01}/P - P'$$

or $$a_1 = a_{01}/(1 - P/P') \tag{68}$$

Similarly it can be shown that

$$a_2 = a_{02}/(1 - P/P') ,$$

and if the ratio of the initial shapes a_{01}/a_{02} is the second critical ratio, the one corresponding to the critical load P'', then

$$a_1 = a_{01}/(1 - P/P'')$$
$$a_2 = a_{02}/(1 - P/P'') .$$

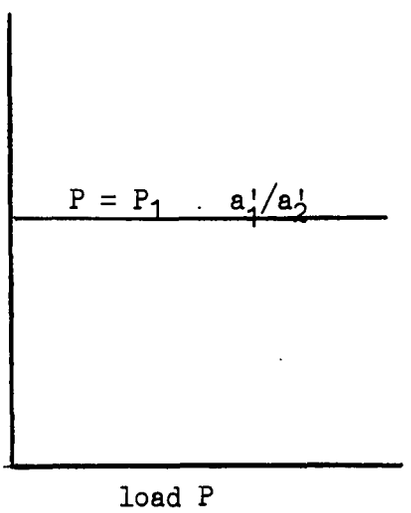

$a_{01}/a_{02} = a_1'/a_2'$

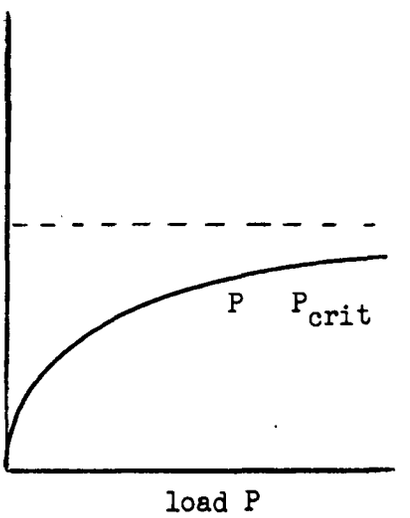

$a_{01}/a_{02} < a_1'/a_2' > 0$

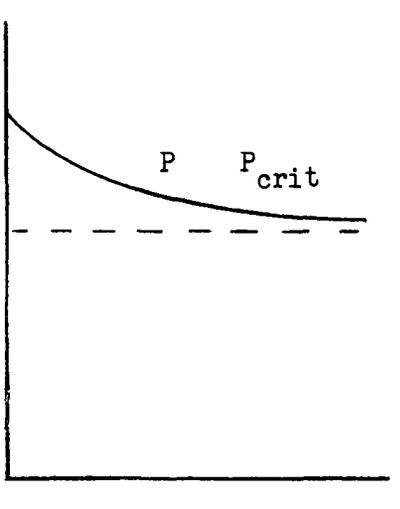

$a_{01}/a_{02} > a_1'/a_2'$

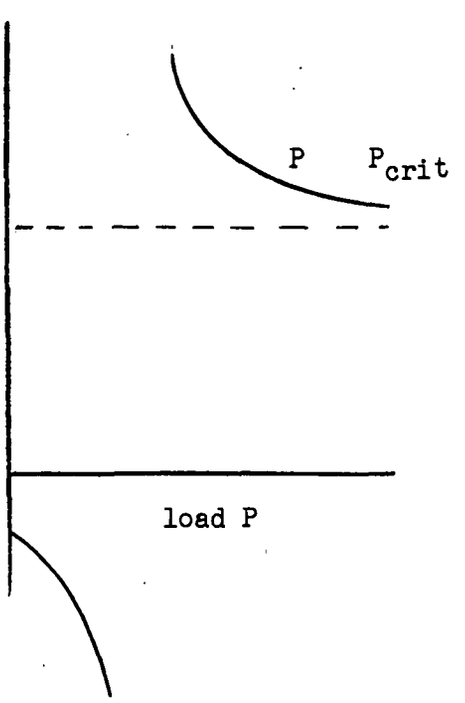

$a_{01}/a_{02} < 0$

a_1/a_2 is the ratio of the measured deflections.
a_{01}/a_{02} is the ratio of the initial shapes.
a_1'/a_2' is the ratio corresponding to the lowest critical load

VARIATION OF THE RATIO OF THE DEFLECTIONS OF THE TWO LEGS OF AN ANGLE-SECTION COLUMN LOADED THROUGH ONE LEG

FIGURE 41

Hence, if the initial shapes are expressed as infinite sums,

$$w_{01} = \sum_{n=1}^{\infty} a_{0n} y(\cos n\pi x/l + 1) + a_{02n} y(\cos n\pi x/L + 1)$$

and (69)

$$w_{02} = \sum_{n=1}^{\infty} R_{1n} a_{01n} y(\cos n\pi x/l + 1) + R_{2n} a_{02n} y(\cos n\pi x/L + 1) ,$$

then the shape of the loaded member is

$$w_1 = \sum_{n=1}^{\infty} (a_{01n}/(1 - P/P_{1n}) + a_{02n}/(1 - P/P_{2n}))y (\cos n\pi x/l + 1)$$

and (70)

$$w_2 = \sum_{n=1}^{\infty} (a_{01n}R_{1n}/(1 - P/P_{1n}) + a_{02n}R_{2n}/(1 - P/P_{2n}))y (\cos n\pi x/l + 1) .$$

When P_{11} is less than any other critical load then these results simplify to

$$w_1 = (a_{011}/(1 - P/P_{11}))(\cos\pi x/l + 1)$$

and $$w_2 = (R_{11}a_{011}/(1 - P/P_{11}))(\cos\pi x/l + 1) ,$$

and it follows that a Southwell plot can be applied to either deflection. In fig. 41 are plotted typical ratio-load graphs. We find there are four types.

The graphs of the last three types have been obtained. However the measured critical ratio was usually considerably different from the calculated value. This is thought to be so because the mathematical model applies only over the central section, whereas the measured ratio is the ratio of the total deflections, and includes the end effects and displacements due to the stress distribution around the bolt.

Second Mathematical Model

The second mathematical model includes the effect of the stress distribution produced by loading the member through a bolt as shown in fig. 38. The geometry of the deformations is assumed to have the same functional form as for the first model, although it must now apply in the vicinity of the bolt, where it is a poor fit to the actual geometric form. The functional form used is

$$w_1 = a_1 y\phi$$

and (71)

$$w_2 = a_2 y\phi$$

* * * *

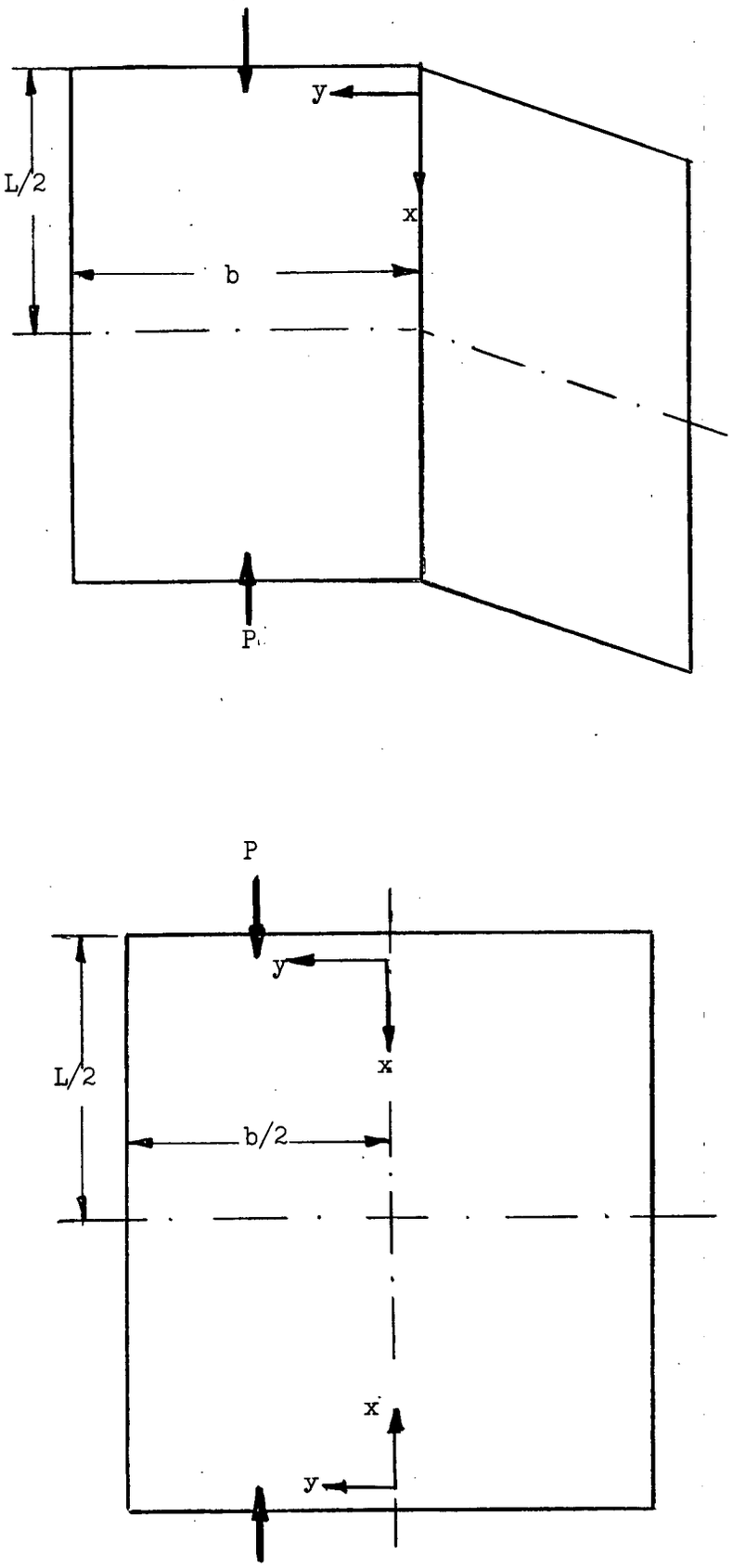

THE CO-ORDINATE SYSTEM USED TO DEFINE THE LONGITUDINAL STRESS DISTRIBUTION FOR AN ANGLE-SECTION MEMBER AND FOR A PLAT PLATE

FIGURE 42.

Stress Distribution Around a Bolt

Before the second mathematical model can be established a function form for the longitudinal stresses N_x in the neighbourhood of the bolt must be obtained. The problem has been simplified by assuming that the difference between the stress distribution and the linear bending theory distribution

$$N_x'' = N_x - P/A \pm Pby/4I_{pp} \qquad (72)$$

is of the same form for an angle-section member as for a plate. The functional form for both will be taken as

$$N_x'' = f(x)(g(y) \pm Cy + D) . \qquad (73)$$

The coordinate system of the angle is: y measured across the leg of the angle from the root and x measured in the direction of the load from the loaded end. Only one half of the member will be considered. The coordinate system of the plate is y is measured across the plate from the centre line of the plate and the x ordinate is the same as for the angle. See fig. 42. The problem has been considered both experimentally and numerically.

Only one model was tested experimentally. This was a $4" \times 8" \times \frac{1}{8}"$ flat, perspex plate. The load was applied $\frac{3}{4}"$ from the free edge through a bolt. The u and v displacements in the plane of the leg of the angle have been measured using the cross-diffraction grating method. Also local strain measurements were made using light, Huggenberger mechanical strain gauges with 1" gauge length to check the results. Numerically, the problem was examined by a finite element technique. The basic ideas of the finite element method are discussed by Zienkiewicz.[1] The digital computer programme used was developed at the University of Tasmania by E. Middleton.

Although only one model was tested in the laboratory the effect of changing the ratio of the length and width of the plate was investigated numerically. The results are indicated in graph 43. It appears that, as a first approximation, the distribution of the stresses is independent of the leg width ratio. The effect of moving the point

---

Ref. 1 O. C. Zienkiewicz, G. S. Holister: "Stress Analysis," John Wiley and Sons.

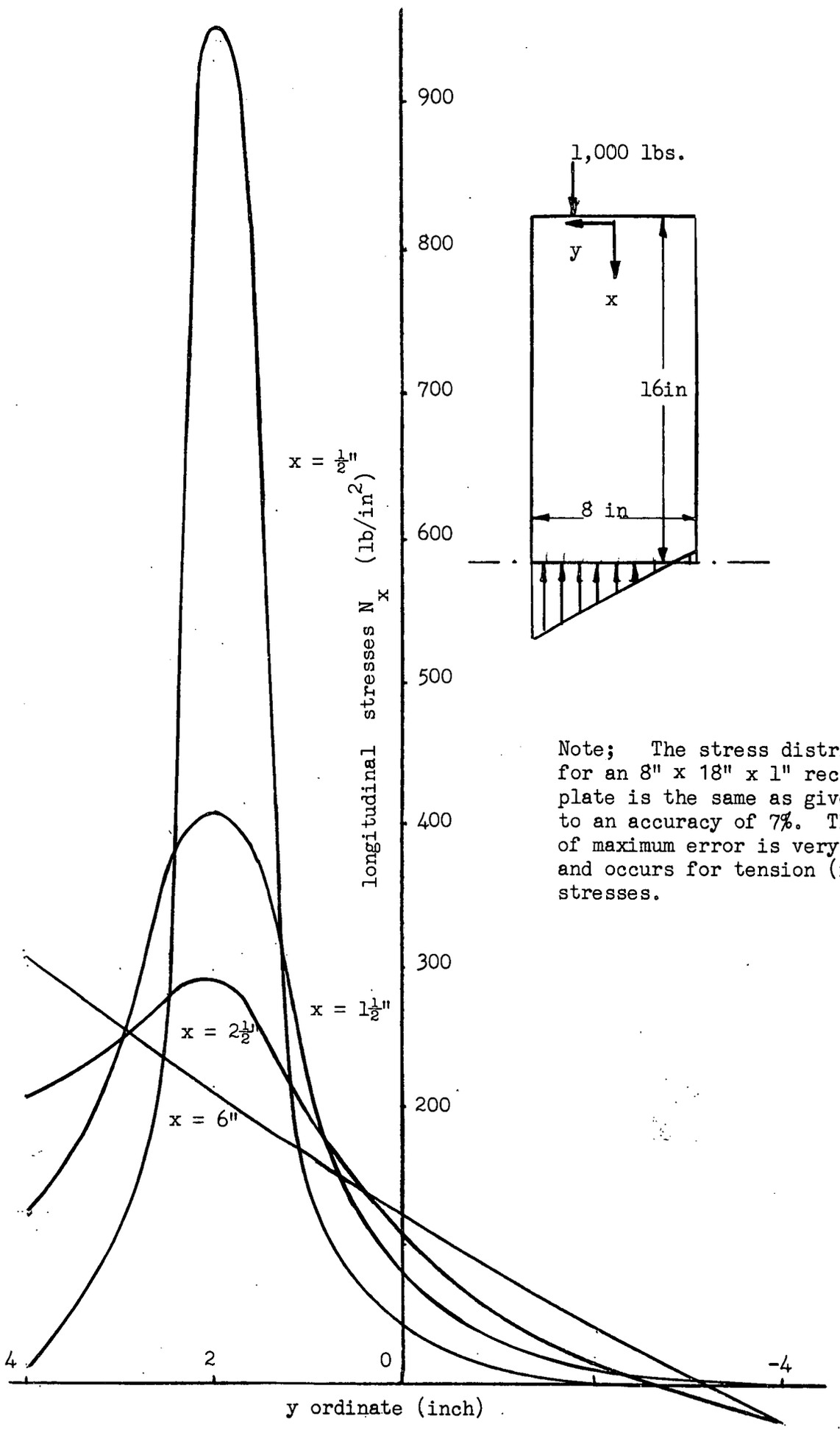

Note; The stress distribution for an 8" x 18" x 1" rectangular plate is the same as given above to an accuracy of 7%. The area of maximum error is very small, and occurs for tension (negative) stresses.

THE LONGITUDINAL STRESSES IN AN 8" x 32" x 1" RECTANGULAR PLATE LOADED THROUGH A QUARTER POINT AND AT AN EDGE.

FIGURE 43.

of application of the load away from the free edge was also considered numerically. The two cases were calculated. The load was applied at the free edge and at a point one quarter of the leg width from the free edge. The results are shown in graph 44. It can be seen that, although the maximum stress under the load was less, the effect was very local.

As the functional form for the stresses will be integrated in considering the overall buckling of the member, its accuracy is not particularly important. The functional form was obtained by using an average fit in the y direction and by fitting the distribution of the stresses along the line through the bolt in the x direction. The one used in the following discussion is

$$N_x = (P/A \pm Pby/4I_{pp}) + Pe^{-x}/dt(e^{-(y-b/2)^2} + C \mp Dy) \qquad (74)$$

where 2b is the width of the plate, t is the thickness and d is the diameter of the bolt. This form applies only in the region

$$0 < x < L/2 \ .$$

Thus, in the following discussion, only half of the angle-section member will be considered. The parameters A and B are evaluated by considering the statical equilibrium of the member. The total axial force and the bending moment on a given cross-section due to the second term N_x'' are zero.

If a more accurate stress distribution is required, it can be obtained from the stress distribution under a point load on a semi-infinite plane. However, a term of the form

$$N_x = f(x)(C \mp Dy)$$

must also be included, to enable the equilibrium of the statical actions on the general cross-section. This model has not been included as the mathematical model which follows is sufficiently complex.

* * * *

Two differential equations can be arrived at, in the same manner as for the first mathematical model, by considering the equilibrium of a part of each leg. The equations are

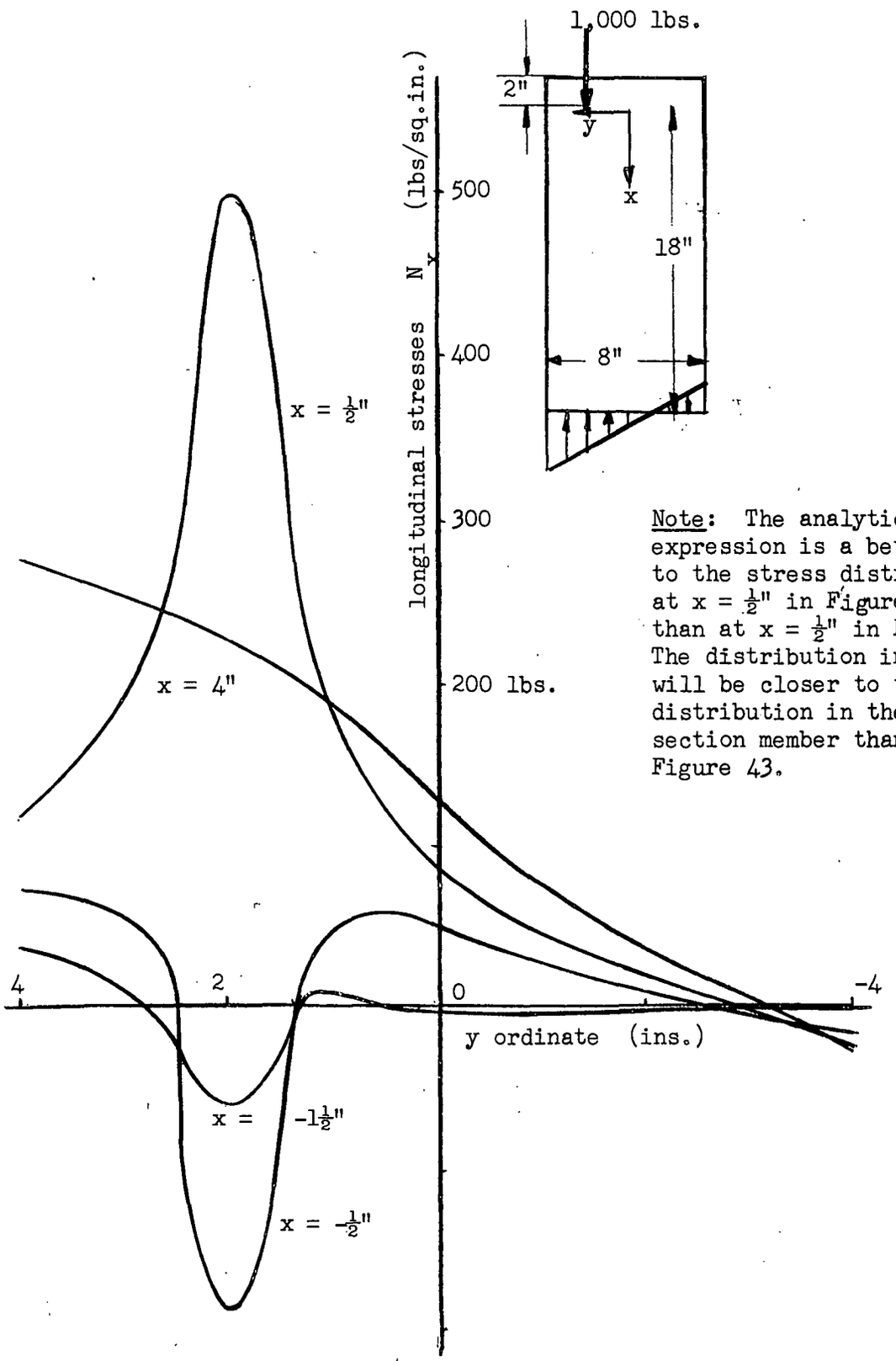

Note: The analytical expression is a better fit to the stress distribution at x = ½" in Figure 44 than at x = ½" in Figure 43. The distribution in Figure 44 will be closer to the stress distribution in the angle-section member than that in Figure 43.

LONGITUDINAL STRESSES FOR AN 8" x 36" x 1" RECTANGULAR PLATE LOADED THROUGH A QUARTER POINT AND 2" FROM AN EDGE

FIGURE 44.

$$a_1 DI_p/2t\, \partial^3\phi/\partial x^3 - a_1 GJ/2\, \partial\phi/\partial x + \int_0^b a_1 N_{x_1} y^2 \partial\phi/\partial x\, dy =$$

$$= (a_1 - a_2)(+ T'2x/L + C \int_0^x \phi\, dx) \qquad (75)$$

and

$$a_2 DI_p/2t\, \partial^3\phi/\partial x^3 - a_2 GJ/2\, \partial\phi/\partial x + \int_0^b a_2 N_{x_2} y^2 \partial\phi/\partial x\, dy =$$

$$= (a_1 - a_2)(- T'2x/L - C \int_0^x \phi\, dx)\ . \qquad (76)$$

When the expression for the longitudinal stress

$$N_x = P/A \mp Py/\sqrt{2}\, I_{pp} + Pe^{-x}(e^{-(y-b/2)^2} - C \pm Dy)/dt \qquad (77)$$

is substituted into the differential equations, the equations become too difficult to solve. An approximate result is obtained by using an averaging, integration process. Firstly, we rewrite equation (75) assuming that the longitudinal stresses can be expressed as a product of a function of x and a function of y. Let N_x' be the function of x and K be the result of the integration with respect to y. Then the first equation becomes

$$a_1 DI_p/2t\, \partial^3\phi/\partial x^3 + GJ/2\, \partial\phi/\partial x + K_1 N'_{x1}\, \partial\phi/\partial x =$$

$$= (T'2x/L + \int_0^x C\phi\, dx)(a_1 - a_2)\ .$$

When the equation is multiplied by $a_1\, \partial^2\phi/\partial x^2$ and integrated twice with respect to x the equation becomes

$$\tfrac{1}{2} \int_0^{L/2} (a_1^2 DI_p/2(\partial^2\phi/\partial x^2)^2 + GJ/2(\partial\phi/\partial x)^2 + K_1 N'_{x1}(\partial\phi/\partial x)^2)dx -$$

$$- \int_0^{L/2} \int_0^x K_1\, \partial N'_{x1}/\partial x (\partial\phi\partial x)^2\, dx\, dx - 2T'/L \int_0^{L/2} a_1(a_1 - a_2)\phi dx +$$

$$+ 3/2 \int_0^{L/2} Ca_1(a_1 - a_2)\phi^2 dx = 0$$

for the given boundary conditions. Similarly the second equation (76) becomes

$$\tfrac{1}{2} \int_0^{L/2} (a_2^2 DI_p/2(\partial^2\phi/\partial x^2)^2 + GJ/2(\partial\phi/\partial x)^2 + K_2 N'_{x2}(\partial\phi/\partial x)^2)dx -$$

$$- \int_0^{L/2} \int_0^x K_2\, \partial N'_{x2}/\partial x (\partial\phi/\partial x)^2\, dx\, dx + 2T'/L \int_0^{L/2} a_1(a_1 - a_2)\phi dx -$$

$$- 3/2 \int_0^{L/2} Ca_1(a_1 - a_2)\phi^2 dx = 0\ .$$

If these two equations are added, the sum, which will be referred to as the "averaging integral", is

$$u = \tfrac{1}{2}\int_0^{L/2}(a_1^2 + a_2^2)DI_p/2t(\partial^2\phi/\partial x^2)^2 - GJ/2(\partial\phi/\partial x)^2) +$$

$$+ (a_1^2K_1N_{x1}' + a_2^2K_2N_{x2}')(\partial\phi/\partial x)^2dx - \int_0^{L/2}\int_0^x (a_1^2K_1\partial N_{x1}'/\partial x +$$

$$+ a_2^2K_2\partial N_{x2}'/\partial x)(\partial\phi/\partial x)^2dxdx - (2T'/L\int_0^{L/2}\phi dx - 3/2C\int_0^{L/2}\phi^2dx)*$$

$$(a_1^2 - 2a_1a_2 - a_2^2) = 0 .$$

The averaging integral can be treated in the same way as an energy expression and the same conditions apply, namely

$$u = 0 \quad \text{and} \quad \partial u/\partial a_1 = \partial u/\partial a_2 = 0 . \tag{76}$$

Also, as the derivative of the differential equations are self adjoint and positive definite, the value of the critical load obtained by applying the averaging integral to an approximate shape will be an upper bound on the true eigenvalue of the simultaneous, linear, differential equations. The same conditions apply to both the "averaging integral" and the energy expression, as both are specific applications of the least square method of obtaining approximate solutions to differential equations.[1] The energy expression for this problem gives the bound to a mathematical model which is inherently more accurate than the mathematical model considered. Thefirst part of the "averaging integral" is identical to the equivalent terms in the energy expression for a plate.

As an example, the first mathematical model will be solved using the "averaging integral" in conjunction with the functional form

$$\phi = \cos 2\pi x/L + 1 . \tag{77}$$

The conditions for the "averaging integral" to be a minimum are

$$\partial u/\partial a_1 = a_1(DI_p(2\pi/L)^4L/8t + GJ(2\pi/L)^2/8 - PI_p(2\pi/L)^2L/4A -$$

$$- LPb^5(2\pi/L)^2/64I_{pp}) - (a_1 - a_2)\phi CL/4 = 0 ,$$

$$\partial u/\partial a_2 = a_2(DI_p(2\pi/L)^4L/8t + GJ(2\pi/L)^2/8 - PI_p(2\pi/L)^2L/4A +$$

$$+ LPb^5(2\pi/L)^2/64I_{pp}) + (a_1 - a_2)\phi CL/4 = 0 .$$

Ref. 1 Applied Mech. Review Vol.19, No.9, Sept. 1966, "The Method of Weighted Residuals", B.A. Finlayson and L.E. Scriven.

The two equations are identical to the equations of statical equilibrium obtained previously.

For the second model, the solution to the differential equation is not known and an approximate shape which satisfies the boundary conditions will be used,

$$\phi = \cos 2\pi/L + 1 .$$

Also the term

$$-\int_0^{L/2}\int_0^{x} (a_1^2 K_1 \partial N_{x1}'/\partial x + a_2^2 K_2 \partial N_{x2}'/\partial x)(\partial \phi/\partial x)^2 dx$$

will be neglected. For the problem considered, this term is always of the same sign as the other terms involving the longitudinal stresses N_x and hence the approximate solution is an upper bound on the solution of the "averaging integral", and hence to the eigen value of the differential equations.

The values of the parameters C and D in the expression for the longitudinal stresses can be evaluated by considering the equations of axial force equilibrium and moment equilibrium. An approximate expression is

$$N_x = Pt/A \mp Ptby/4I_{pp} + Pe^{-x}(e^{-(y-b/2)^2} - \sqrt{\pi}/A \mp \sqrt{\pi}by/4I_{pp})/dt . \quad (78)$$

The term

$$\int_0^{L/2}\int_0^{b} N_x y^2 (\partial \phi/\partial x)^2 \, dy \, dx$$

of the averaging integral consists of two parts

$$\int_0^{L/2}\int_0^{b} (y^2 Pt/A \mp Ptby^3/4I_{pp})(\partial \phi/\partial x)^2 \, dy \, dx$$

$$+ \int_0^{L/2}\int_0^{b} y^2 Pe^{-x}(e^{-(y-b/2)^2} - \sqrt{\pi}/A \mp \sqrt{\pi}by/4I_{pp})(\partial \phi/\partial x)^2/dt \, dy \, dx .$$

The second part involves the stresses around the bolt. The double integral can be considered as the product of the two integrals

$$\int_0^{L/2} e^{-x} \sin^2(2\pi x/L)dx = -8(e^{-L} - 1)\pi^2/(16\pi^2 + (L/2)^2)$$

$$\simeq 8\pi^2/(16\pi^2 + (L/2)^2)$$

and

$$\int_0^{b} y^2 e^{-(y - b/2)^2} dy \simeq \sqrt{\pi}/2 + b^2\sqrt{\pi}/4 .$$

It should be noted that these results are approximate, as all terms involving exponentials have been neglected. Also, the results do not appear to be dimensionally correct. This arose because the exponents of the exponential terms in the functional form are not non-dimensional.

Thus the conditions for the "average integral" of the second mathematical model to be a minimum are

$$a_1(DI_p(2\pi/L)^4/2t + GJ(2\pi/L)/2 - PI_p(2\pi/L)^2/A2 - Pb^5(2\pi/L)^2/16I_{pp} + + P8\pi^2(\sqrt{\pi}/2 + b^2\sqrt{\pi}/4 - b^3\sqrt{\pi}/3A - \sqrt{\pi}b^5/16I_{pp})/d(16\pi^2 + (L/2)^2)) - - C(a_1 - a_2) = 0 \quad (79)$$

and

$$a_2(DI_p(2\pi/L)^4/2t + GJ(2\pi/L)^2/2 - PI_p(2\pi/L)^2/A2 + b^5P(2\pi/L)^2/16I_{pp} + + P8\pi^2(-b^3\sqrt{\pi}/3A + \sqrt{\pi}b^5/16I_{pp})/d(16\pi^2 + (L/2)^2)) + C(a_1 - a_2) = 0 . \quad (80)$$

A non-trivial solution to the two homogeneous, linear equations can be obtained when the determinant is zero, which gives the critical value of the load parameter.

For a column with leg width $b = 4"$, thickness $t = 0.065"$, length $L = 24"$ Young's modulus $E = 10^7$ p.s.i. and constant $C = 143$ lbs. the two equations are

and $$\begin{bmatrix} (261 - 0.369P), & +143 \\ +143, & (261 + 0.015P) \end{bmatrix} \begin{bmatrix} a_1 \\ a_2 \end{bmatrix} = 0$$

and the lowest critical load is 500 lbs.

The results for other members are quoted in the table below. The first value refers to the critical load obtained when the cross-section distorts but the stresses around the bolt are neglected, and the third value includes the effect of the stress distribution. The fourth value is the "critical load" obtained experimentally.

Member	Critical Load			Ratio
4" 4" 24" .065"	625	485	500	470
4" 4" 8" .065"	1770	880	1180	
4" 4" 12.5" .065"	1040	580	670	640
3" 3" 24" .065"	770	620	630	645

As is to be expected, the effect of the stress distribution around the bolts is negligible for long members. The ratio of the deflections of the two flanges does not change appreciably with the inclusion of the secondary stresses. The largest change was for the 4" x 4" x 8"x 0.065" member, in which case the change was an increase of ten percent.

As for previous models tested, some of the members stiffened for loads greater than the "critical load". The member with a leg width of four inches and length of twenty four inches carried an ultimate load of 720 pounds, compared with a critical load of 470 pounds. On the other hand, the ultimate load and the critical load of the member with the leg width of three inches were identical. For the second member, the material yielded before any significant longitudinal strains due to the twisting of the section were produced.

The angle-section members tested were all bent from thin aluminium sheet, and consequently the roots of the angle-section members were weak. Extruded angle-section members quite often have a heavy fillet at the root of the section. For these members, the author does not think that the mathematical model developed in this section will apply. One would expect that for these members the angle contained between the two legs of the member would remain constant, and that there would be an appreciable amount of bowing of the legs. If this is the case, a mathematical model could be developed using a functional form of the type,

$$w_1 = (a_1 y^2 + by)\phi(x) \quad \text{and} \quad w_2 = (a_2 y^2 + by)\phi(x) .$$

The problem could also be treated by the usual method of considering each leg as a plate, and applying compatibility of geometry and statical actions at the root. This method, used often in published work, will be discussed in the conclusions at the end of this thesis.

TORSIONAL-FLEXURAL BUCKLING

One of the basic assumptions of the previous part of this chapter was that the line of shear centres remained straight and that the section rotated in an undeformed state about the shear centre. For long members, the foregoing assumption is no longer justified because the member bends. In this chapter on buckling it has been shown how Euler developed a mathematical model which took into account the possibility

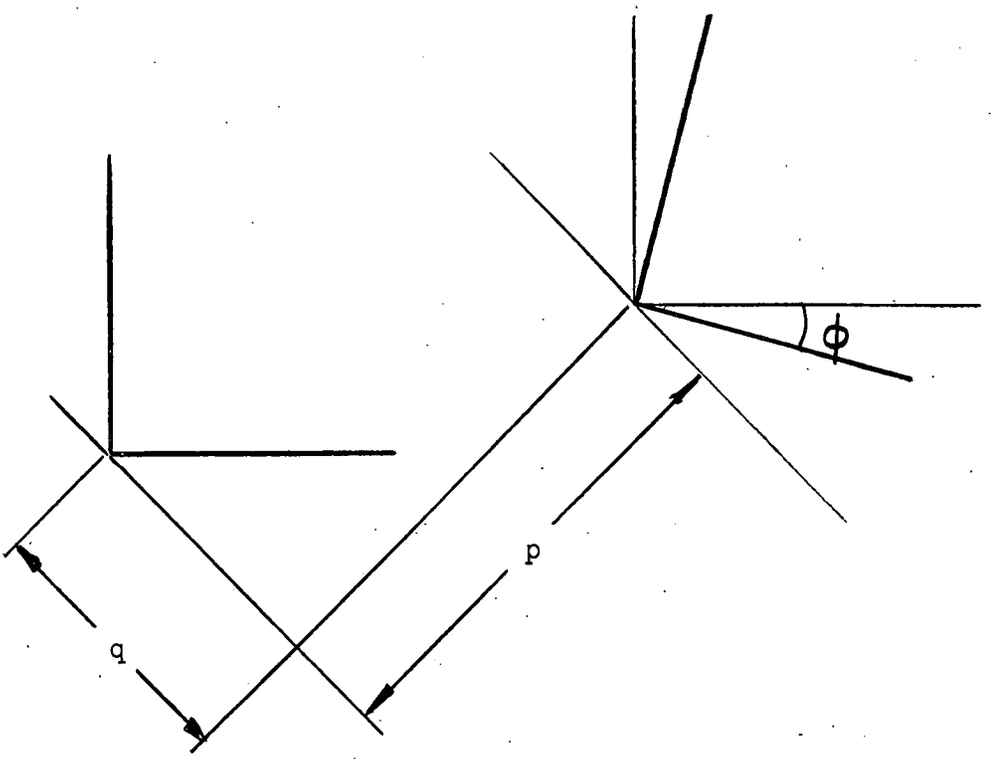

FIGURE 45

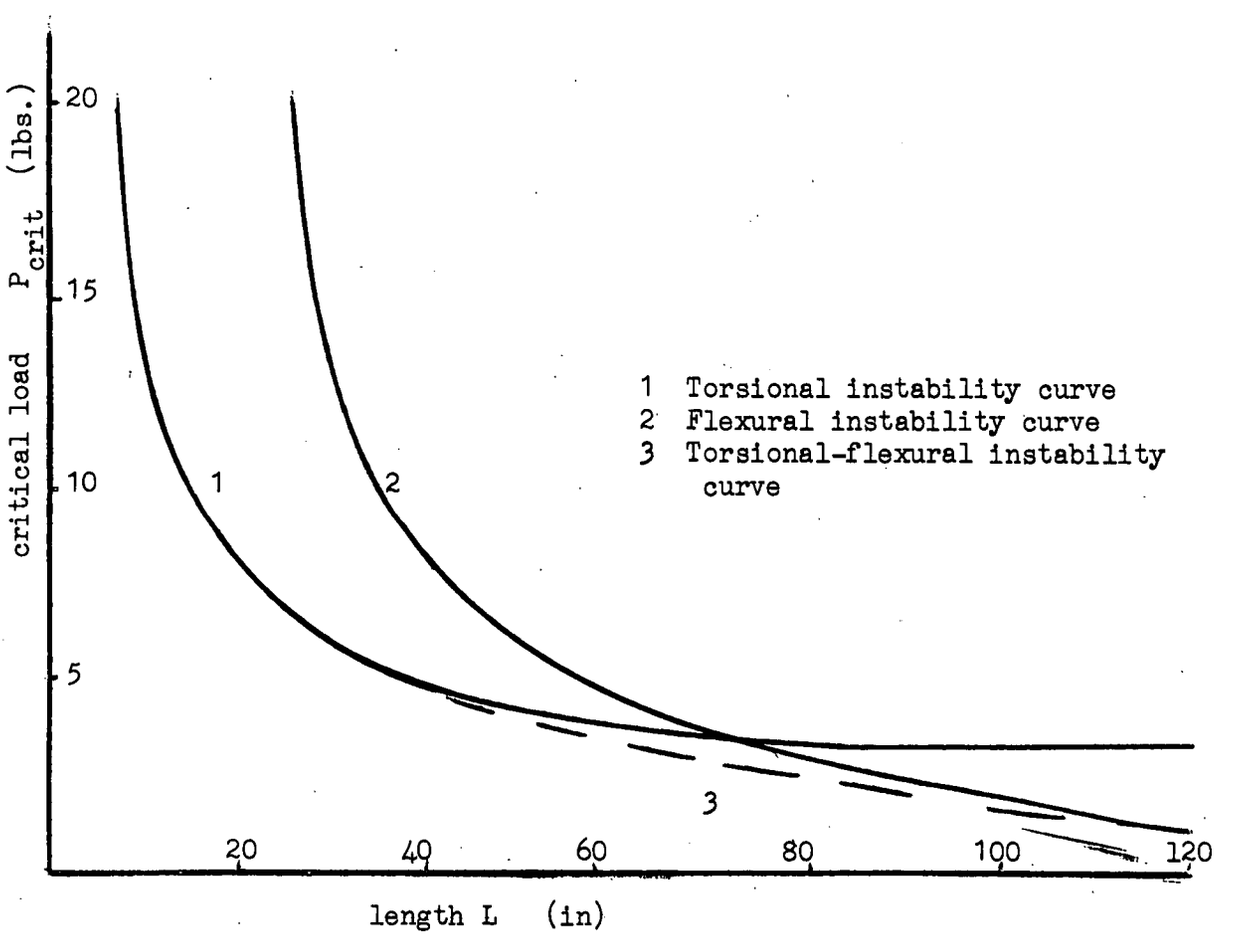

THE VARIATION OF THE CRITICAL LOAD OF THE TORSIONAL-FLEXURAL MODE OF A 4" x 4" x 1/8" ALUMINIUM, ANGLE-SECTION COLUMN

FIGURE 46.

of the members buckling by bending. In the following section the interaction of the torsional mode and the flexural mode will be considered. This exercise has been carried out before by various people, including Bleich[2], Timoshenko[2] and Goodier[3], but in this thesis the equations of statics will be established directly by the same method as that used in the models developed previously.

The notation introduced before will be maintained except that the deflections of the shear centre not the centroid in the directions of the two principal axes will be denoted by p and q. Thus as the polar-coordinate of the centroid is $b/2\sqrt{2}$ the displacements of the centroid are $q + \phi\, b/2\sqrt{2}$ and p. Thus the total moments about the two principal axes of the cross section are

$$M_P = P(q + \phi b/2\sqrt{2}) \qquad (81)$$

and

$$M_Q = Pp \ ,$$

which, in conjunction with the load deformation relationship, gives the two differential equations

$$EI_{pp}\, \partial^2 q/\partial x^2 = -P(q + \phi b/2\sqrt{2})$$

and

$$EI_{QQ}\, \partial^2 p/\partial x^2 = -Pp \ .$$

The longitudinal stresses produced by bending of the member are

$$N_x = P/A + Pp(y - b/2)/\sqrt{2}\, I_{QQ} \mp P(q + \phi b/2\sqrt{2})y/\sqrt{2}\, I_{pp} \ .$$

The St. Venant shear stresses are

$$GJ\, \partial^2 w/\partial x \partial y = GJ\, \partial\phi/\partial x$$

and the plate bending, shear stresses Q_x are

$$-Dy\, \partial^3\phi/\partial x^3 + N_x y\, \partial\phi/\partial x - N_{xy}\phi \ .$$

The equation of torque equilibrium on a section, with x constant, using the values quoted above, becomes

---

Ref. 1 F. Bleich: "Buckling Strength of Metal Structures", McGraw-Hill Book Co. Inc.

Ref. 2 S. P. Timoshenko & J. M. Gere: "Theory of Elastic Stability", McGraw-Hill Book Co. Inc.

Ref. 3 J. N. Goodier: "Torsional and Flexural Buckling of Bars of Thin Walled Open Sections Under Compressive and Bending Loads", A.S.M.E., Trans. 1942.

$$T = 0 = (DI_p/t)\partial\phi^3/\partial x^3 - GJ\partial\phi/\partial x -$$

$$-\int_0^b (Pt/A)((\partial q/\partial x - \partial p/\partial x)/\sqrt{2} + y\partial\phi/\partial x)y\ dy -$$

$$-\int_0^b (Pt/A)((\partial q/\partial x + \partial p/\partial x)/\sqrt{2} + y\partial\phi/\partial x)y\ dy -$$

$$-\int_0^b (Ptp(y - b/2)/\sqrt{2I_{QQ}})((\partial q/\partial x - \partial p/\partial x)/\sqrt{2} + y\partial\phi/\partial x)y\ dy -$$

$$-\int_0^b (Ptp/y - b/2)/\sqrt{2I_{QQ}})((\partial q/\partial x + \partial p/\partial x)/\sqrt{2} + y\partial\phi/\partial x)y\ dy -$$

$$-\int_0^b (Pt(q + b\phi/2\sqrt{2I_{pp}})((\partial q/\partial x - \partial p/\partial x)/\sqrt{2} + y\partial\phi/\partial x)y\ dy -$$

$$-\int_0^b (Pt(q + b\phi/2\sqrt{2I_{pp}})((\partial q/\partial x + \partial p/\partial x)/\sqrt{2} + y\partial\phi/\partial x)y\ dy\ , \quad (82)$$

which simplifies to

$$DI_p/t\ \partial^3\phi/\partial x^3 + (PI_p/A - GJ)\partial\phi/\partial x + Ptb^2/\sqrt{2}A\ \partial q/\partial x +$$

$$+ P_p t/6I_{QQ}(\tfrac{1}{2}\partial q/\partial x + 1/\sqrt{2}\ \partial\phi/\partial x) - Ptb^4(q + b\phi/2\sqrt{2})/4I_{pp}\partial p/\partial x = 0.$$

A set of solutions to the three simultaneous differential equations (81a), (81b) and (82) in ϕ, p and q for simply supported boundary conditions is

$$\phi = \phi_0 \sin n\pi x/L$$

$$p = p_0 \sin n\pi x/L \quad (83)$$

and $$q = q_0 \sin n\pi x/L\ ,$$

provided the conditions

$$p_0\phi_0 = 0\ , \quad (84)$$

$$\phi_0 Ptb^2/A\sqrt{2} + PtI_p/A\phi_0 - DI_p(\pi/L)^2/t\phi_0 - GJ\phi_0 = 0\ , \quad (85)$$

$$EI_{pp}q_0(\pi/L)^2 = P(q_0 + b\phi/2\sqrt{2}) \quad (86)$$

and $$EI_{QQ}p_0(\pi/L)^2 = Pp_0 \quad (87)$$

are fulfilled.

The conditions indicate that there are two independent modes of failure, either $p = p_0$, $\phi = 0$ and $q = 0$, which is the case of pure flexural buckling about the minor axis, of $q = q_0$ and $\phi = \phi_0$ $p = 0$, which is a mode in which there is an interaction between bending about the major axis and torsion. The critical load for the first type of failure is Euler's buckling load.

For the second type of failure to occur the two equations, (85) and (86), must be satisfied. To give a non-trivial solution the determinant must be zero, which gives the following characteristic equation

$$(P - P_n)(P - Q_n) + 3P^2/8 = 0 \qquad (88)$$

if the notation

$$P_n = EI_{pp}(n\pi/L)^2$$

and $$Q_n = A((DI_p/t)(n\pi/L)^2 + GJ)/tI_p$$

is introduced. There are two solutions to this equation, hence there are three types of failure in all, one of pure bending, and two of combined bending and torsion.

If we consider the mode in which the torsional displacements predominate, then the torsional critical load Q_n is less than the axial critical load and the critical load is approximately equal to the torsional critical load. The displacement in the QQ direction of any point on the cross-section is $q + r\phi$, where r is the polar ordinate of the point. For the point to be stationary $r = -q/\phi$. From equation (85)

$$q/\phi = A(GJ + 2Pt/3A - 2Db^3\pi^2/3L^2)/Pt ,$$

which is zero when $P = Q_n$. That is the section rotates about the shear centre, which is the assumption used when the pure torsional mode was being investigated.

Graph (46) indicates how the lowest critical load varies with the length of the member. The relationships obtained by the simpler model is also indicated, and, as expected, the result it gives is not conservative for slender members. The result obtained from the flexural-torsional mode is more complicated than necessary; for any member where it is necessary to use this model, the term $DI_p/t\ \partial^3\phi/\partial x^3$ may be neglected. However, if this model is adapted for any other cross-section by replacing DI_p/t by a warping constant, then the term cannot be neglected.

It is interesting to note that Timoshenko, in developing his model for torsional-flexural buckling, has taken the longitudinal

stresses as constant, when he considers the torque equilibrium. In the previous calculations the variation in the stresses due to bending has been included and this has produced the equation,

$$P_0\phi_0 = 0 ,$$

which is a redundant equation.

* * * *

Eccentric Loading

Both Timoshenko and Goodier have produced models for the buckling of members experiencing axial loads and end moments. Although the approaches adopted differ, the assumptions are the same, and so are the resulting differential equations. Both assume that the longitudinal stresses depend only upon the applied loads. Goodier gives the three equations of statics as

$$EI_{QQ}\,\partial^2 p/\partial x^2 + Pp + M_Q\phi = - M_Q , \tag{89}$$

$$EI_{pp}\,\partial^2 q/\partial x^2 + Pq + (M_p + Pb/2\sqrt{2})\phi = - M_p , \tag{90}$$

and

$$DI_p/t\;\partial^3\phi/\partial x^3 - (GJ - M_p 7b/4\sqrt{2} - PI_p/A)\,\partial^2\phi/\partial x^2 + + M_Q\,\partial^2 q/\partial x^2 - (Pb/2\sqrt{2} + M_p)\,\partial^2 p/\partial x^2 = 0 . \tag{91}$$

Both Timoshenko and Goodier assume that the graphs of the deformations p, q and ϕ against the loads are asymptotic to a given load condition. At a load near the critical load the equations of statics, stated above, are satisfied. If p', q' and ϕ' now denote the change in deformations from this state, the new equations of statical equilibrium have zeroes on the right hand side, as the change in the loads is negligible. In making this assumption the problem has been forced into an eigen value problem. Thus while the load-deformation relationships obtained will be erroneous, the critical loading conditions obtained should approximate to the asymptote of the real relationship.

The end moments of the models tested have been applied by means of an eccentric load, thus, if the moments are $M_p = - Pe_p$ and $M_Q = - Qe_Q$ the critical conditions become

$$EI_{QQ}(\pi/L)^2 p_0 - Pp_0 + Pe_Q\phi_0 = 0$$

$$EI_{pp}(\pi/L)^2 q_0 - Pq_0 - P(b/2\sqrt{2} - e_p)\phi_0 = 0$$

and $$DI_p(\pi/L)^3\phi_0/t + (GJ - 7M_p b/4\sqrt{2} - PI_p/A)(\pi/L)^2 + + (Pb/2\sqrt{2} - Pe_p)p_0(\pi/L)^2 = 0 .$$

It should be noted that when the load is eccentric about both axes all three types of instability are combinations of the torsional modes and the flexural modes about both axes. The three critical loads are the solutions to the cubic, characteristic equation obtained from the determinant of the above equations.

For the case where $e_Q = 0$, the characteristic equation is

$$(P_n - P)(Q_n I_0/A - P(I_0/A - 7be_p/4\sqrt{2})) - P(b/2\sqrt{2} - e_p)^2 = 0 . \quad (92)$$

The critical load is infinity when the eccentricity is approximately $0.38b/\sqrt{2}$, which compares well with $b/3\sqrt{2}$ for the simpler model.

When $e_p = 0$ the characteristic equation condenses to

$$(P - P_n')((P - Q_n)(P - P_n) - P^2 e_p{}^2 A/I_0) + Pb^2 A(P - P_n)/8I_0 = 0 ,$$

which indicates that the lowest critical load is not independent of bending about the major axis, as obtained from the simpler model. P_n' is the other flexural critical load. However, if the characteristic equation is expressed in the form

$$P = Q_n - PA/I_0(e_p{}^2/(P_n'/P - 1) + b^2/8(P_n/P - 1)) ,$$

it follows that as the ratios P/P_n' and P/P_n tend to zero, as would be the case for a torsionally weak member, the critical load tends to the critical load for the torsional mode of a column loaded through the centroid.

This section of the thesis has extended the mathematical model to make it more applicable to members met frequently in engineering practice. It has also shown that the simpler model is the limiting case of the more complex model.

SUMMARY

In this chapter has been established mathematical models to describe the behaviour of the columns tested by the author. Although each mathematical model has been discussed at the end of each major section of the chapter, it is thought worthwhile to briefly summarize

the chapter.

Mathematical models have been developed to describe the buckling mode of short columns loaded with an axial load, with an end moment about the minor axis, or an end torque. The second mathematical model is recommended as the most practical model.

The next section of the chapter deals with columns loaded through one leg. While the mathematical models developed are really only relevant to the type of member tested, that is angle-cross-sections with little or no fillets, the mathematical models indicate two things. The assumption that the cross-section does not distort when the column is loaded eccentrically about the major axis is a non conservative estimate. The second point is the actual manner in which the load is applied, or the longitudinal stress distribution near the ends, has no important effect on the overall buckling mode and load of the member. However, end connections are important as far as regards secondary effects, such as local buckling due to high stress concentrations or weakness in the metal due to heating.

The third section develops a mathematical model describing the flexural-torsional buckling modes of long members. The mathematical model is basically the same as the ones developed by Timoshenko, Bleich and Goodier.

All the mathematical models use the basic functional form of straight lines across the leg of the angle remain straight during buckling, and all the problems are attacked by the same approach.

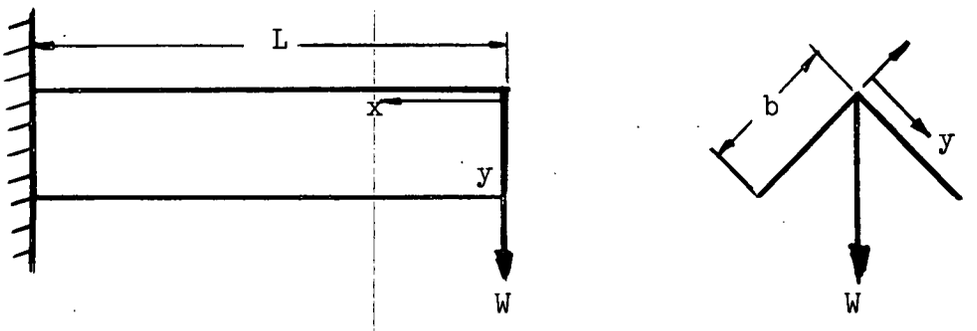

FIGURE 47

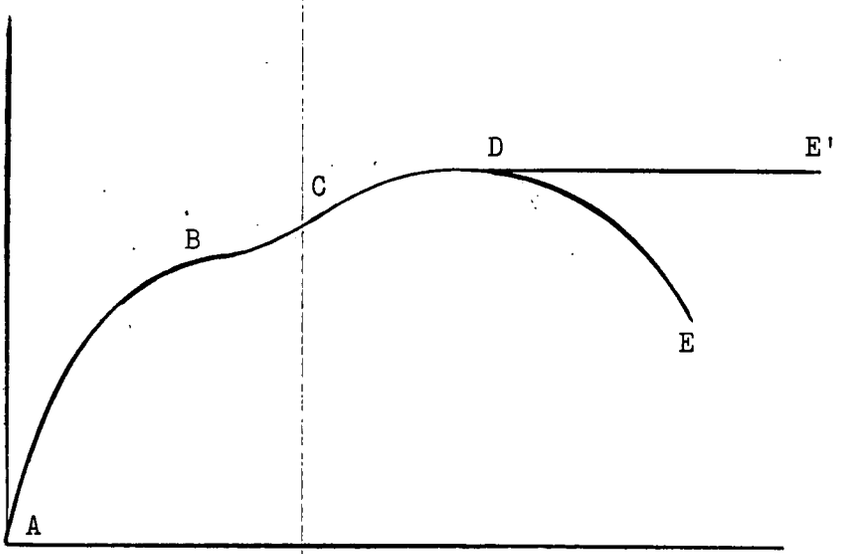

AB - small, elastic deformations
BC - large, elastic deformations
CD - elasto-plastic deformations
DE - plastic unloading with a control on the deformation
DE' - plastic collapse

TYPICAL LOAD-END ROTATION RELATIONSHIP FOR A CENTILEVER.

FIGURE 48.

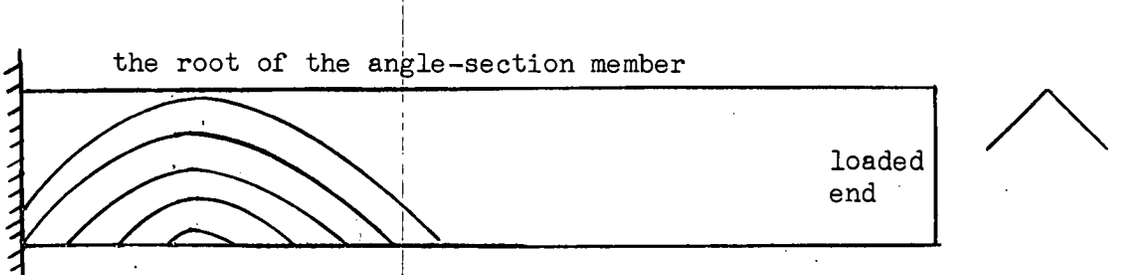

LIGTENBERG FRINGES ($\partial w/\partial x$) for A POINT LOADED CANTILEVER

FIGURE 49

STABILITY OF ANGLE-SECTION BEAMS

This chapter deals with the stability of angle-section beams in bending. The majority of the experimental work associated with this chapter was done on cantilevers. However, the ideas obtained from the results and the mathematical models developed are used to discuss the general stability of angle-section beams and to predict the behaviour in a number of cases. Some simply supported, centrally loaded beams have also been tested. The chapter is limited to the case of bending about the minor axis, although, following the work done on columns with eccentric loads, the effect of bending about the major axis will be discussed.

The members tested failed by local instability, but the failure of members by overall lateral instability is also discussed.

STABILITY OF ANGLE-SECTION CANTILEVERS

To examine the stability of angle-section beams in bending, several cantilevers were tested. When a cantilever was loaded so that compressive stresses were produced at the root of the angle the instability was due to plastic bending deformations and it was found that the failure load could be estimated using the common, fully plastic analysis method for beams.[1] When the outstanding legs of the angle member were in compression, the member was unstable in the elastic range. For the members tested the instability mode was one of pure torsion, the deflections caused by twisting being much larger than those caused by the bending of the member. The loads at which the members failed were considerably smaller than those calculated from the lateral buckling model of Timoshenko.[2] The mode obtained was due to local buckling of the legs of the angle. The main body of the chapter will be devoted to establishing a mathematical model describing the local buckling mode. The relevance of the lateral buckling mode will be considered at the end of the chapter.

A typical graph of load against total rotation is shown in fig. 48. The graph can be divided into four sections. In section AB the

---

Ref. 1 J. Baker, M. R. Horne, J. Heyman: "The Steel Skeleton", Vol. II, Cambridge University Press.
Ref. 2 S. P. Timoshenko: "Theory of Elastic Stability".

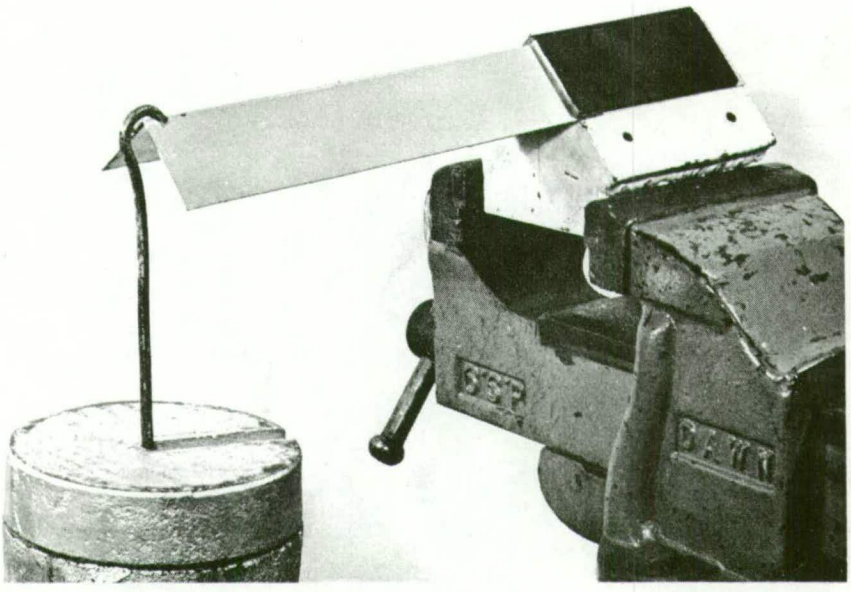

The loading of an angle-section cantilever.

FIG. 50

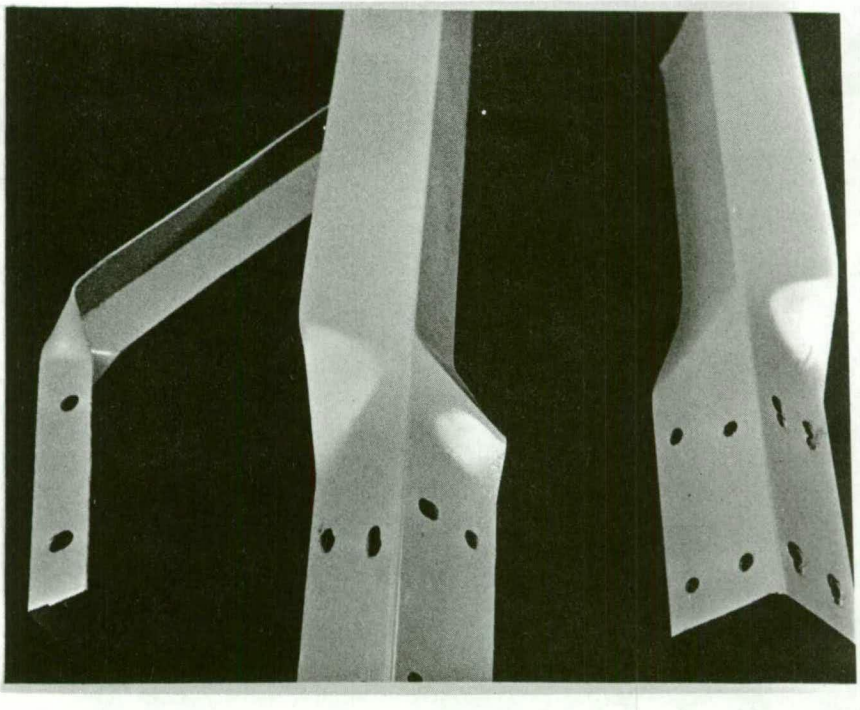

The plastic deformations of a cantilever. The member on the left has been allowed to collapse without any control on the deformations.

FIG. 51

rotations are small and the section rotates in an un-deformed state. In section BC the rotations are large but elastic. In section DE most of the deformation takes place in a relatively short length and the cross section experiences plastic distortion. The plastic mode is shown in fig. 51. An isosceles triangle is seen in both legs. The total rotation is approximately 30°. This mode is independent of the leg width and the length. Section CD is an intermediate state between the elastic large deformation mode and the fully plastic "triangular" mode.

Apparatus

All the angle section cantilevers were bent from 0.050 inch aluminium sheet. For all the members the ratio of the leg-width b to the thickness t far exceeded the allowable structural design code value 16 . Models were tested with various leg-widths b and overall lengths L .

To produce a "built-in" end, each leg of the cantilever was clamped between a flat plate and a side of a vee block as shown in fig. 47. The plates were held securely with four quarter inch diameter bolts. The mounting was such that zero twist $\partial \phi / \partial x$ occurred at the "built-in" end of the cantilever. The models were loaded using dead weights. However, in the plastic range, the deflections were controlled so that measurements could be made while the member unloaded plastically (that is on the downwards sloping part DE of the load-deflection curve).

The loaded shape of a cantilever was measured using the Ligtenberg reflective method. When the Ligtenberg apparatus was used the model was mounted so that one leg was vertical. This necessitated loading the model through a pulley system. Strains at required places on the legs were measured using mechanical, Huggenburger strain gauges. Point rotation measurements were taken using a light source and a small mirror mounted on the model.

Small Deflection, Elastic Mathematical Model

First, the discussion of the problem will be limited to one involving small rotations. The mathematical model will attempt to

describe section AB of the load-deformation graph. The elastic, small deflection plate theory is relevant, and the results derived in appendix A, will be employed. The Ligtenberg moire fringes show that all sections rotated without deformation of the cross-section. They also show that for some members only part of the member twisted. The fraction of the cantilever which deformed depended upon the ratio of the leg width to the length. This fraction decreased as the ratio decreased.

To establish the mathematical model the following co-ordinate system is set up. The co-ordinate is measured along the cantilever from the free end and the y co-ordinate is measured across the leg from the root of the angle. The deformations out of the plane of the leg are denoted by w and the rotations, that is $\partial w/\partial y$, by ϕ (see fig. 47). A basis for the mathematical model will be $w = y\phi(x)$, where $\phi(x)$ is a function of x only. The longitudinal stresses N_x will be linear in y and unaffected by the deformations. Initially the unloaded member will be taken to be straight. The expression for the shear stresses, Q_x derived in Appendix A under these conditions becomes

$$Q_x = - D \partial^3 w/\partial x^3 - N_x \partial w/\partial x + D(1 - \nu)\partial^2 w/\partial x \partial y - $$

$$- M_{xy} \partial w/\partial y .$$

From the moment equilibrium and the axial force equilibrium on a section, x constant, the longitudinal stresses are

$$N_x = Wx(y - b/2)/I_{QQ}\sqrt{2} , \qquad (93)$$

where W is the point load applied at the end of the cantilever. The torque equilibrium about the x-axis produces the differential equation,

$$(2b^3D/3)\,\partial^3\phi/\partial x^3 + (b^4tWx/6\sqrt{2}I_{QQ})\partial\phi/\partial x - GJ\,\partial\phi/\partial x = 0 \qquad (94)$$

which can be simplified to

$$\partial^3\phi/\partial x^3 + dx\,\partial\phi\,\partial x - a\partial\phi/\partial x = 0 \qquad (95)$$

by substituting $d = Wbt/42DI_{QQ}$ and $a = 3GJ/2b^3D$.

The stability of the differential equation can be investigated

by examining the adjoint properties of the equation, as explained in the chapter on buckling. The differential equation is of the form

$$\partial^2\phi/\partial x^2 + x\lambda W\phi + \gamma\phi = 0 .$$

If ϕ_r and ϕ_s are any two solutions of the differential equation which also satisfy the boundary conditions; $\phi = 0$ at $x = 0$ and $x = L$ then the integrals

$$\int_0^L \phi_r(\partial^2\phi_s/\partial x^2 + \gamma\phi_s) - \phi_s(\partial^2\phi_r/\partial x^2 + \gamma\phi_r)dx$$

and

$$\int_0^L x\phi_r\phi_s - x\phi_s\phi_r \, dx$$

are zero if the equation is self adjoint. The second integral is zero and the first simplifies to

$$\int_0^L (\phi_r \partial^2\phi_s/\partial x^2 - \phi_s \partial^2\phi_r/\partial x^2) \, dx ,$$

which on integration by parts leads to

$$\phi_r \partial\phi_s/\partial x \Big]_0^L - \phi_s \partial\phi_r/\partial x \Big]_0^L + \int_0^L (\partial\phi_s/\partial x)(\partial\phi_r/\partial x) -$$

$$- (\partial\phi_r/\partial x)(\partial\phi_s/\partial x) \, dx .$$

Under the boundary conditions the second integral takes the value zero. Hence the differential equation is self adjoint and there are an infinite number of orthogonal, eigen functions and eigen values (P_r, ϕ_r) . That is, the mathematical model predicts that the rotation is zero for all loads except the eigen values, at which loads the rotation is infinite.

When the member has an initial crookedness ϕ_0 the differential equation can be expressed in the form

$$\partial^2(\phi - \phi_0)/\partial x^2 + \gamma(\phi - \phi_0) + xW\lambda\phi = 0 .$$

From the self-adjoint properties of the differential equation of the initially straight member it follows that the initial shape can be expressed as a unique sum of the orthogonal eigen functions,

$$\phi_0 = \sum_{r=1}^{\infty} A_r\phi_r$$

and the shape ϕ for any initially crooked member is

$$\phi = \sum_{r=1}^{\infty} \frac{A_r}{1 - W/W_r} \phi_r \, .$$

Physically, this means that the rotation tends to infinity as the load approaches the lowest eigen value.

The differential equation (95) can be solved directly. An expression for the lowest critical load, or eigen value, will now be obtained. The solution of the equation is

$$\partial \phi/\partial x = A_1 \sqrt{dx - a}\, J_{1/3}(2(dx - a)^{3/2}/3d) + A_2 \sqrt{dx - a}\, J_{-1/3} (2(dx - a)^{3/2}/3d)) \qquad (96)$$

where A_1 and A_2 are constants. It can be seen that for small x this expression is immaginary as $dx - a$ is negative. If $d(L - l) - a = 0$, then we define l as the effective length over which the member deforms. For $x = L - l$ it is assumed that $\partial\phi/\partial x = 0$. From the moire fringe photographs (fig. 49) the boundary conditions are $\partial\phi/\partial x = 0$ at $x = L$ and $x = L - l$. The second condition gives $A_2 = 0$, as $J_{-1/3}(0) = \infty$, and the first condition gives

$$2(dL - a)^{3/2}/3d = 2.9 \, , \qquad (97)$$

as 2.9 is the first zero of the Bessell function of the one third order. This implicit equation can be solved for the critical load. The other eigen values can be obtained by replacing 2.9 by the appropriate zero of the Bessell function.

As an example consider a cantilever with $b = 2"$, $t = 1/20"$, $L = 10.25"$, $E = 10^7$ and $\nu = 0.3$. Then

$$a = 3GJ/2b^3D = 6(1 - \nu)/b^2 = 1.05$$

and

$$d = 3W/2b^2D = 0.00464 \, .$$

The implicit equation can be solved by trial and error to give $W_{crit} = 41$ pounds. The length of the member which is distorted is

$$l = L - a/d = 10.25 - 1.05/0.00464 = 4.5" \, .$$

These values compare well with the experimental values of 40 pounds and 4.75". The shape predicted mathematically is compared graphically with the one obtained experimentally on graph 52. The

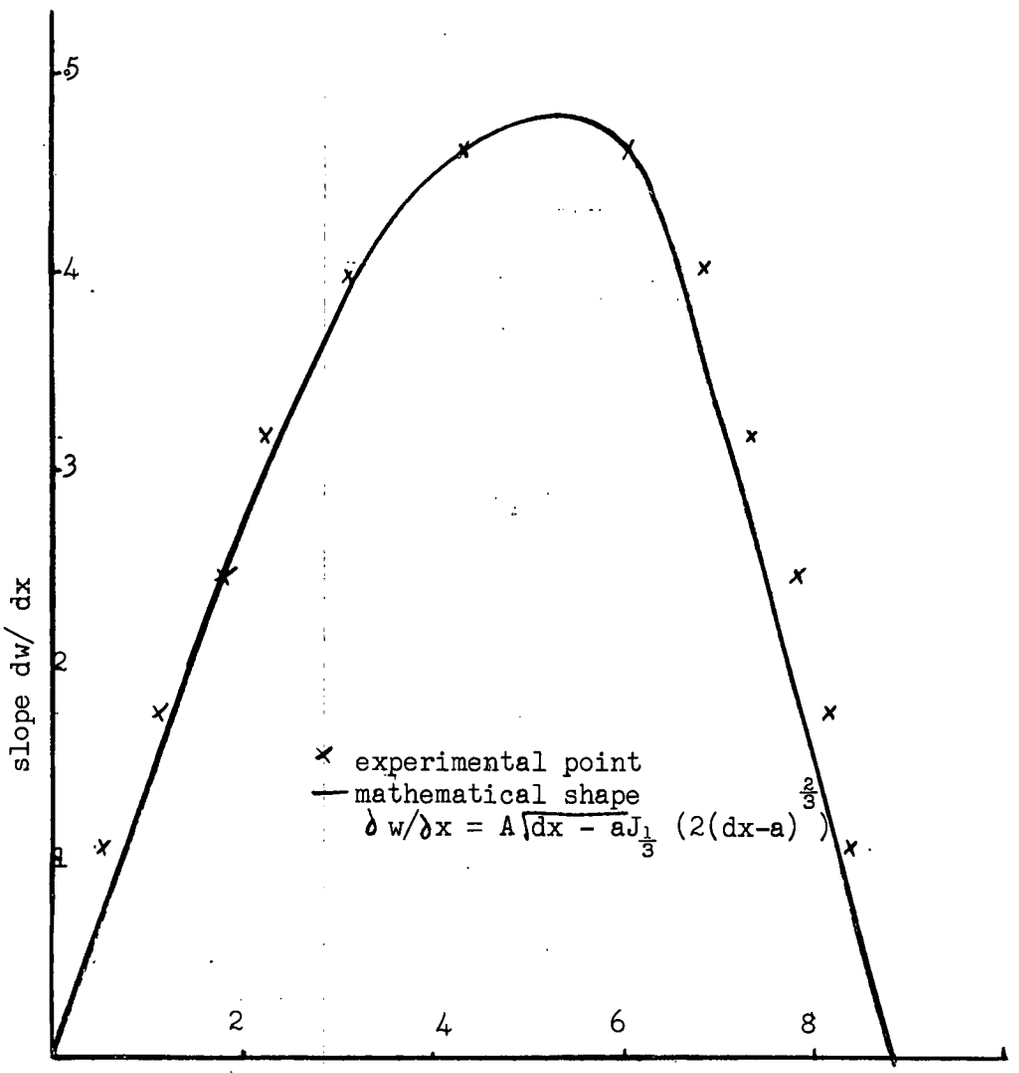

COMPARISON OF EXPERIMENTAL AND MATHEMATICAL SHAPE OF A 2" x 2" x 1/20" ALUMINIUM CANTILEVER, LENGTH L = 10.25"

FIGURE 52

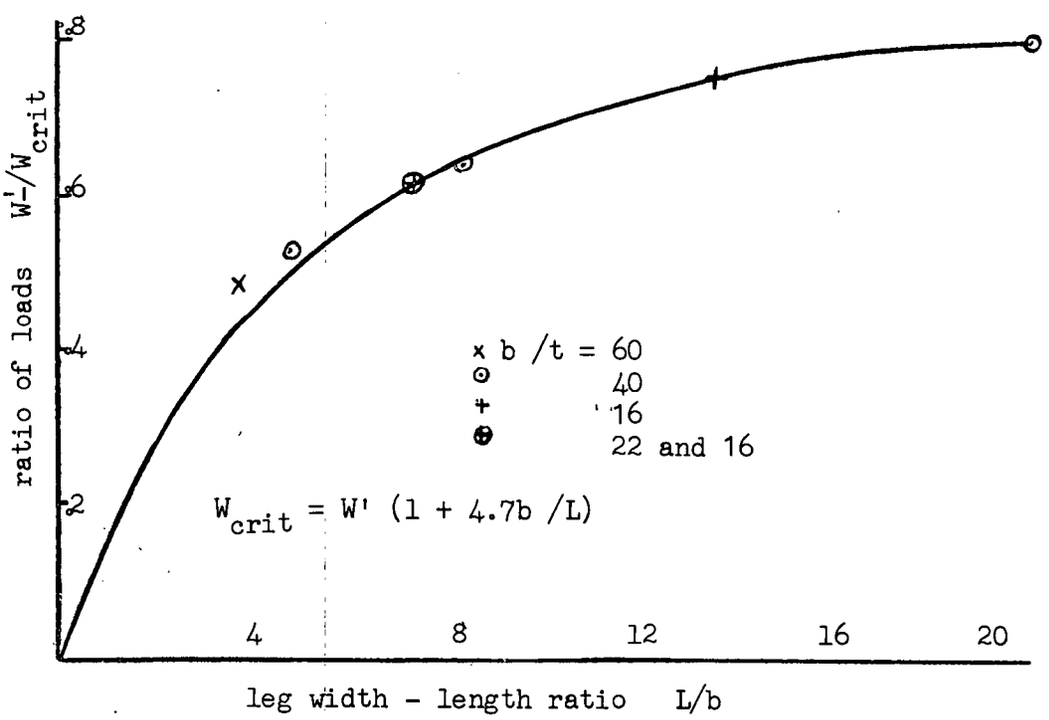

NUMERICAL DETERMINATION OF APPROXIMATE EXPRESSION FOR THE CRITICAL LATERAL LOAD

FIGURE 53.

agreement between the two shapes is acceptable although the following table indicates the agreement is not always as good.

length L inch	leg width b inch	thick-ness t inch	b/t	L/b	P_{crit} (lbs)	P'/P_{crit}	effect-ive length l	measured length l
12.5	3	0.05	60	4	36.5	0.50	6.2	7.4
10.25	2	0.05	40	5	41	0.54	4.70	4.75
18	2	0.05	40	9	19	0.66	6.1	6.9
41.5	2	0.05	40	20.5	6.8	0.80		
60	4	0.25	16	15	62.5	0.77		
30	4	0.25	16	7.5	1400	0.63		
6	0.8	0.037	22	7.5	110	0.63		

From inspection of the implicit equation (97) it is obvious that

$$W' = 2\sqrt{2}(1-\nu)D/L$$

is a lower bound to the critical load. The ratio of the lower bound to the critical load has been calculated for various sections. The ratios appear in the above table. It has been found that, as a first approximation, the ratio is independent of the leg-width to thickness ratio b/t, but varies with the length to leg-width ratio L/b. The ratio is plotted against L/b on graph (53) for various b/t. The algebraic expression for the relationship is

$$\frac{W_{crit}}{W'} = \frac{L/b}{L/b + 4.71}$$

or

$$W_{crit} = W'(1 + 4.7b/L) .$$

This leads to an approximate expression for the critical load.

$$W_{crit} = 2\sqrt{2}(1-\nu)D\,(1 + 4.7b/L)/L . \qquad (98)$$

Although the approximate formula was derived empirically, a numerical justification can be made. If the load is found by an iterative process it becomes

$$W = a/dL,$$

then $$W = a(1 + 1.65\,(b/L)^{2/3})/dL,$$

and then $$W = a(1 + 1.65\,(b/L)^{2/3}(1 + 1.65\,(b/L)^{2/3})^{2/3})/dL,$$

or in simple terms $$P = (a/dL)\ (\text{a function of } b/L) .$$

For most practical members the function of b/L is the function

$$1 + 4.7b/L \ .$$

For members with large length to leg-width ratios, an approximate functional form is

$$\partial w/\partial x = ay \cos (x - L - 1)/l \ .$$

This is the functional form if it is assumed that the longitudinal stresses are constant over the deformed length,

$$N_x = W(L - 1/2)(y - b/2)/I_{QQ} \sqrt{2} \ .$$

The approximate functional form is used in the following sections to obtain approximate values of rotation from the experimental values of twist.

Elastic, Large Deflection Mathematical Model.

The rotation of the member does not run away to infinity at the critical load as shown by the first model. In fact the stiffness of the member increases if the member is loaded above the critical load. In an earlier chapter on twisting of an angle section member, it was shown that longitudinal strains are developed during twisting. The expression for these strains is

$$\epsilon_x = (\partial \phi/\partial x)^2(r^2/2 + b^2/12 - by/2)$$

(see equation 25). The following calculation will indicate the relative magnitudes of the strains due to twisting and the strains due to bending of a cantilever. The cantilever measured had the following dimensions, leg-width = 2" , thickness = 1/20" and length = 18" . The strain due to bending given by the linear bending model is

$$\epsilon_x = My/I_{pp}E = 6WL/\sqrt{2}b^2tE$$

$$= 3.4P \times 10^{-4}$$

To calculate the twist at the point of measurement the approximate functional form is used

$$\phi = a(\cos \pi x/l + 1)$$

or

$$\partial\phi/\partial x = \theta \pi/2l \sin \pi x/l \ ,$$

where θ is the total rotation of the end of the cantilever. From

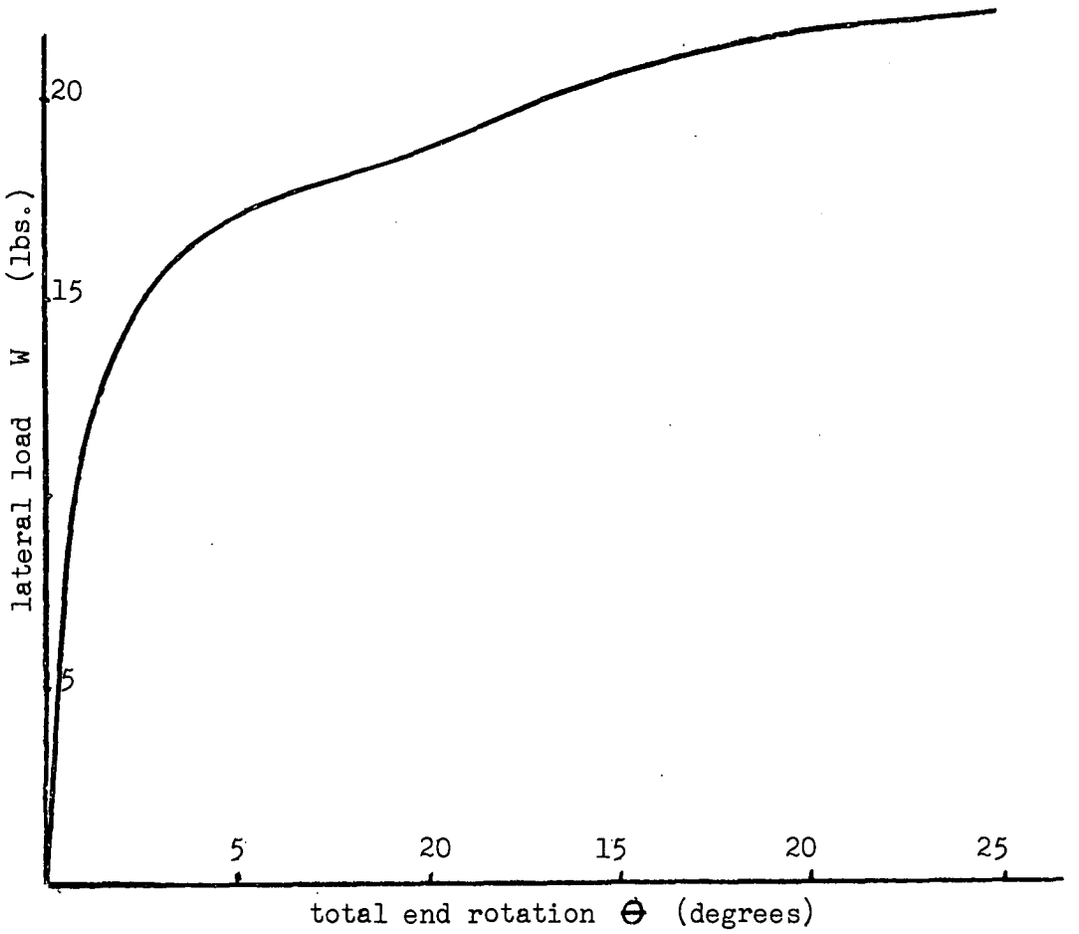

LOAD -END ROTATION GRAPH FOR A 2" x 2" x 20" ALUMINIUM CANTILEVER, 18" LONG.

FIGURE 54.

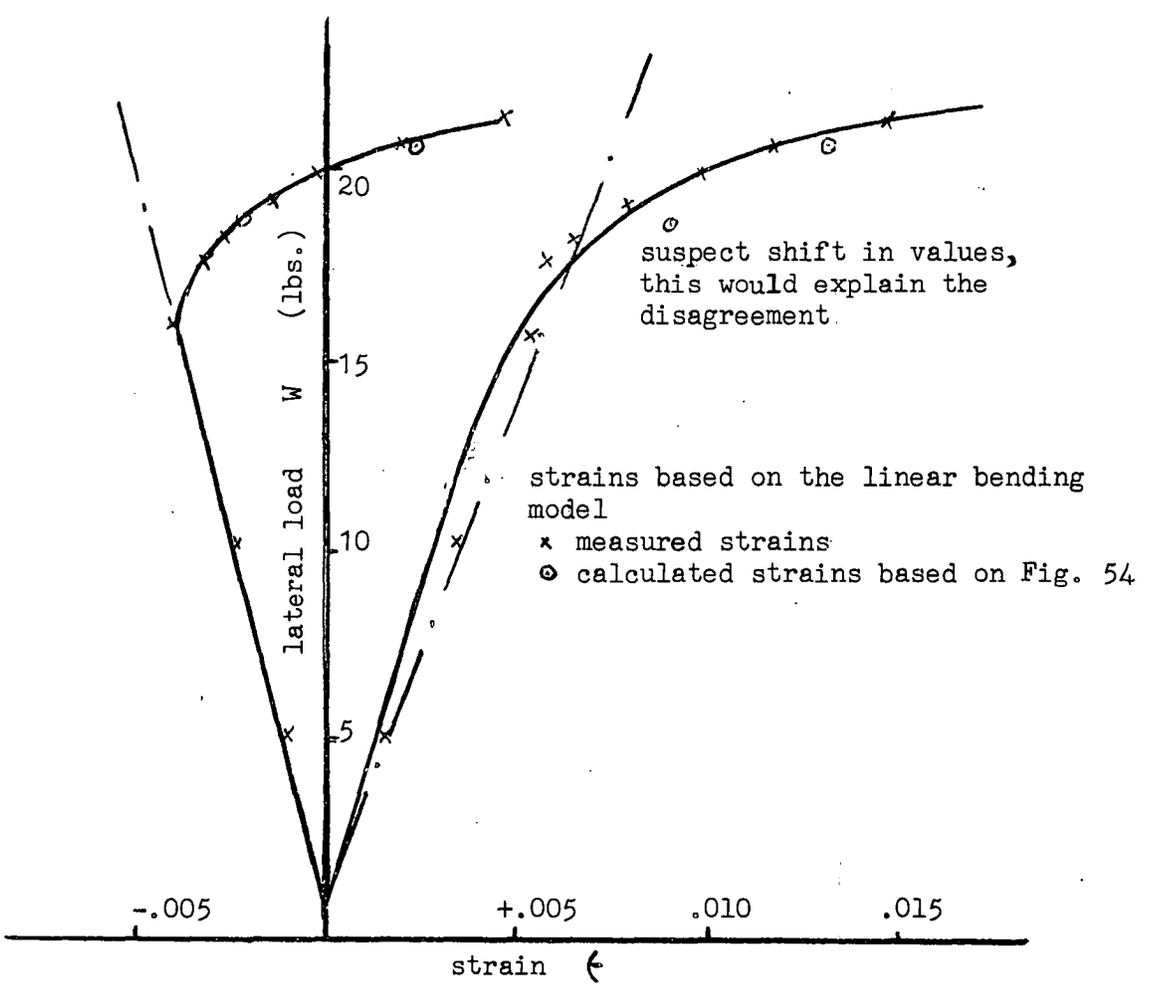

LOAD -STRAIN GRAPH FOR TWO POINTS ON A 2" x 2" x 1/20" ALUMINIUM CANTILEVER, 18" LONG

FIGURE 55.

the load-rotation graph for the values of the end rotation for the loads 19, 21 and 21.5 pounds, are 10^{o}, 16^{o} and 19^{o} respectively. See graph 54.

For P = 21 pounds, $\theta = 16^{o} = 0.28$ rads, therefore $\partial\phi/\partial x = (0.28/2)(\pi/7) \sin(2\pi/7) = 0.049$, therefore $t_x' = (0.049)^2/3 = 0.0008$. At a load of 21.5 pounds the maximum strain is 0.0015 and at 19 pounds it is 0.0003.

The experimental and calculated strains are compared in graph 55. As was to be expected, the twisting strains are of the same order as the bending strain near the critical load. Consequently the small deflection model breaks down. It should be noted that the load at which the twisting strains become important depends upon the initial crookedness of the member.

If the twisting strains are taken into account, the moment about the shear centre of the w-component of the longitudinal stresses must be modified. The integral becomes

$$\int_0^b N_x y\, \partial w/\partial x\, dy = (Wxb^4/6\sqrt{2}\, I_{QQ})\, \partial\phi/\partial x + Eb^5 t(\partial\phi/\partial x)^3/180 .$$

The approximation for the curvature $K_x = \partial^2 w/\partial x^2$, is still applicable even for the largest twist measured, which is of the order of 0.05 rads. per inch. When this integral is included the differential equation describing an initially straight member becomes

$$(DI_p/t)\,\partial^3\phi/\partial x^3 + (Wxb^4 t/6\sqrt{2}\, I_{QQ} - GJ)\,\partial\phi/\partial x + Eb^5 t(\partial\phi/\partial x)^3/180 = 0 \qquad (99)$$

No solution has been found for this equation. However, for the members with large leg width-thickness L/b ratio an approximate model could be established, if it is assumed that the longitudinal bending stresses do not vary within the deformed length of the member. In this case, the large deflection model for a column could be used to obtain an approximate load deformation relationship.

Fully Plastic Mathematical Model

As the deformations become large, the material yields and plastic effects become pronounced. The cross section distorts and finally the member collapses, or unloads if it is loaded so that the

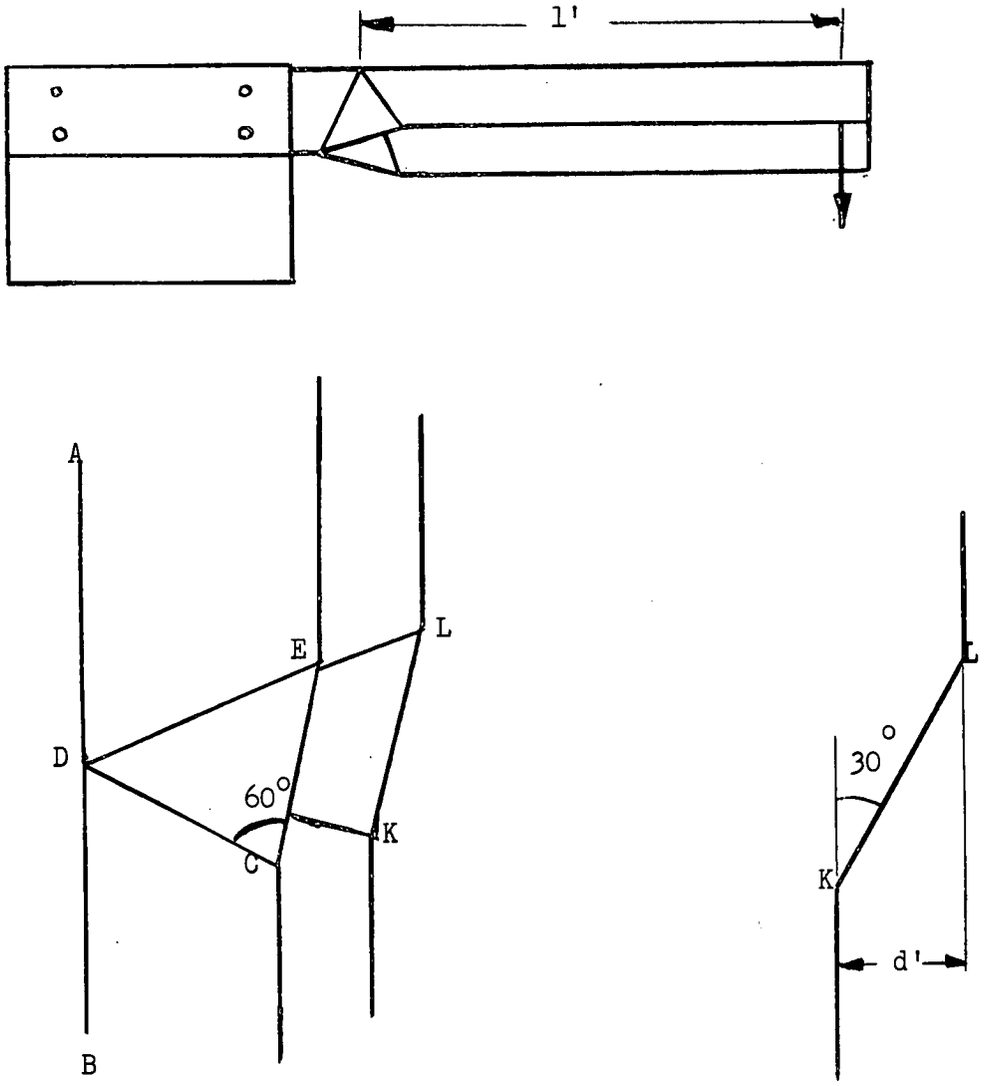

PLASTIC MODE OF COLLAPSE OF A CANTILEVER

FIGURE 56

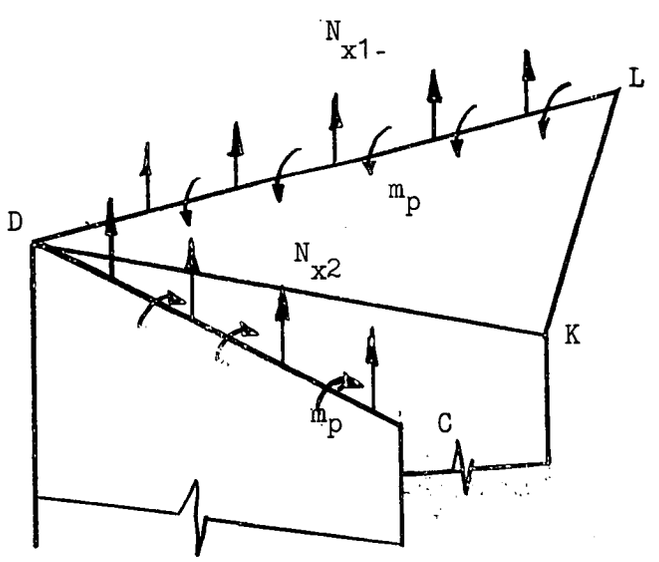

THE INTERNAL ACTIONS ON A PLASTIC HINGE

FIGURE 57

deflections are controlled. The fully plastic mode of failure by buckling is shown in figs. (56) and (57). It is interesting to note that the apices of the triangles form at the plane of maximum twist. Here, the maximum moment is at 45° to the axis. In practice the line of plastic moment is formed at sixty degrees. The difference in the angle is probably due to changes both in the twist and the moment over the deformed length.

A mathematical model was developed for this mode, as it was hoped to produce an upper bound on the load the member can carry. This did not prove successful, as, in most cases, the fully plastic mode was formed after the member partially unloaded. The functional form for the mathematical model as shown in fig. 56. Both triangles DEC and DLK are isosceles triangles and the lines EC and LK are both at thirty degrees to DA . The line ADB remained straight when the mode was first formed. The mode was the same for all the different members considered.

Using the notation, that N_{x1} and N_{x2} are the longitudinal stresses in the two legs on either side of the "plastic hinge", l' is the distance from the load to the apex of the triangle, d is the maximum displacement and m_p is the plastic moment per unit length, the following equilibrium equations are obtained:

The moment equilibrium about the minor axis for the material to the left of CDK gives

$$2\int_0^b N_{x1} p \, dy = Wl' + 4bm_p \cos 60^{\circ}/\cos 60^{\circ} . \qquad (100)$$

The moment equilibrium about the minor axis for the material to the left of CDL gives

$$2\int_0^b N_{x1} p \, dy + 2\int_0^b N_{x2} p \, dy = 2Wl' . \qquad (101)$$

Vertical stress resultant equilibrium gives

$$\int_0^b N_{x1} \, dy = -\int_0^b N_{x2} \, dy . \qquad (102)$$

Now consider moment equilibrium on triangle DEC , and we obtain

$$\int_0^b N_{x1} \, dy/2b \, dy + \int_0^b N_{x2} \, dy/2b \, dy = -2bm_p . \qquad (103)$$

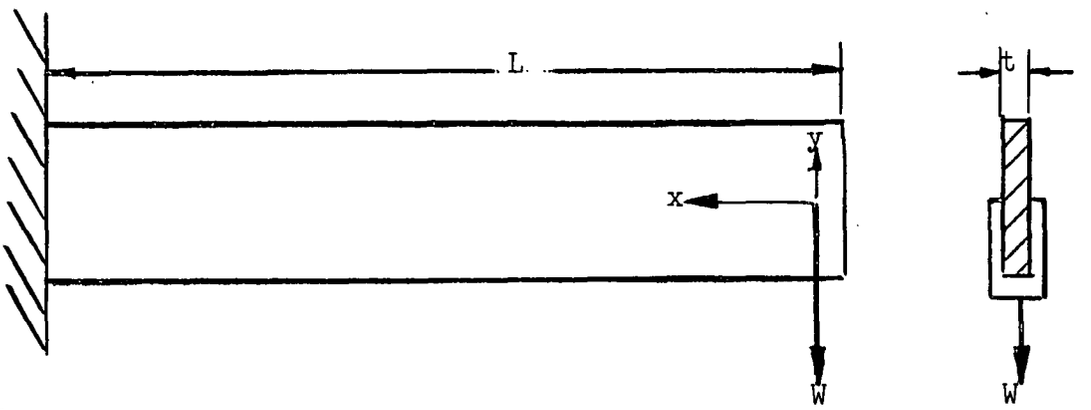

FLAT PLATE CANTILEVER

FIGURE 58.

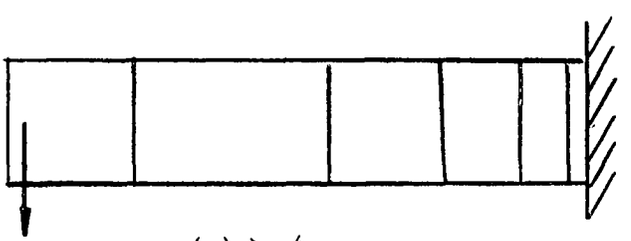

(a) $\partial w/\partial y$

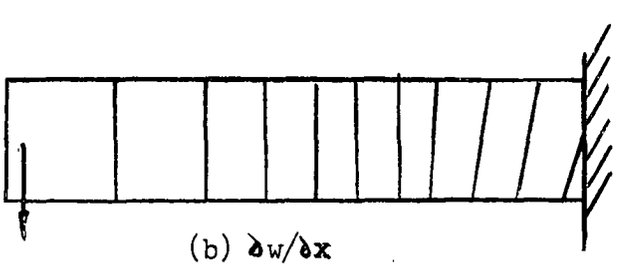

(b) $\partial w/\partial x$

..he Ligtenberg fringes predicted by Timoshenko's model of lateral buckling of a cantilever

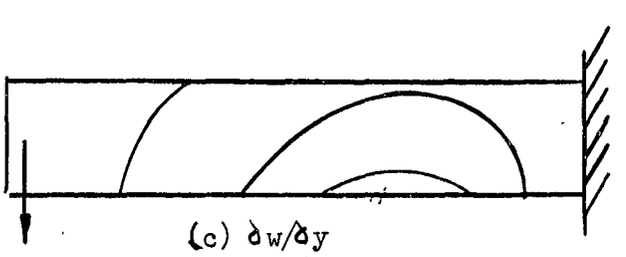

(c) $\partial w/\partial y$

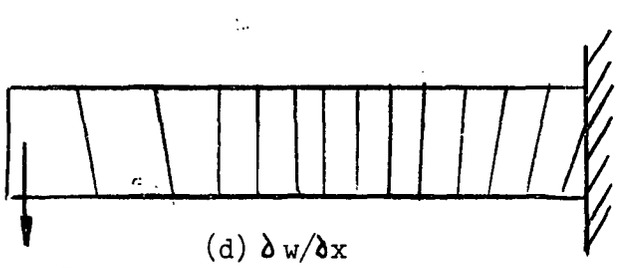

(d) $\partial w/\partial x$

The Ligtenberg fringes obtained experimentally

FIGURE 59.

If equations (100), (101), (102) and (103) are combined, and we note that $y = \sqrt{2}p + b/2$, then

$$d\sqrt{2}W1'/4b + d\sqrt{2}(W1'/2 + 2mb_p)2b = 2bm_p \text{ .} \qquad (104)$$

For a cantilever of length, $L = 10.25"$, and leg width $b = 2"$ and plastic moment $m_p = 12$ pounds per inch, the expression gives the load $P = 23$ pounds, which compares favourably with the measured value of the load 27 pounds. For a cantilever of length forty-three inches the estimated load is 4.9 pounds and the measured value is 6.1 pounds.

LATERAL BUCKLING OF A CANTILEVER

As mentioned before, none of the cantilevers tested failed by lateral buckling. However the members tested would not find general use in practice. All members should be tested both for local buckling and lateral buckling.

Lateral Buckling of a Strip

Timoshenko's lateral buckling model[1] is identical for both an angle-section cantilever and a flat plate cantilever as for both sections the primary warping is neglected. A flat plate cantilever was tested to check the validity of Timoshenko's model (see fig. 58).

Fringes typical of Timoshenko's model are shown in fig. (59) a and b, while fringes which were obtained are shown in fig. (59) c and d. Fig. c indicates that the bending deformations are large compared with the twisting deformations. Fig. d indicates that the built-in end does not prevent warping of the cross-section to any extent, in this respect the boundary conditions agree with Timoshenko's model, which states that the maximum twist is at the built-in end. Fig. d indicates that the cross section has deformed.

The local buckling of the section is due to the variation of the strain across the model due to the applied moment. The same type of local buckling occurred when the author tested a flat plate loaded eccentrically as a column. In the case of the column the function form was

---

Fig. 1 S. P. Timoshenko & Gere: "Theory of Elastic Stability", McGraw-Hill Book Co.

$$w = A(y + B)^2 \sin \pi x/L$$

where A and B are parameters, L is the length, y is measured across the plate and x in the direction of the load. One would expect the distortion of the cross-section of the cantilever to be more prominent than that of the column, as no axial load is present.

The local section deformation appears to be a secondary effect and has no effect on the load capacity of the member. For a 2" × .052" × 9.25" aluminium cantilever with a Young's modulus of 10×1^{6} p.s.i., Timoshenko gives the critical load as

$$P_{crit} = 2Ebt^3/2\sqrt{2(1 + \nu)}\, L^2 \qquad (105)$$

$$= 13.6 \text{ pounds.}$$

The critical load of 13.6 pounds is obtained from the Southwell plot on the bending strains.

Timoshenko gives the critical load for an angle cantilever as

$$4.013Eb^2t^2/3L^2\sqrt{1 + \nu} \quad . \qquad (106)$$

For the sake of the comparison we shall use the approximate local buckling load. For the member to fail by lateral buckling, the following inequality must apply,

$$4.013Eb^2t^2/3L^2\sqrt{1 + \nu} < 2\sqrt{2}(1 - \nu)D(1 + 4.7b/L)/L$$

or $$b/L < (t/b(1 + 4.7b/L)/4.013\sqrt{2(1 + \nu)} \; . \qquad (107)$$

For most extruded aluminium section the ratio of the leg width to the thickness is sixteen, the ratio laid down by steel codes. For such members, lateral buckling will occur if L/b is greater than 104 .

The bending stiffness of the leg of the angle-section member can be taken into account using Timoshenko's model for the lateral buckling of cantilever in which warping of the cross-section is included. Timoshenko gives the buckling load as

$$P_{crit} = Eb^2t^2/3L^2\sqrt{1 + \nu}$$

and quotes values of γ for value ratios of L^2GJt/DI_p or $6(1 - \nu)(L/b)^2$. As the ratio tends to infinity, γ tends to 4.013 . For large ratios Timoshenko gives the approximate relationship

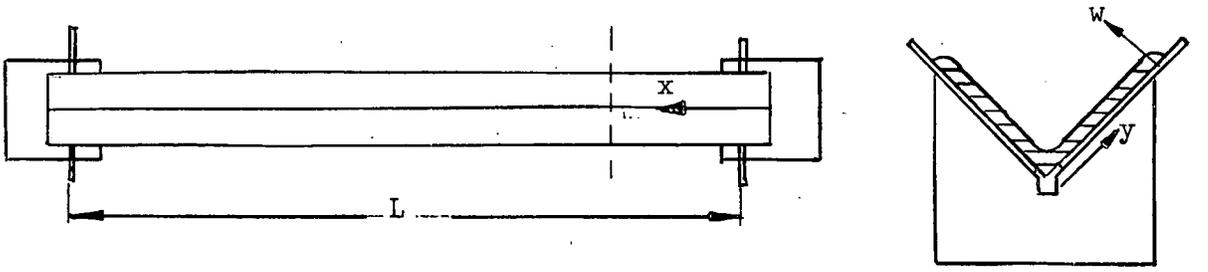

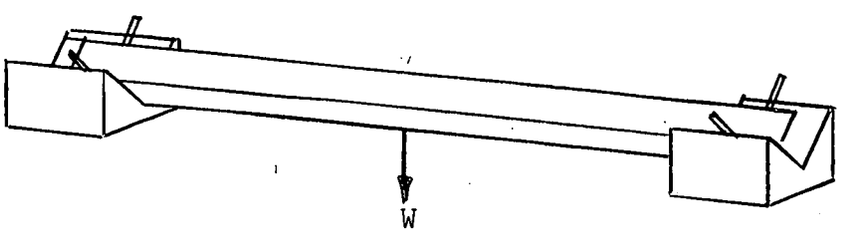

ONE OF THE SETS OF SUPPORTS USED FOR TESTING SIMPLY SUPPORTED BEAMS

FIGURE 62

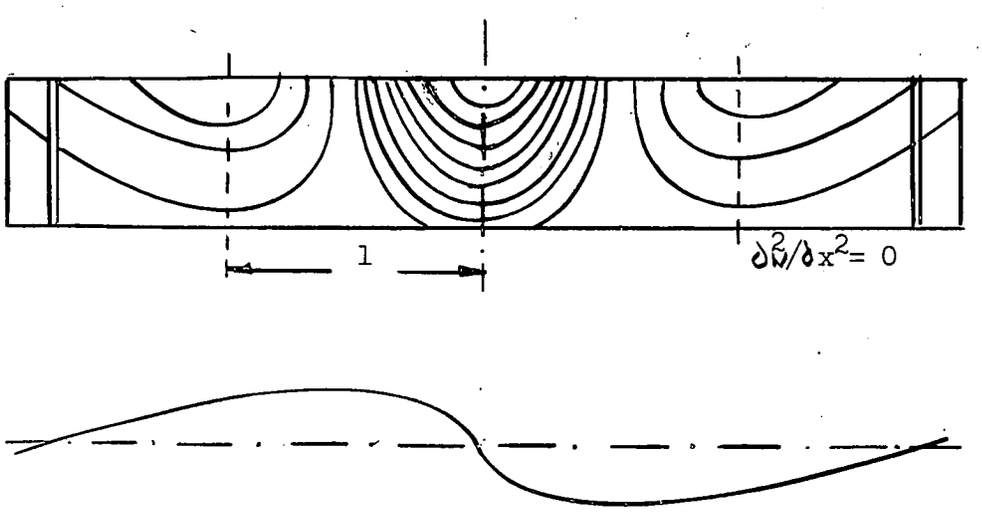

the shape of the free edge of the loaded member

FIGURE 63

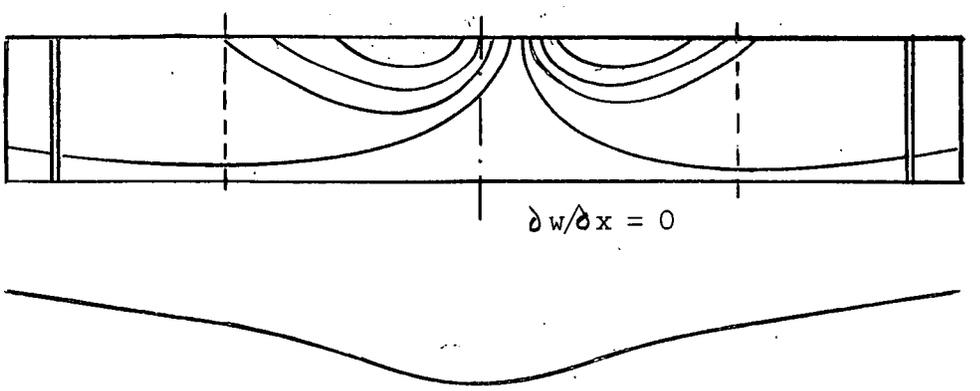

the shape of the free edge of the loaded member

THE LIGTENBERG FRINGES OF $\partial w/\partial x$ OF ONE LEG OF AN ANGLE-SECTION BEAM FOR THE TWO POSSIBLE MODES

FIGURE 64

$$\gamma = 4.013/(1 - b/L\sqrt{6(1 - \nu)})$$

which for practical applications, equals 4.013 . For the more detailed model the twist at the built-in end is zero. Thus there must be a very local change from zero twist to maximum twist in the vicinity of the built-in end.

It is possible to consider the interaction between the local buckling mode and the lateral buckling mode. The three equations of statical equilibrium on a section normal to the axis of the cantilever are

$$EI_{QQ}\,\partial^2 p/\partial x^2 + Px = 0$$

$$EI_{pp}\,\partial^2 q/\partial x^2 + Px\phi = 0$$

and $DI_p/t\,\partial^3\phi/\partial x^3 - GJ\partial\phi/\partial x + Plx\,\partial q/\partial x + P(q_1 - q) +$

$$+ (Plb^4t/6\sqrt{2}I_{QQ})\partial\phi/\partial x = 0 ,$$

which combine to give

$$DI_p/t\,\partial^4\phi/\partial x^4 + (PLb^4t/6\sqrt{2}\,I_{QQ} - GJ)\partial\phi/\partial x - P^2x^2\phi/EI_{pp} = 0 .$$

This equation must be solved by an approximate method, and as the equation can not be expressed in a form so that the self adjoint test can be applied, there would appear to be no available indication of the relationship between the approximate eigen value and the true value.

SIMPLY SUPPORTED BEAMS

Central Load

The bending moment diagram for a simply supported, centrally loaded beam is linear. The boundary conditions for the twist are such that half the beam can be considered as a cantilever. The maximum bending moment for the beam is $WL/4$. Thus the differential equation is

$$b^3D(\partial^3\phi/\partial x^3)/3 + b^4tWx(\partial\phi/\partial x)/12\sqrt{2} - GJ(\partial\phi/\partial x) = 0 , \quad (108)$$

or $$\partial^3\phi/\partial x^3 + (dx - a)\partial\phi/\partial x = 0 ,$$

and the critical load is

$$W_{crit} = 4\sqrt{2}(1 - \nu)D(1 + 9.4b/L)/L . \quad (109)$$

The notation is for a cantilever and is defined in fig. 62.

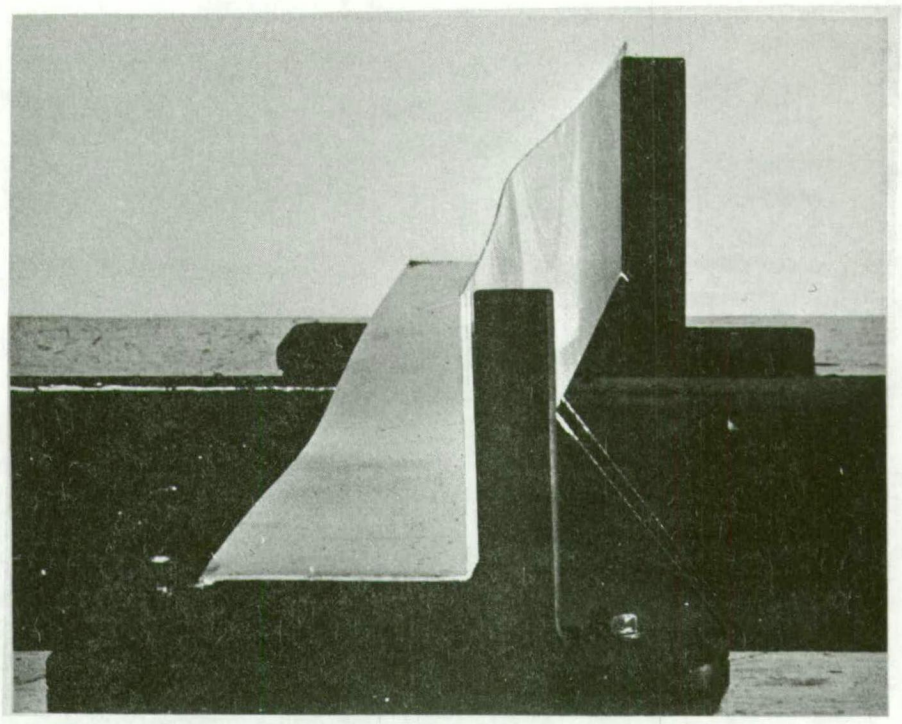

A simply supported beam as arranged when the Ligtenberg apparatus is used to measure the shape. The buckling mode is the elastic symmetric mode.

FIG. 60

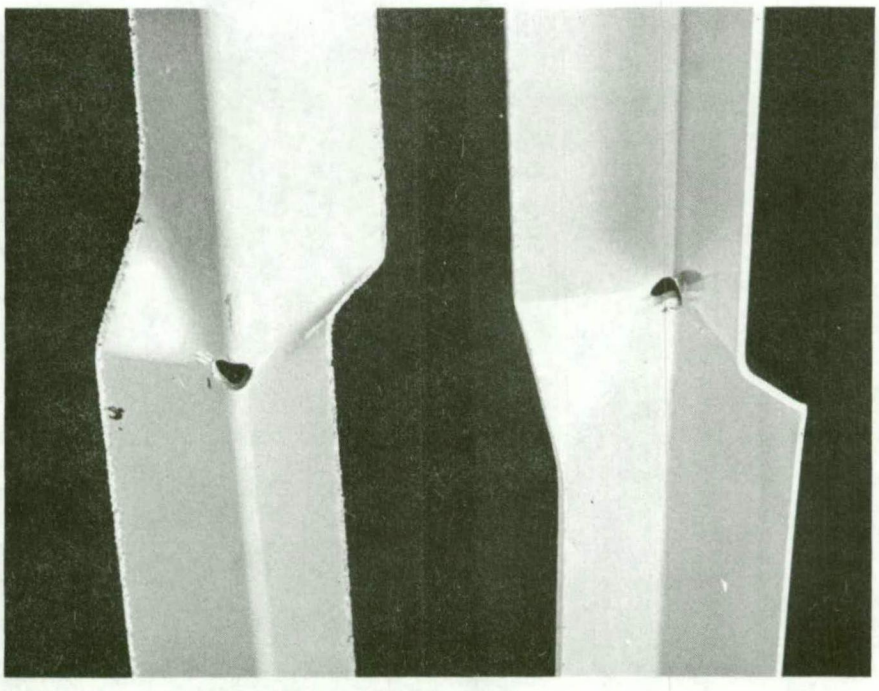

The plastic deformation of a simply supported, centrally loaded beam.

FIG. 61

A few beams were tested under two sets of conditions. One set of supports consisted of rollers in vee-blocks as shown in fig. 62. The alternative set of supports, illustrated in fig. 60, was used in conjunction with the Ligtenberg apparatus. Some experimental results obtained by Gregory were also used to extend the available information. Some of the beams which were tested buckled in the symmetric mode described above, see Ligtenberg fringes in fig. 63. For this mode the implicit equation is

$$2(dL/2 - a)^{3/2}/3d = 2.9 . \qquad (110)$$

(See equation 97.) Other beams buckled in an antisymmetric mode. The fringes obtained are shown in fig. 64. The boundary conditions for this mode are, the moment is zero at the midpoint and at a point where

$$x = a/d .$$

For these boundary conditions the shape is

$$\partial \phi/\partial x = A_2 \sqrt{dx - a}\, J_{-1/3}(2(dx - a)^{3/2}/3d) \qquad (111)$$

(see equation 96) and the implicit equation is

$$2(dL/2 - a)^{3/2}/3d = 3.1 . \qquad (112)$$

The critical loads obtained from equations (110) and (112) are very close in value. Thus the mode the model deforms into depends largely upon the initial shape and the boundary and loading conditions. For the second mode (equation 111) all the beam deforms, although most of the deformations take place in the central region of the beam.

The plastic mode was asymmetric. The mode was triangular and of the same form as the cantilever (see fig. 61). However, because of the asymmetry the relative rotation of the two ends is thirty degrees. To enable this relative rotation to occur, one end of the beam jumps out of its support. For beams with large L/b ratios the elastic deformations are negligible and the failure is catastrophic.

Gregory tested a series of beams in which one parameter, the leg width, varied. The results were suplemented by some tested by the author. The members were tested both with the root of the angle in tension and compression. The members either failed by plastic bending or elastic or plastic buckling. All the members with their

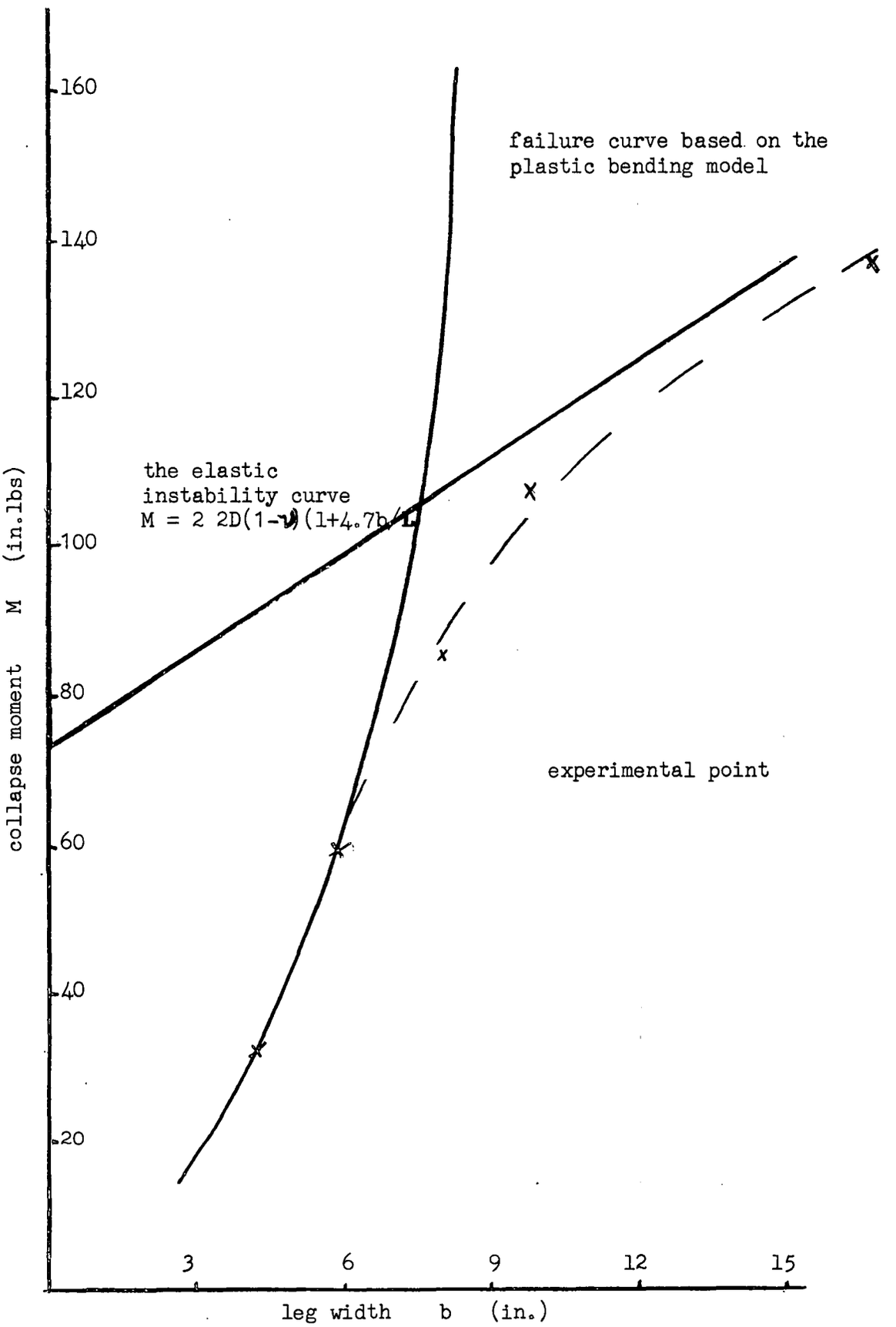

THE COLLAPSE CURVES FOR AN ANGLE- SECTION BEAM OF THICKNESS 0.036" AND SPAN 12"

FIGURE 65

roots in compression attained the plastic moment. In fact, some had added strength due to the opening of the cross-section. For the members with the free edge in compression the failure was either by instability or by plastic deformation. The elastic, instability curve and the fully plastic moment curve are plotted in fig. 65. Both curves are unsafe estimates of the loads carried by the beam. However, most of the beams tested failed in instability mode after the strains were plastic. One way of estimating the critical load is to use the tangent modulus, in the way Bleich has applied it to plates (refer to Conclusions).

Uniform Bending Moment

The local buckling of a beam bending under a uniform moment has been discussed previously in the section on eccentrically loaded columns. However, it will be repeated here briefly for the sake of completeness.

When a bending moment M_Q is applied about the minor axis of the cross-section thelongitudinal stresses are

$$N_x = M_Q t(y - b/2)/\sqrt{2}\, I_{QQ}$$

and the differential equation for torsional equilibrium on a section normal to the axis of the beam is

$$DI_p/t\ \partial^3\phi/\partial x^3 + (M_Q t b^4/6\sqrt{2}\, I_{QQ} - GJ)\partial\phi/\partial x = 0 .$$

The solution to the equation for a beam of length L with simply supported end conditions is

$$\phi = A \sin n\pi x/L$$

and the critical moments are

$$M_{crit} = (DI_p(n\pi/L)^2/t + GJ)6\sqrt{2}\, I_{QQ}/b^4 t ,$$

where n is an integer. The maximum stress at the critical condition is

$$\sigma_c = E(t/b)^2((\pi b/L)^2 + 6(1 - \nu))/6(1 - \nu^2) . \qquad (113)$$

This expression is of the same basic form as for the buckling of a centrally loaded, simply supported beam.

$$\sigma_c = E(t/b)^2(6(1 - \nu^2) + f(b/L))/6(1 - \nu^2), \qquad (114)$$

where $f(b/L)$ is a function of the ratio of the leg width to the length.

When a moment M_p is applied about the major axis and the cross-section rotates as a whole, the critical load is infinite. As for an eccentrically loaded column, two mathematical models can be developed if it is assumed that the cross-section distorts.

COMBINED AXIAL AND LATERAL LOADINGS

In the following section, some ideas are presented which help with the understanding of the behaviour of members under the action of combined axial loads and central lateral loads. The ideas suggested have not been intensively tested and have been included mainly to tie together the work previously presented. Also, this material is presented to indicate the ease with which the basic assumptions of torsional buckling can be extended to most problems.

The beam-columns tested had simply supported end connections and were loaded in an Amsler machine as shown in fig. 66. Initially the aluminium base plates were welded on to the member. However the heat affected the aluminium and the member failed in the regions near each end. The American Society of Civil Engineers Committee investigating aluminium alloys has recommended a separate code to apply within a region of one inch from any aluminium weld. In the code the allowable stresses are reduced considerably near the weld. In the models finally used, the base plate was rivetted to the angle member.

Only beam columns with one set of dimensions were tested. The shape was recorded using the Ligtenberg apparatus. The test was further limited in that only small lateral loads could be applied. The highest lateral load used was sixty pounds.

Previous work has shown that the shape of a simply supported, centrally loaded, beam is antisymmetrical about its central point and the curvature is zero at the centre. However, the deformations of a column are symmetric about the central point and the twist at the centre is zero. Hence there must be a change from one mode to another as the lateral and axial loads are altered.

Measuring the buckling mode was difficult, as it was not

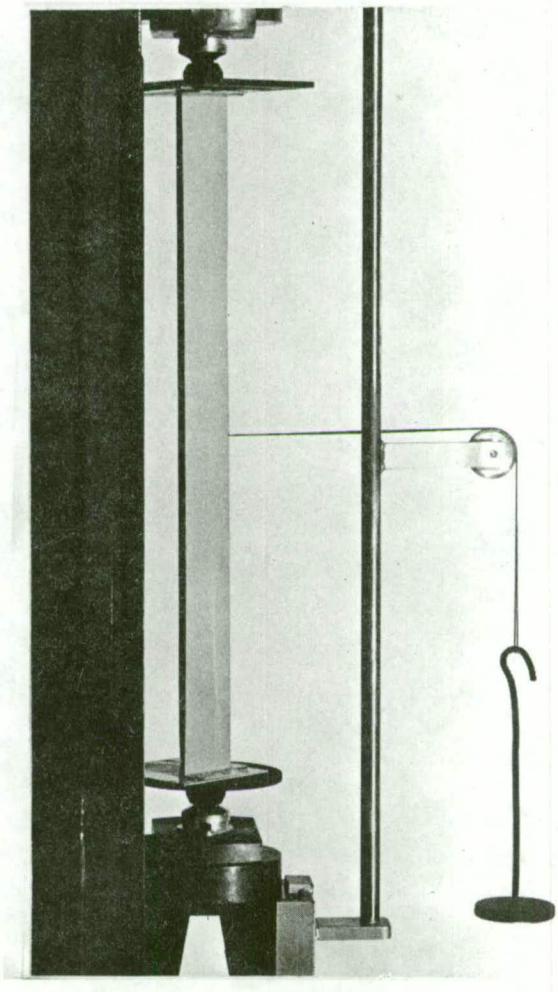

The mechanisms for loading a simply supported column both axially and laterally.

FIG. 66

possible to apply the axial and lateral loads proportionally. With the apparatus used, a large axial load was required before a lateral load could be applied and hence the symmetric component of the shape often predominated, even near the buckling load. A typical progression of shape is shown in fig. 67. For some models, an axial load was applied, then a lateral load and finally the axial load was increased until the critical interaction was obtained. For large lateral loads, the shape is assumed to be the same as for a simply supported beam.

A third mode was often present. As the ends of the beam column were not prevented from rotating the beam often snapped from the symmetric, simply-supported mode into a mode in which half the beam took the same shape as a cantilever, that is there was zero twist at the centre and near the end. The beam column in snapping from one mode to the other experiences a change in load. This is possible as the axial loading machine applies a given strain not a given load.

A mathematical model can be developed for the torsional buckling of a beam column, whose outstanding legs are in compression, if it is assumed that the section rotates as a whole. A differential equation for the member can be obtained by considering the torque equilibrium on a section normal to the axis of the column. The notation used is: x is the ordinate measured from the end of the beam, ϕ is the rotation of the beam, P is the axial load, W is the lateral load and L is the length of the beam. The differential equation is

$$DI_p/t\ \partial^3\phi/\partial x^3 + (PI_p/A - GJ + Wxb^4t/12\sqrt{2}\ I_{QQ})\ \partial\phi/\partial x = 0$$

or

$$\partial^3\phi/\partial x^3 + (dx - a)\,\partial\phi/\partial x = 0\ , \qquad (115)$$

the solution of which is

$$\partial\phi/\partial x = C\ \sqrt{dx - a}\ J_{1/3}(2/3d^{-1}(dx - a)^{3/2}) + D\ \sqrt{dx - a}\ J_{-1/3}(2/3d^{-1}(dx - a)^{3/2})\ .$$

The values of the constants C and D must be determined by considering the boundary conditions.

For small axial loads the mode will be assumed to be the same as for a centrally loaded beam. The curvature is zero at the centre, $x = L/2$, and at

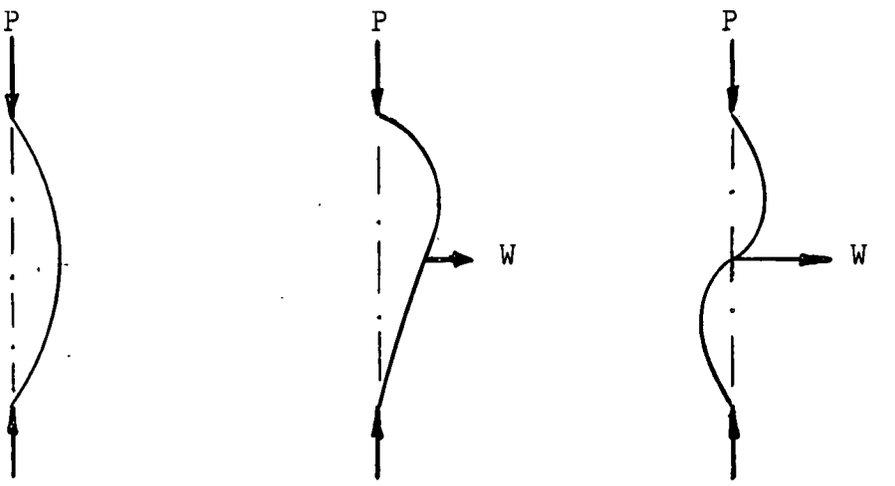

CHANGE IN SHAPE OF THE FREE EDGE OF A BEAM COLUMN AS THE LATERAL LOAD CHANGES

FIGURE 67.

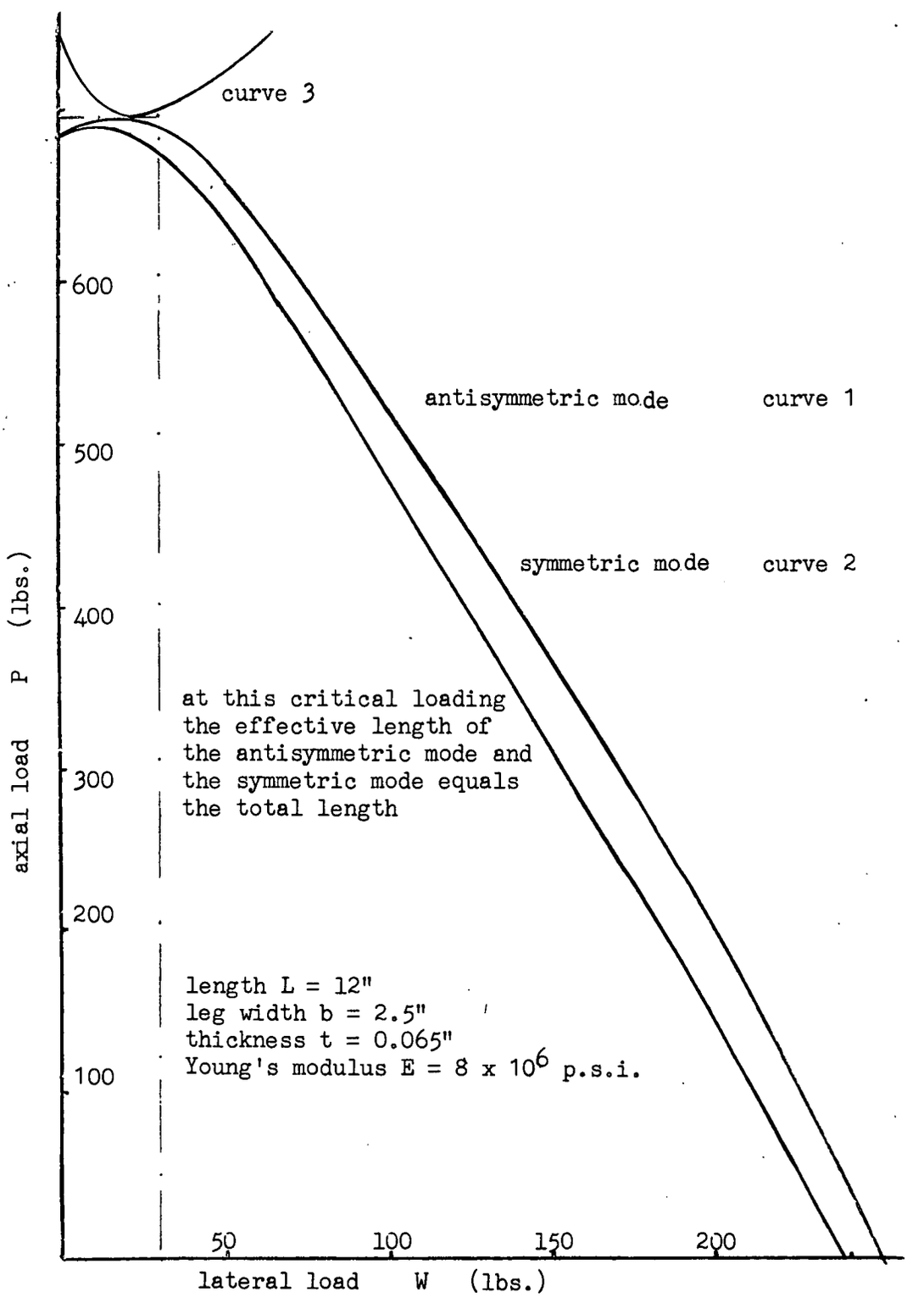

THE INTERACTION CURVE FOR A BEAM COLUMN

FIGURE 68.

$$x = 1 = a/d = (PI_p/A - GJ)12\sqrt{2}\, I_{QQ}/Wb^4 .$$

Thus the constant C is zero and we have

$$2(dL/2 - a)^{3/2}/3d = 3.1 . \qquad (116)$$

For x less than 1 the curvature is unreal. The second condition gives a critical relationship between the axial load and lateral load, and it is assumed to apply provided the quantity 1 is greater than or equal to zero. The relationship is plotted as curve 1 in fig. 68, for a member with L = 12" , b = 2.5" , t = 0.065" and $E = 8 \times 10^6$ p.s.i.

As stated before, the beam column snapped through to another mode. For this mode, the twist is zero at the centre, x = L/2 , and at the point x = 1 , in which case the constant D is zero and the critical relationship between the two loads is

$$2(dL/2 - a)^{3/2}/3d = 2.9 . \qquad (117)$$

The relationship is plotted as curve 2 in fig. 68. For lateral loads which are approximately one third of the critical load of a centrally loaded beam the difference between curves one and two is small. The snap through buckling occurred in this region. The snap through occurred after the total, lateral load was applied and the axial load increased.

If the quantity 1 is less than zero, the shape does not fulfil the boundary condition of zero moment at the end. Under these conditions, that is for small lateral loads, the mode will be taken to satisfy the boundary conditions, zero twist at the centre and zero moment at the ends, which leads to two simultaneous, linear equations in the parameters C and D .

$$\partial\phi/\partial x = 0 = C\ dL/2 - a\ J_{1/3}(2(dL/2 - a)^{3/2}/3d) + D\ dL/2 - a\ J_{-1/3}(2(dL/2 - a)^{3/2}/3d)$$

$$\text{and}\quad \partial^2\phi/\partial x^2 = 0 = C\ -a\ J_{1/3}(2(a)^{3/2}/3d) + D\ -a\ J_{-1/3}(2(-a)^{3/2}/3d) \qquad (118)$$

The determinant of the two equations (118) must be zero for the solution to be non trivial. This produces a critical relationship

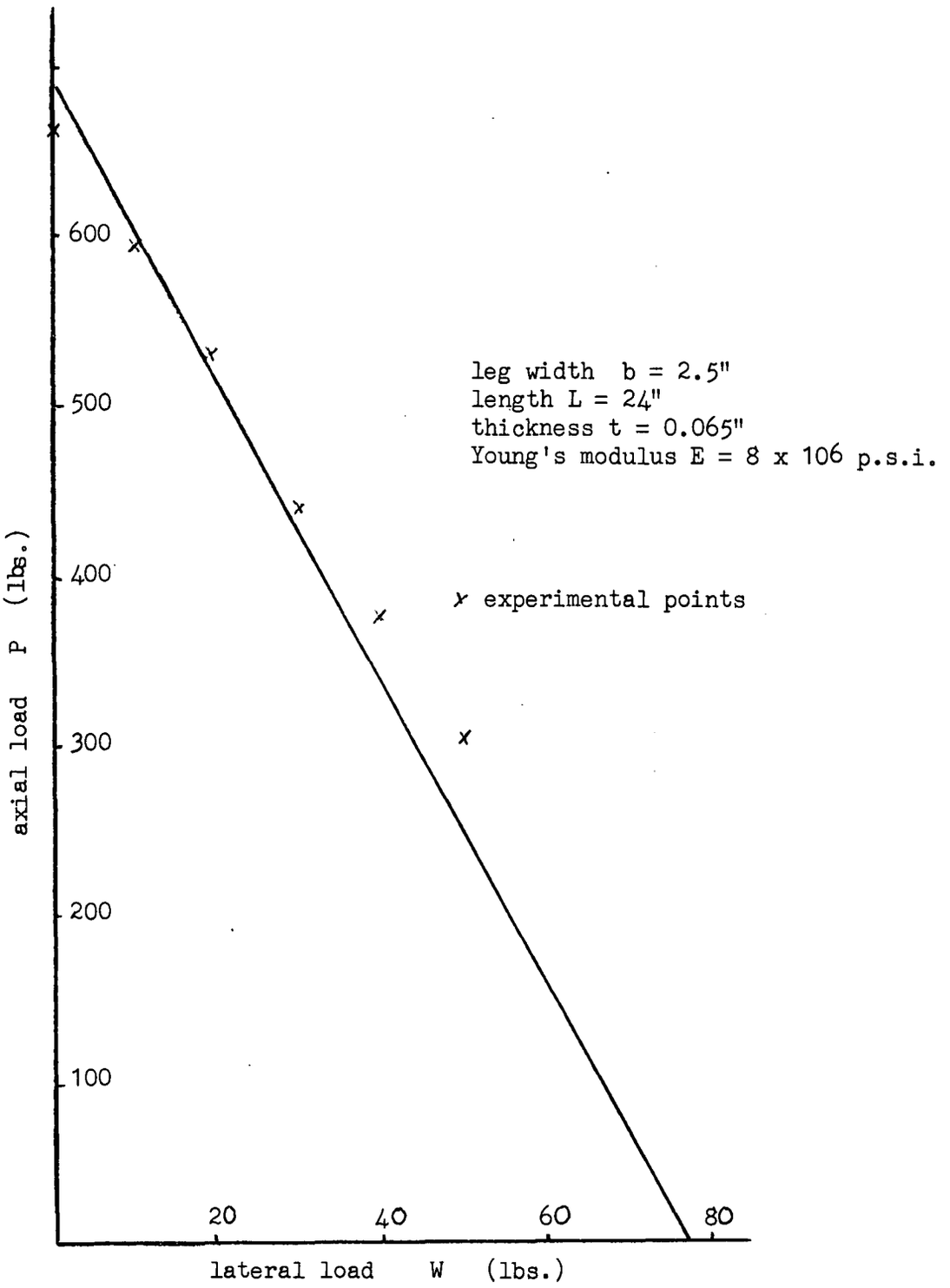

APPROXIMATE INTERACTION CURVE FOR A BEAM COLUMN

FIGURE 69.

between the two loads. The relationship appears as curve 3 in fig. 68. For the member considered, curves 3 and 1 are tangential in the neighbourhood of the loading at which the change of mode was assumed to take place.

If equation (116) or (117) is assumed to extend for very small lateral loads the critical load for a column is

$$P_{crit} = GJA/I_p ,$$

which is the same value as was obtained from the first mathematical model for a column, that is when the bending stiffness of the legs was neglected. The first model for a column gave the critical load as independent of the shape of the column. For a long column this value is a good approximation to the actual critical load of the column. For long beam-columns the critical relationship between the lateral and axial loads may be taken conservatively as a straight line between the critical axial load and the critical bending load.

The lateral load W' at which the quantity 1 is zero is

$$W' = (4.95)^2 \quad 8DI_p I_{QQ} 12\sqrt{2}/L^3t^2b^4$$

and the ratio of this load to the critical bending load is

$$W'/W_{crit} = 16.3b^2/(1 - \nu)(L^2 + 9.4bL) ,$$

if the appropriate value of the bending load is used. As the length L decreases the ratio increases. Also as the length decreases the difference between critical axial load and the approximate value, given by the first mathematical model increases. Hence it becomes more important to consider the symmetric mode of buckling. The straight line approximation appears to be a good approximation to the critical relationship, even for short columns if the true critical, axial and bending loads are used; see fig. 68. A linear relationship is often used, both in design codes and empirical experimental relationships, for interaction problems. It is used when the lateral buckling or flexural-plastic buckling of a beam column is considered.

The member tested had the following dimensions, length $L = 24"$, leg width $b = 2\frac{1}{2}"$, and thickness $t = 0.065"$. The approximate relationship for the member is plotted in fig. 69.

The member may be considered as a long member. The experimental values are also plotted, and are less than the values given by the mathematical model.

In the previous calculations, the central lateral load has been applied so that the free edge of the leg is in compression. In the case of a centrally loaded beam with the free edge in tension the beam fails by plastic collapse. Thus the question arises, "What is the behaviour of a beam column when a negative moment is applied so the extreme fibre is in tension?" This question will not be answered here, although it is obvious that both the buckling mode and the plastic failure due to bending will have to be considered. In considering the buckling properties, new modes will have to be investigated. For the plastic analysis, an estimate of the moment must be made. A suitable first approximation might be

$$WL/4 + PWL^3/48EI(1 - P/P_E) = M_p ,$$

where P_E is the flexural, Euler buckling load.

Returning to the general problem, we may note that the possibility of the beam-column failing by flexural or lateral-torsional buckling or plastic failure should be considered. Taking the problem one step further, the interaction between the modes could be considered.

SUMMARY

A detailed mathematical model has been developed in this thesis to describe the behaviour of a point loaded cantilever. The estimated shapes and critical loads agree well with the measured values. This model has been extended to cover a centrally loaded simply supported beam and a laterally loaded column. However, the beams and laterally loaded columns have the difficulty that more than one mode exists. As already pointed out the two modes of the beam are thought to depend upon the initial shape and the loading of the beam. It is also probable that the mode depends upon the dimensions of the beam, especially the leg width-length ratio.

The critical load of a beam is virtually independent of the length of the beam for most practical members. It also appears that

the lower limit of the critical, maximum moment is independent of the way in which the beam is loaded. The following conditions can be used as conservative design criteria:

for a column the axial stress $\sigma a_{crit} = GJ/I_p$

for a beam the maximum bending stress $\sigma m_{crit} = E(t/b)^2/(1 + \nu)$

and for a laterally loaded column $\sigma a/\sigma a_{crit} + \sigma m/\sigma m_{crit} = 1$.

The mathematical model for a laterally loaded column is very limited in its application and the problem needs more consideration, but it appears from the model developed that the linear relationship between the axial and bending stresses is sufficiently accurate for design purposes.

It should be emphasized that this chapter has introduced many unsolved problems and the ideas presented are only a guide to the fundamental understanding of the problem. Problems which arise from the work done are the non-elastic buckling modes and loads, the interaction of the lateral and local buckling modes of beams, general loading of beams, flexural-torsional buckling of laterally loaded columns, and also the effect of opposing lateral and axial loads. The mathematical solutions of most of these problems will involve complex mathematical models, which will be of little practical benefit, and thus it appears that the expressions for the stresses in this summary are good design criteria.

CONCLUSIONS

In this chapter four topics will be considered. The relationships between the mathematical models developed in this thesis and those developed previously will be discussed,and it will also be shown how these mathematical models can be extended to apply to a general cross-section. The design codes established as a guide in designing members of the type will be studied and the unanswered questions rising from the work carried out will be stated and possible lines of attack will be suggested. Mention will also be made of plastic buckling, although this topic has only been touched upon in the thesis.

Timoshenko[1] has considered the torsional buckling of short, equal leg, angle-section members. He arrived at a simple mathematical model, called the first mathematical model in this thesis. He also derived a more complex model which included the plate stiffness of the member. The angle-section member was considered as two flat rectangular plates buckling under a uniformly distributed compressive load. The assumed boundary conditions were that the line of shear centres remains straight and that this line acts as a pin-joint between both legs, as the moment m_y round the corner is zero, The ends of the member were assumed to be pin-jointed. The problem then reduced to one of the buckling of a rectangular, flat plate with one free edge and three pin-jointed edges, under uniform compression in the axial direction x. In fact it was assumed that any change in the longitudinal stresses N_x due to the deformations was negligible and the stresses were taken as constant and equal to the ratio of the force P to the cross-sectional area A.

The deflections w normal to the leg were taken to be of the form

$$w = f(y) \sin (\pi x/L) ;$$

where $f(y)$ is a function of y only, and w satisfies the boundary conditions at $x = 0, L$. If w satisfies the equilibrium equation for a plate element,

$$\partial^4 w/\partial x^4 + 2\,\partial^4 w/\partial x^2 \partial y^2 + \partial^4 w/\partial y^4 = N_x/D\;\partial^2 w/\partial x^2$$

then $$w = A(\cosh \alpha y + B \sinh \beta y) \sin \pi x/L$$

Ref. 1 S. P. Timoshenko: "Elastic Instability".

for a unique load given by

$$P = 2mD/b ,$$

where D is $Et^3/12(1-\nu^2)$ is the flexural rigidity, E is Young's modulus, ν is Poissons ratio, t is the leg thickness, and m is a parameter which depends upon the ratio of the length of the member L to the leg width b and the elastic properties of the material. For a Poisson's ratio of 0.3 the constant m becomes

$$m = 0.425 + b^2/L^2 .$$

Bleich has made a detailed survey of the local buckling of columns of general cross-section. He treats each leg of the member as a plate with either one or two elastic supports. The coefficient of restraint of the support depends upon the neighbouring elements. The analysis includes both an elastic and an inelastic treatment. For an inelastic material the elastic modulus is replaced by the tangent modulus. It was also assumed that the ratio of the tangent and elastic moduli is the same for both shear and normal deformations at any given axial loading. Bleich treats equal-leg angle-section members as a special case. The average critical stress is

$$\sigma = \pi^2 E \sqrt{\tau}(t/b)^2(\sqrt{\tau}(b/l)^2 + 0.425)/12(1-\nu^2) \qquad (119)$$

for $\nu = 0.3$.

Bulson also gives a detailed analytic treatment for local buckling of thin, open section members. He gives the experimental results he obtained and compares them with the analytic results. For a member which buckles inelastically, he suggests an average modulus E' (where E_t is the tangent modulus and E_{sec} is the secant modulus) given by

$$E' = \tfrac{1}{4}E_t + \tfrac{3}{4}E_{sec} .$$

The expression for the critical load of a member buckling torsionally, derived in this thesis is

$$= E(t/b)^2((b/l)^2 + 6(1-\nu)/\pi^2)/12(1-\nu^2) . \qquad (120)$$

When a Poisson's ratio of 0.3 is considered the expression is identical to the one obtained by Timoshenko and Bleich[1] (equation

119). However, it has the advantage that it is simply derived and the value of the constant m can be readily evaluated for various Poisson's ratio values.

Bleich also discussed the thickness of plates required so that a column fails by flexural buckling before local buckling occurs. The inequality expressing this condition is

$$(\pi/l)^2 Eb^3 t/12 = \pi^2 E/(l/\rho)^2 \leq \pi^2 E/12(1-\nu^2)(t/b)((b/l^2 + 0.425)$$

$$\leq k(t/b)^2 \pi^2 E/12(1-\nu^2)$$

or

$$t/b \leq C\sqrt{k}, \qquad (121)$$

where C is a function of the slenderness ratio l/ρ. Bleich also extends the inequality for inelastic buckling, by assuming a linear relationship between C and the square root of the slenderness ratio. For equal leg, angle section members Bleich gives

$$b/t \leq 0.652C .$$

The Column Research Council Guide to Design Criteria for Metal Compression Members states that the American Institution of Steel Construction bases its code for local buckling on any supported edge being simply supported and that a local buckling must not form before the material yields, which gives the yield stress

$$\sigma_y = (t/b)^2 \, {}^2E/12(1-\nu^2)((b/l)^2 + 0.425)$$

for an outstanding leg. For a steel with a yield stress of 36kpsi the allowable leg width-thickness ratio is 17.6. A.I.S.C.[2] practice gives the limits:

for an outstanding leg: $b/t \leq 3000/\sqrt{\sigma_y}$

and for an element supported along each edge:

$$b/t \leq 8000/\sqrt{\sigma_y}$$

The German code DIN 4114 follows the same attitude as was used by Bleich, and designs the column so that local buckling does not occur

---

Ref. 1: F. Bleich "Buckling Strength of Metal Structures"
Ref. 2: American Institute of Steel Construction, "Manual of Steel Construction".

before overall buckling. The code states, for the outstanding leg; if the slenderness ratio $l/\rho > 75$ then $b/t = 0.2\, l/\rho$ else $b/t = 15$.

For a member supported along each edge, a table is provided, in which a formula for the permissible ratio is quoted. The ratio depends upon the shape and dimensions of the overall cross-section. The code also allows for the stiffness of the joints between two con tituent plates.

The British Code BS449 1959 gives a formula for the following ratio for the three steels mentioned. The ratios are based upon the yield criteria. For steel BS15 the allowable leg width thickness ratio is sixteen, for BS548 and 968 the ratio is fourteen. The draft (1966) for the Australian Code SAA Inst. 351 uses the AISC formulae for the detailed design of compression members.

The American Society of Civil Engineers[1] suggested specifications for different aluminium alloys. In determining the allowable dimension of members governed by local buckling of the constituent elements it is assumed that all supported edges are simply supported. This is conservative.

Few codes consider the local buckling of a leg with non uniform stress. However the ASCE committee has included the cases when a member is bending about the minor or major axis. Timoshenko has solved the problem of the buckling of a plate with linearly distributed longitudinal stresses using an energy approach. The mathematical model developed in this thesis gives the maximum allowable bending stress in a cantilever or centrally loaded simply supported beam as

$$\sigma = Mb/2\sqrt{2}\, I_{QQ} = W_{crit} L/8\sqrt{2}\, I_{QQ} = E(t/b)^2(1 + 9.4b/L)/(1+\nu)$$

For large L a conservative allowable stress is

$$= E(t/b)^2/(1+\nu) \quad \text{or} \quad \pi^2 E(b/t)^2/(3.5)^2 , \qquad (122)$$

which is the value quoted by the ASCE committee. This value is also a conservative estimate for a beam bending under a uniform bending

---

Ref. 1 Proc. Am. Soc. of Civ. Eng. Journal of Structural Div. Vol. 88 Dec. 62, "Suggested Specifications for Aluminium Alloys".

moment as for that loading

$$\sigma = (E(t/b)^2/(1+\nu))(1+\pi^2(b/L)^2/6(1-\nu)) .$$

In fact equation (122) is conservative estimate of the stress for all beams.

When an angle section member is loaded about the major axis a conservative assumption would be to assume each leg was simply supported and the stress varied linearly from zero to a maximum, which gives an allowable stress of

$$\sigma = \pi^2 E(t/b)^2/(4.4)^2 \qquad (123)$$

for long members.

In the work presented previously it be assumed that the root of the angle-section member is weak and the included angle changes when a moment is applied about the major axis. Most extruded or rolled sections have a fillet, which strengthens the root of the angle. Consequently the tendency will be for the included angle to be maintained and for the legs of the cross-section to deform. It is possible to analyse this functional form by considering each plate separately and applying compatibility of statics and geometry at the root. When the functional form is taken to be rotation of the cross-section in an undeformed state, bending about the major axis does not cause torsional instability. The experimental analysis of beams has been limited to bending about the minor axis. Bending about the major axis can be considered by either of the methods described above, although it is reasonable to assume that the true functional form is a combination of the two forms.

All the design codes quoted are based on a conservative estimate of the load capacity of a member. The mathematical models developed by the author allow for a less conservative design of both beams and columns, with very little extra computation. However in the case of a general beam, it is unlikely that the differential equations which are derived from the mathematical model will prove solvable.

Flexural-torsional buckling of thin-open section members in compression has been studied in some detail by Timoshenko, Weber,

Wagner and Goodier[1]; the stiffness of the plates of which the member consists was neglected. For a long member this assumption is satisfactory. However, the plate action of a short member is important and increases the load a member can carry. Bleich has used an energy approach to arrive at a solution for the flexural-torsional buckling of short members. However, the results obtained vary from those obtained in this thesis as Bleich[1] has neglected the Poisson's ratio effect in allowing for the bending stiffness. The author considers the approach used in this thesis is more satisfactory as it is a direct approach.

The characteristic equation for the critical load of a general cross-section is

$$I_p(P - P_1)(P - P_2)(P - P_3)/A - P^2 y_0^2(P - P_1) - \\ - P^2 x_0^2(P - P_2) = 0 , \qquad (124)$$

where P_1 and P_2 are the two flexural, Euler buckling loads and

$$P_3 = A(GJ + C_w(n\pi/L)^2)/I_p ,$$

which is the torsional buckling load. The constant C_w is the warping constant introduced in the section on torsion. For an equal leg angle section member the constant C_w is zero.

The results obtained in the section on torsional-flexural buckling and by Timoshenko, Bleich and Goodier depend upon the boundary condition for the three variables, the two deflections, u, v and the rotation w, being compatible. Baker and Roderick[2] have tested a variety of members of varying cross-sections and dimensions. But the boundary conditions of the models tested were not compatible, as the warping was restrained at the ends. They suggested using the same basic, characteristic equation (124) except that the values of P_1, P_2 and P_3 used, should be the values obtained when the flexural and torsional buckling are considered as independent and each mode satisfies the appropriate boundary condition. Renton[3] solved the

---

Ref. 1 See sections on Torsion and Torsional-Flexural Buckling
Ref. 2 J. F. Baker & J. W. Roderick: "Strength of Light Alloy Struts" Al. Dev. Assoc. Report No. 3.
Ref. 3 J. D. Renton: "A Direct Solution of Torsional-Flexural Buckling of Axial Loaded Thin-Walled Bars", The Structural Eng., Vol. 18, No. 9, Sept. 1960.

problem for any set of end conditions, both statical and geometric. He compared his analytic results with Baker and Roderick's results. The difference between Renton's mathematical model and the approximate mathematical model is very small. The difference is most noticeable for a T-section and angle section members.

Bleich gives some diagrams which show the susceptibility to flexural and torsional-buckling of members having cross-sections of various shapes. Only tee-members and the angle section members are prone to torsional buckling. Bijlaard and Fischer[1], in discussing the interaction between local and overall buckling, state: "The interaction effect is negligible for box sections as indicated by both theory and experiment...; the same conclusions apply to common size of H and channel sections, but not to sections for which torsional instability is an important factor, such as the tee and angle sections".

One of the conditions for calculating the critical loads for the various types of buckling was that the mode being investigated predominated. In the case of local buckling it was assumed the line of shear centres remained straight. In the case of torsional-flexural buckling it was assumed the cross-section did not distort.

A. Chajes and G. Winter[2] have arranged the torsional-flexural model into a form suitable for a design office tool. The critical load P for a cross-section with one axis of symmetry can be expressed as

$$P/P_1 + P/P_3 - KP^2/P_1P_3 = 1 , \qquad (125)$$

where P_1 and P_3 are the flexural and torsional critical loads and K is a factor which depends only upon the geometry of the cross-section. He also gives the values of the torsional load P_3, the constant K, and the type of failure as graphs plotted against a non-dimensional parameter of the cross-section.

Most codes mention that a column should be checked for torsional instability. However, only Addendum No. 1 (1961) to the British

---

Ref. 1 Column Research Councils Guide to Design Criteria for Metal Compression Members.

Ref. 2 A. Chajes and G. Winter, Proc. A.S.C.E. Struct. Vol. 91, Aug. 1965.

Code BS499 tackles the problem numerically. A table of equivalent slenderness ratios l/ρ are quoted for various cross-sections. Also the Joint Committee of the British Instruction of Structural Engineers and the Institute of Welding mention torsional buckling in their report on "Fully rigid multi-storey steel frames". They set limits on the distribution factor at a joint so that sufficient restraint is provided to overcome torsional instability.

When a column is loaded laterally a straight line interaction curve is usually considered sufficient,

$$P/P_{ult} + M/M_{ult} = 1 , \qquad (126)$$

where P_{ult} and M_{ult} are the load capacity of the member under an axial load P and as moment M respectively. This is the case for the local buckling of the member. However, in general the ultimate moment can either be the lateral buckling load, plastic moment or the moment to cause local buckling. Curves of the form

$$P/P_{ult} + M/(K\, M_{ult}\,(1 - P/P_{ult})) = 1$$

or

$$P/P_{ult} + (M/M_{ult})^2/K = 1 \qquad (127)$$

have also been considered. The first alternative is quoted in some codes, for example the AISC Manual of Steel Construction. The second alternative is used in connection with lateral buckling, and also as an upper bound on the true load capacity. The work in this thesis indicates that the linear relationship is a good approximation for local buckling.

The large deflection, elastic model for the torsional instability of a column indicates that an elastic member is able to carry a load greater than the critical load, if the deformations are not important. However, the increased load capacity of the member decreases as the leg width-thickness ratio decreases. If we consider an initially straight member and denote the increase in load above the critical load at which a unit twists is achieved by P', then the ratio of the increase to the critical load P_{crit} is

$$P'/P_{crit} = (1 - \nu)b^2(b/t)/40((b/l)^2\ \ ^2 + 6(1 - \nu)) .$$

If the thickness is increased or the leg width decreased the ratio

decreases.

This thesis has not considered the behaviour of a member once the material becomes plastic. Most design codes are based upon the Bleich approach of replacing the modulus of elasticity by a "modulus of plasticity". The codes also include an empirical expression for the ratio of the two moduli τ . One of the most interesting facts observed is that all members tested, whether as beams or columns, failed in the same plastic "triangular" mode (figs. (61), (51) and (38). However as pointed out, this functional form cannot be used to obtain an upper bound on the load capacity, as it appears that the member has partially unloaded before the true "triangular" mode is formed.

Codes also take into account the load capacity of a member in which a local buckle has occurred. But the suggested specifications of the ASCE specifically state that single angle, double angle, crucifix and tee members should not be included, their reason being that the interaction between local buckling and overall buckling is important for these sections. The effective leg width for other sections is taken as a fraction of the leg width which depends upon the load being carried and the critical load to cause local buckling. The effective leg width is used in calculating the load capacity of the member.

In all the mathematical models developed in this thesis, the change of loading as the deformations increase has been neglected. In the case of both the cantilevers and the beams tested the direction of the load was independent of the deformations. The beams were loaded through the shear centre and although the mathematical models describing the local buckling is not effected by the way the model is loaded, when the lateral buckling of the beam is considered this is important. For large deflections of an eccentrically loaded column, it is thought that the bearing stresses on the base redistribute in such a manner as to increase the eccentricity and consequently stiffen the model. The discrepancy between the measured and the estimated graph in Fig. 33 could be explained by this fact.

All the members investigated have been tested as single members, and have not been integrated into a truss. Thus the problem rises as to how a member acts in a truss. The primary problem is the boundary conditions. Both the beams and the columns have been considered as pin-ended. While it would appear reasonably simple to consider a column with any boundary conditions, the boundary conditions of a laterally loaded beam would be more difficult to apply, especially as the mode is complex and it is possible to obtain two modes. Already the possibility of including the variation of the torsional strength of a member with the axial load and end moment to the overall buckling of a frame has been mentioned. However, the problem is not as serious as it first appears as the critical load, both for long columns and long beams, is independent of the length.

Other applications of angle section members must be considered. Often two angles are bolted together to act as a strut. The local buckling of the individual angle members can be considered by using the mathematical models developed. However, in considering the overall torsional and flexural buckling of the member, the member must be considered as a tee-member. The problem of double bulb angle struts is considered by Cullimore.

The torsional buckling of a member about a fixed axis of rotation is considered by Bleich.[1] Maurice Sharp[2] investigates the use of longitudinal stiffeners on flat angle, one application of angle-section member. If a lip is added to the free edge of the leg of the angle member the load capacity of the member is increased. Bulson[3] discusses analytically the effect of lips on cross-section. Sharp also includes the action of a lip in his paper.

The last section of this chapter has been devoted to common applications of angle-section members. All the references quoted have treated the problem using the classical approach. It is quite poss-

---

Ref. 1 F. Bleich "Buckling Strength of Metal Structures"
Ref. 2 M. L. Sharp "Longitudinal Stiffness for Compression Members" Proc. Am. Soc. of Civ. Eng., Struct. Div., October 1966.
Ref. 3 P. S. Bulson "Local Instability Problems of Light Alloy Struts". Al. Dev. Assoc. Report No. 29.

ible to attack these problems in the same manner as used in this thesis, and the author feels that, as a result, a more simplified mathematical model can be obtained, based upon a clear understanding of the problem.

While the mathematical models developed by the author have in general not broken new ground, the approach used has enabled an examination to be made of the local buckling of all structural members using basically the same functional form for the geometry, the same underlying ideas, and similar mathematical models. The author feels that this approach is of benefit, as the review of existing literature on this topic has shown that many different approaches are required to cover the topics considered, and most of these approaches involve complicated and somewhat abstract mathematics. The geometric approach will be of particular importance when more complex problems are considered. For these problems an advanced numerical or algebraic analysis of each member will most likely have to be used. The geometric functional form approach can be simply and logically applied to these problems.

APPENDIX A

ELASTIC BENDING OF THIN PLATES

In the following section of the thesis, the mathematical model of bending of thin plates is developed. The results obtained have been applied repeatedly throughout the thesis. The analysis closely follows the lines followed by Timoshenko[1] except that some of the symbols have been defined differently. The model is based upon the fact that all the strains vary linearly across the section, that is, throughout the thickness. The model includes the case when the centre plate deforms.

The coordinate system with which the model will be developed will be x, y axes in the plane of the unloaded plate and the z direction normal to the x-y plane. The deflections in the z direction will be denoted by w. (see fig. 29) The element to be considered is of thickness, t and defined by the planes x, $x+dx$, y and $y+dy$. The following notation will be used

	N_x, N_y	longitudinal stresses on the central plane
	N_{xy}	shear stresses on the central plane
	Q_x, Q_y	normal shear stresses
	m_x, m_y	bending moments about x and y axis
and	m_{xy}	twisting moments

All symbols are quantities per unit length.

	t	thickness
	D	flexural rigidity, $D\ Et^3/12(1-\nu^2)$
and	K_x, K_y	curvatures

The symbols are defined graphically in fig. 29.

In general the shape of the plate is known, so that the aim will be to develop expressions for the internal actions of the plate in terms of known geometry using the load deformation relationship. In the case of small deflections the change in the curvatures is

$$K_x = \partial^2 w/\partial x^2$$

and

$$K_y = \partial^2 w/\partial y^2$$

Ref. 1 S. P. Timoshenko "Plates and Shells", McGraw-Hill Book Co., Inc.

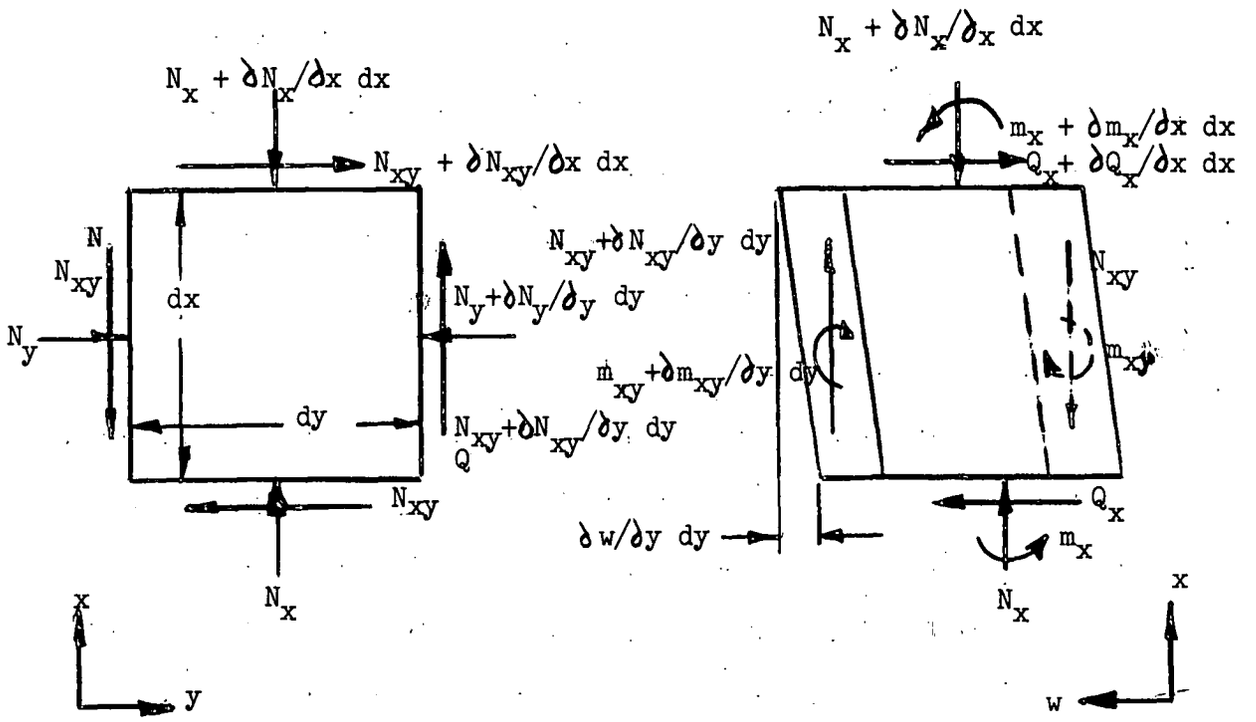

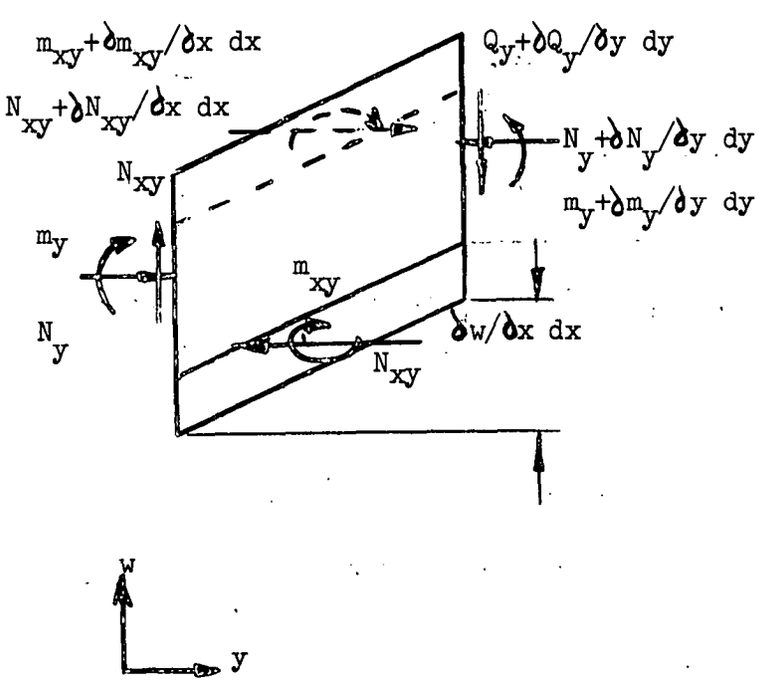

All cuts are parallel to the x, y, z axes.

All forces are parallel to the x,y and z axes.

Thickness of element t
N_{xy}, Q_x, Q_y shear forces
N_y, N_x, longitudinal forces
m_x, m_y, m_{xy} moments.

All forces are forces per unit length.

FORCES ON AN ELEMENT dx · dx · t

FIGURE 29

and the change in twist is

$$K_{xy} = \partial^2 w/\partial x \partial y .$$

If the problem is further restricted and only linear load deformation relationships are considered, that is the materials are elastic, the moments per unit length required to maintain the deformations are

$$m_x = - D(K_x + \nu K_y) = - D(\partial^2 w/\partial x^2 + \nu \partial^2 w/\partial y^2)$$

$$m_y = - D(K_y + \nu K_x) = - D(\partial^2 w/\partial y^2 + \nu \partial^2 w/\partial x^2)$$

and $m_{xy} = D(1 - \nu) \partial^2 w/\partial y \partial x = K_{xy} D(1 - \nu) .$

The internal shearing stresses can be obtained by considering the equilibrium of an element of the plate. The equations of equilibrium are

force equilibrium in the z direction

$$\partial Q_x/\partial y + \partial Q_y/\partial x = 0 ,$$

force equilibrium in the x direction

$$\partial N_{xy}/\partial y + \partial N_x/\partial x = 0 ,$$

force equilibrium in the y direction

$$\partial N_{xy}/\partial x + \partial N_y/\partial y = 0 ,$$

moment equilibrium in the zx plane

$$Q_x = \partial m_x/\partial x - \partial m_{xy}/\partial y - N_x \partial w/\partial x - N_{xy} \partial w/\partial y ,$$

moment equilibrium in the zy plane

$$Q_y = \partial m_y/\partial y - \partial m_{xy}/\partial x - N_y \partial w/\partial y - N_{xy} \partial w/\partial x .$$

The equilibrium equations in conjunction with the load deformation relationships give an expression for the shearing forces for unit length in terms of the geometry,

$$Q_x = - D(\partial^3 w/\partial x^3 + \partial^3 w/\partial x \partial y^2) - (1 - \nu) D \partial^3 2/\partial y^2 \partial x - $$

$$- N_x \partial w/\partial x - N_{xy} \partial w/\partial y$$

and

$$Q_y = - D(\partial^3 w/\partial y^3 + \partial^3 w/\partial x^2 \partial y) - (1 - \nu) D \partial^3 w/\partial y \partial x^2 - $$

$$- N_y \partial w/\partial y - N_{xy} \partial w/\partial x .$$

It should be noted that although the final expressions depends upon having small deflections and a linear mode deformation relationship, the equations of equilibrium are independent of both these restrictions.

APPENDIX B

Solution of the differential equation, third model for a column loaded through a base plate

$$\partial^2\phi/\partial x^2 + \Omega^2\phi - \phi^3\beta = 0 .$$

Multiply by $2\partial\phi/\partial x$;

$$2\partial\phi/\partial x\ \partial^2\phi/\partial x^2 + 2\Omega^2\phi\,\partial\phi/\partial x - 2\beta\phi^3\partial\phi/\partial x = 0 .$$

After integrating with respect to x the equation becomes

$$(\partial\phi/\partial x)^2 + \Omega^2\phi^2 - 2/3\beta\phi^4 = c$$

or $$\partial\phi/\partial x = (c - \phi^2(\Omega^2 - 2/3\beta\phi^2))^{-\frac{1}{2}} .$$

Properties of the elliptic functions

$$\text{cnz} = (1 - \text{sn}^2 z)^{\frac{1}{2}} ,$$

$$\text{dnz} = (1 - k^2\text{sn}^2 z)^{\frac{1}{2}} ,$$

$$\text{dsnz/dz} = \text{cnz dnz} ,$$

$$\text{dcnz/dz} = -\text{snz dnz} ,$$

$$\text{d dnz/dz} = -k^2\,\text{snz dnz} ,$$

and $$d^2\,\text{snz}/dz^2 = k^2\,\text{sn}^3 z - k^2\,\text{snz} - \text{snz} + k^2\,\text{sn}^3 z .$$

NOTATION

b	leg width of angle
L	length
l	effective length
t	thickness of leg
D	flexural rigidity $Et^3/12(1-\nu^2)$
J	torsional rigidity $2bt^3/3$
I_p	polar moment of inertia about the shear centre
I_{pp}, I_{QQ}	moments of inertia about the principal axes
ρ	radius of gyration
A	cross-sectional area
x, y	co-ordinates associated with the leg of an angle-member
p, q	principal co-ordinates of cross-section of angle members
r	polar ordinate about the shear centre
w	deflection normal to the leg of the angle
w_1, w_2	deflections of the individual leg; often the same, $w_1 = w_2 = w$.
u, v	displacements in the x, y directions
ϕ	rotation of the cross-section
a, B	twist parameters
E	Youngs modulus
$\bar{E}$	plastic modulus
τ	ratio of Youngs and plastic moduli
G	shear modulus
ν	Poisson's ratio
C_w	warping constant
T	torque
P	axial load
W	lateral load
W_{crit}, P_{crit}	critical loads
M_p, M_Q	moments about the principal axes
m_x, m_y, m_{xy}	moments per unit length of plate
N_x, N_y	longitudinal forces per unit length of plate

N_{xy}	shear force per unit length of plate
Q_x, Q_y	shear forces per unit length plate acting a cross the thickness of the plate
K_x, K_y	curvatures in x and y directions
K_{xy}	twist
ϵ	strain
σ	stress
e	eccentricity
λ	eigen value
u	potential energy